

PHOTOCHROMIC CHARACTERISTICS OF
SPIROOXAZINE-CONTAINING MEDIA

By
XIAODONG SUN

Bachelor of Science
Peking University
Beijing, China
1986

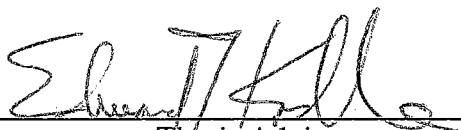
Master of Science
Peking University
Beijing, China
1989

Submitted to the Faculty of the
Graduate College of the
Oklahoma State University
in partial fulfillment of
the requirements for
the Degree of
DOCTOR OF PHILOSOPHY
May, 1997

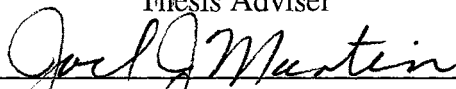
Thesis
1997D
5957p

PHOTOCHROMIC CHARACTERISTICS OF
SPIROOXAZINE-CONTAINING MEDIA

Thesis Approved:

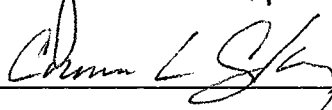


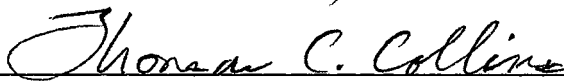
Thesis Adviser











Dean of the Graduate College

ACKNOWLEDGMENTS

I wish to express my deepest appreciation to my major advisor, Dr. Edward T. Knobbe for his invaluable guidance, assistance and understanding throughout the course of study. My sincere appreciation extends to my other advisory committee members – Drs. Elizabeth M. Holt, Corinna L. Czekaj, Warren T. Ford, Joel J. Martin and George S. Dixon. Special thanks to Dr. Knobbe and the Department of Chemistry for providing me with this research opportunity and their generous financial support.

I would like to thank Professor Meigong Fan for generously providing the samples and his inspiration and constructive discussions. Much appreciation goes to those who provided suggestions and assistance for this study: Drs. Elizabeth M. Holt, Kai Dou, Xiao-jun Wang, Feng Qiu, James Wicksted, Wei Shan, John Guthrie, Steven Paulin, Margaret Eastman and Ms. Marie Coutant. I also want to thank the past and present researchers in Ed Knobbe's group with whom I have had pleasure of working, including (in no particular order) Robert, Lowell, Trace, James, Diane, Robbie and Monica.

I would like to give special appreciation to my wife, Lin Fan. This research would not be possible without her understanding, love, patience and encouragement. My appreciation is extended to my parents and parents-in-laws for their constant support and understanding.

TABLE OF CONTENTS

Chapter	Page
1. Introduction to Photochromic Effect in Spirooxazines.....	1
References.....	4
2. Crystal Structure Analysis of Photochromic Spirooxazine Compounds and Non-Photochromic Thiazolinospirooxazine Compounds	5
2.I. Introduction	5
2.II. Experimental Methods	11
2.II.A. Synthesis of Title Compounds.....	11
2.II.B. Preparation of Single Crystals.....	12
2.II.C. Crystallography.....	12
2.III. Results and Discussion	12
2.IV. Summary and Conclusions.....	16
2.V. References.....	17
3. Acidichromic Effects in Photochromic Spiro(1,3,3-trimethylindolo-2,3'-naphth[1,2- <i>b</i>]-1,4-oxazine): Absorption Characteristics.....	69
3.I. Introduction	69
3.II. Experimental Methods	70
3.III. Results and Discussion	70
3.IV. Summary and Conclusions.....	78
3.V. References.....	79
4. Acidichromic in Photochromic Spirooxazines: Structural Effects	80
4.I. Introduction	80
4.II. Experimental Methods	81
4.III. Results and Discussion	81
4.III.A. Proton Activity Dependence of Absorption Spectra.....	81
4.III.B. Photochromic Character of the Acidichromic Compounds.	84
4.III.C. Substituent Effects on the Absorption Maxima of Acidichromic Products.....	86
4.III.D. Discussion of the Acidichromic Mechanism for the Hydroxylated Spirooxazine Compounds.....	87
4.IV. Summary and Conclusions.....	89
4.V. References.....	90
5. Acidichromic Effects in Photochromic Spiro(1,3,3-trimethylindolo-2,3'-naphth[1,2- <i>b</i>]-1,4-oxazine): Fluorescence Studies.....	91
5.I. Introduction	91
5.II. Experimental Methods	92
5.III. Results and Discussion	92

5.III.A.	Fluorescence Emission and Excitation Spectra of SP1.....	92
5.III.B.	Fluorescence Emission and Excitation Spectra of SP1•HCl.....	93
5.III.C.	Proton Activity Dependence of Fluorescence Spectra.....	96
5.III.D.	Fluorescence Emission of PMC1•HCl.....	97
5.IV.	Summary and Conclusions.....	100
5.V.	References.....	101
6.	NMR Spectroscopic Studies on Structure of Spiro(1,3,3-trimethylindolo- 2,3'-naphth[1,2- <i>b</i>]-1,4-oxazine).....	102
6.I.	Introduction.....	102
6.II.	Experimental Methods.....	103
6.III.	Results and Discussion.....	103
6.III.A.	¹ H Assignments by DQFCOSY.....	103
6.III.B.	¹³ C Assignment by HMQC.....	106
6.III.C.	Conformational Structure of SP1.....	114
6.III.D.	Structure Determination of the Protonated Product of SP1.....	116
6.IV.	Summary and Conclusions.....	116
6.V.	References.....	117
7.	Study of Aluminosilicate Gels Doped with Photochromic Spirooxazine.....	120
7.I.	Introduction.....	120
7.II.	Experimental Methods.....	121
7.II.A.	Materials and Sample Preparation.....	121
7.II.B.	Apparatus and Spectral Measurements.....	122
7.III.	Results and Discussion.....	123
7.III.A.	SP1 Spectra in the DBATES.....	123
7.III.B.	SP1 Spectra in the Aged Gel.....	128
7.III.C.	SP1 Spectra in Air-stable Xerogel Specimens.....	131
7.IV.	Summary and Conclusions.....	133
7.V.	References.....	134
8.	Preparation of Air-Stable Photochromic Xerogel Using Spirooxazine Dopants.....	135
8.I.	Introduction.....	135
8.II.	Experimental Methods.....	138
8.II.A.	Materials.....	138
8.II.B.	Sample Preparation.....	138
8.II.C.	Spectral Measurements.....	139
8.III.	Results and Discussion.....	141
8.III.A.	Photochromic Effects in SP1-doped ORMOSIL Xerogels.....	141
8.III.B.	Decay Rate Measurements.....	142
8.III.C.	Fluorescence Studies of SP1-doped ORMOSIL Xerogels.....	144
8.III.D.	Time-resolved Fluorescence Decay of SP1 Doped Gels....	145
8.IV.	Summary and Conclusions.....	147
8.V.	References.....	148

LIST OF TABLES

Table	Page
2-1 Interplanar Angle (°) of Compounds	12
2-2 Bond Length (Å) Related to Spiro <i>C</i> vs. Photochromic Behavior	14
2-3 Bond Angle Totals at <i>N8</i> (°) vs. Photochromic Behavior.....	15
2-4 Bond Length (Å) Related to <i>S1</i> and <i>N8</i> for Compounds I, II and III	16
2-5 Crystal Data for Compound I.....	19
2-6 Atomic Coordinates and Equivalent Isotropic Displacement Coefficients for Compound I.....	20
2-7 Bond Lengths (Å) for Compound I.....	22
2-8 Bond Angles (°) for Compound I.....	23
2-9 Anisotropic Displacement Coefficients for Compound I.....	25
2-10 Hydrogen Atom Coordinates and Isotropic Displacement Coefficients for Compound I.....	27
2-11 Crystal Data for Compound II.....	29
2-12 Atomic Coordinates and Equivalent Isotropic Displacement Coefficients for Compound II.....	30
2-13 Bond Lengths (Å) for Compound II.....	32
2-14 Bond Angles (°) for Compound II.....	33
2-15 Anisotropic Displacement Coefficients for Compound II.....	34
2-16 Hydrogen Atom Coordinates and Isotropic Displacement Coefficients for Compound II.....	36
2-17 Crystal Data for Compound III.....	38
2-18 Atomic Coordinates and Equivalent Isotropic Displacement Coefficients for Compound III.....	39
2-19 Bond Lengths (Å) for Compound III.....	41
2-20 Bond Angles (°) for Compound III.....	42

2-21	Anisotropic Displacement Coefficients for Compound III.....	43
2-22	Hydrogen Atom Coordinates and Isotropic Displacement Coefficients for Compound III.....	45
2-23	Crystal Data for Compound IV.....	48
2-24	Atomic Coordinates and Equivalent Isotropic Displacement Coefficients for Compound IV.....	49
2-25	Bond Lengths (Å) for Compound IV.....	51
2-26	Bond Angles (°) for Compound IV.....	52
2-27	Anisotropic Displacement Coefficients for Compound IV.....	54
2-28	Hydrogen Atom Coordinates and Isotropic Displacement Coefficients for Compound IV.....	56
2-29	Crystal Data for Compound V.....	59
2-30	Atomic Coordinates and Equivalent Isotropic Displacement Coefficients for Compound V.....	60
2-31	Bond Lengths (Å) for Compound V.....	62
2-32	Bond Angles (°) for Compound V.....	63
2-33	Anisotropic Displacement Coefficients for Compound V.....	65
2-34	Hydrogen Atom Coordinates and Isotropic Displacement Coefficients for Compound V.....	67
4-1	λ_{\max} of Protonated Product in Isopropanol Solutions.....	87
6-1	Chemical Shifts (δ /ppm) of Protons and H-H Coupling Constants.....	112
6-2	Chemical Shifts (δ /ppm) of Carbon Atoms.....	113

LIST OF FIGURES

Figure	Page
1-1 Chemical Structure of SP1 (Spiro-form) and the Corresponding UV-Induced Photomerocyanine Form (PMC form)	3
1-2 Four Isomers of Photomerocyanine Form.....	3
2-1 Mechanism of Photochromism in Spirooxazine Compounds	7
2-2 Example of photochromic thiazo compound.....	7
2-3 Chemical Structure of 1-Methylbenzothiazolinospiro-2,3'-(2'-methyl-[3H]phenanthro [9,10- <i>b</i>][1,4]oxazine) (Structure I)	9
2-4 Chemical Structure of 1-Methylbenzothiazolinospiro-2,3'-(2'-methyl-[3H]naphth [2,1- <i>b</i>][1,4]oxazine) (II).	9
2-5 Chemical Structure of 1-Methylbenzothiazolinospiro-2,3'-(2'-methyl-9'-methoxy-[3H]naphth [2,1- <i>b</i>][1,4]oxazine) (III)	10
2-6 Chemical Structure of Spiro(1,3,3-trimethyl-2'-methylindolo-2,3'-naphth[1,2- <i>b</i>]-1,4-oxazine) (IV).....	10
2-7 Chemical Structure of Spiro(1,3,3-Trimethyl-indolo-9'-methoxy-2,3'-naphth[1,2- <i>b</i>]-1,4-oxazine) (V).....	10
2-8 Projection View of I	18
2-9 Projection View of II	28
2-10 Projection View of III	37
2-11 Projection View of IV	47
2-12 Projection View of V	58
3-1 Absorption Spectra of Alcoholic Spirooxazine Solutions as a Function of Proton Activities	72
3-2 Absorption Spectra of Four Species, A, B, C and D.....	74
3-3 Proposed Transformation among A, B, C and D Forms.....	75
3-4 Proposed Acidichromic Process of the Photomerocyanine Form.....	76

3-5	Proposed Acidichromic Process between SP1(A) and SP1•HCl (B)	77
3-6	Time Evolution of Alcoholic SP1•HCl Solution Absorbance at 526 nm, Following UV Irradiation. Inset: $\ln (A/A_0)$ Versus Decay Time	78
4-1	Chemical Structure of Photochromic SP1, SP2, SP3 and SP4 Compounds....	81
4-2	The Absorption Spectra Changes of SP3 in Acidic Isopropanol Solutions at Different HCl Activities	82
4-3	The Absorption Changes of SP3 in Basic Isopropanol Solutions at Different Sodium Hydroxide Concentrations.....	83
4-4	Absorption Intensity Changes of SP3•HCl with Various 450 nm Irradiation Times.....	85
4-5	The Absorption Spectra Change of Basic Isopropanol Solution of SP3 with Various Irradiation Time by 365 nm Light.....	86
4-6	Proposed Mechanistic Scheme of Acidichromism for SP3 and SP4 Behavior in Isopropanol Solutions.....	88
5-1	Fluorescence Emission and Excitation Spectra of Alcoholic SP1 Solution	94
5-2	Fluorescence Emission and Excitation Spectra in Acidified SP1 Solution.....	95
5-3	Fluorescence Emission Spectra of SP1 in Isopropanol Solution at Different HCl/SP1 Value ($\lambda_{ex} = 370$ nm).....	97
5-4	Fluorescence Emission Spectra of SP1, SP1•HCl and PMC1•HCl in Isopropanol Solution.....	98
5-5	Photophysical and Photochromic Processes of SP1 and Its Product.....	99
6-1	Chemical Structure of Spiro(1,3,3-trimethylindolo-2,3'-naphth[1,2- <i>b</i>]-1,4-oxazine) (SP1) (I).....	104
6-2	2D DQFCOSY Spectrum of SP1	105
6-3	Tentative Assignment of ^1H by DQFCOSY	106
6-4	PFG-HMQC Spectrum of SP1.....	107
6-5	^{13}C Assignment by PFG-HMQC	108
6-6	HMBC Spectrum of SP1	109
6-7	Assignment of Proton and Carbon Atoms in the Spiro Ring from HMBC	110
6-8	Assignment of Proton and Carbon Atoms in the Oxazine Ring from HMBC ...	111
6-9	Conformational Structure of Oxazine Ring (Structure II)	114

6-10	Conformational Structure of SP1 (Structure III)	115
7-1	Chemical Structure of Di- <i>sec</i> -butoxyaluminoxytriethoxysilane (DBATES).....	121
7-2	Fluorescence Emission Spectra of SP1 Doped DBATES Sol, $\lambda_{ex} = 350$ nm ...	124
7-3	Fluorescence Emission Spectra of SP1 Doped DBATES Sol, $\lambda_{ex} = 540$ nm ...	125
7-4	An Equilibrium between SP1, PMC1 and Their Excited States.....	126
7-5	Absorption Spectra of SP1 Doped DBATES Sol before and after UV Irradiation.....	127
7-6	Fluorescence Emission Spectra of SP1 Doped Aluminosilicate Aged Gel at Different Excitation Wavelength	129
7-7	Absorption Spectra of SP1 Doped Aluminosilicate Aged Gel before and after UV Irradiation.....	131
7-8	Fluorescence Emission Spectra of SP1-Xerogel at Different Excitation Wavelength	133
8-1	Chemical Structure of 3-Glycidoxypropyltrimethoxysilane (GPTMS)	135
8-2	Ideal Structure of Epoxy-Diol Ormosil.....	136
8-3	Schematic Diagram of Experimental Setup for Time-Resolved Measurements of Photochromic SP1-Doped Gels.....	140
8-4	Absorption Spectra of SP1-Doped Epoxide Ormosil Gels before and after UV Irradiation.....	142
8-5	Time Evolution for SP1 Doped Air-Stable Epoxide Ormosil Xerogel Absorbance at 612 nm Following UV Irradiation. Inset: $\ln (A/A_0)$ Versus Decay Time	143
8-6	Fluorescence Emission Spectra of SP1 Doped Epoxide Ormosil Gels.....	145
8-7	Radiative Decay Curve of SP1 Doped Epoxide Ormosil Gel.....	146

CHAPTER 1

INTRODUCTION TO PHOTOCHROMIC EFFECT IN SPIROOXAZINES

Photochromism in organic molecules, which involves the switching between two states of the compound by optical means, has long been of interest from both theoretical and practical viewpoints. ^{1.1-1.4} Structural transformation is induced, in at least one direction, by photon excitation. Relaxation back to the initial state is usually correlated with a thermal activation process. Photochromic compounds are of great interest to materials researchers, as they can be used in photonic media as optical limiters, switches, or as optical information storage media.

Photochromic compounds have been widely studied for more than 100 years. ^{1.2,1.5,1.6} The first study of photochromic reactivity was reported by Fritsche in 1867. ^{1.7} In 1871, the first systematic study of photochromic compounds was published by Houston. ^{1.8} However, the term "photochromism" did not appear in the literature until it was suggested by Hirshberg in 1950. ^{1.3} The spiropyrans represent a family of photochromic compounds which have not been extensively utilized in device applications, as they have proven to suffer from poor cycling fatigue resistance. [Cycling fatigue is defined to occur when a photochromic compound is exposed in a cycling manner to light such that the photochromic transition is repeatedly induced, eventually leading to a loss of color changeability. It results from photo-induced decomposition of the photochromic species]. ^{1.1} Thus, photonic media based on photochromic spiropyrans have only been studied as a laboratory "curiosity". Recently a new class of photochromic compounds, the spirooxazines, has been the subject of renewed interest in the field. The spirooxazines have been found to be resistant to cycling fatigue, a characteristic which makes them

especially attractive from an applications perspective. ^{1,2} Assessment of spirooxazine crystal structure, study of the influence of the local environment on photochromic behavior, and the preparation of photonically-active solid state media based on spirooxazine dopants serve as major focus for the research described herein.

Spirooxazines comprise a collection of photochromic compounds which are reasonably well characterized, but poorly understood compared to the spiropyrans.

^{1,2,1.9,1.10} A dilute alcoholic solution containing spiro(1,3,3-trimethylindolo-2,3'-naphth[1,2-*b*]-1,4-oxazine), a particularly efficient photochromic compound, is colorless in the absence of a suitable photoexcitation source, but becomes intensely blue upon exposure to ultraviolet light. The intense blue color disappears rapidly when ultraviolet irradiation ceases. The colored form, also called the photomerocyanine (or PMC form), is reported to have a lifetime of about 0.5 seconds in common solvents. ^{1.9} Alcoholic spirooxazine solutions are also observed to be highly fluorescent, a characteristic which may be explored for the purpose of detailing guest-host interactions. Photochromism in spirooxazine compounds generally involves the UV-induced dissociation of the spiro C–O bond, from the oxazine ring, to form the open planar PMC structure. The normal chemical structure of the spiro(1,3,3-trimethylindolo-2,3'-naphth[1,2-*b*]-1,4-oxazine) (also referred as SP1 hereinafter), and the UV-induced photomerocyanine form, are shown in Figure 1-1. The photomerocyanine form is reported to be a mixture of four structurally distinguishable isomers (e.g., *cis* and *trans* conformations) in common solvents as shown in Figure 1-
2.1.11

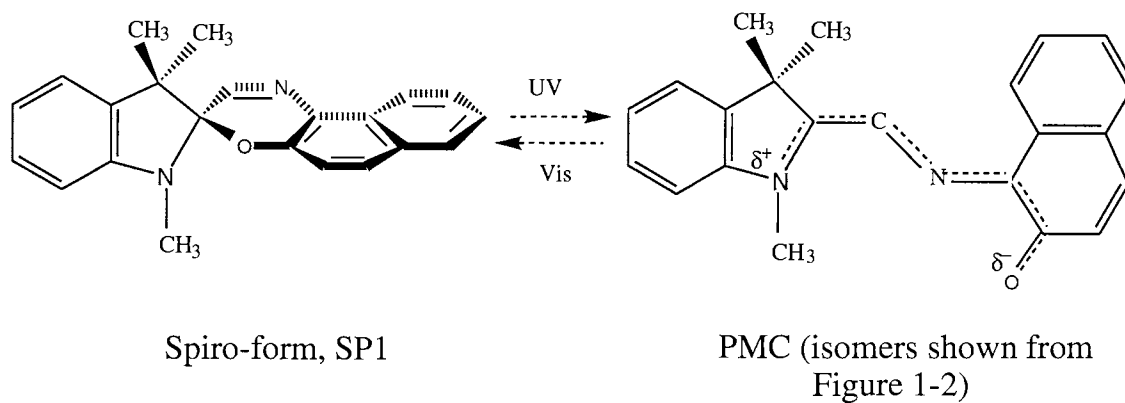


Figure 1-1. Chemical structure of SP1 (spiro-form) and the corresponding UV-induced photomerocyanine form (PMC form).

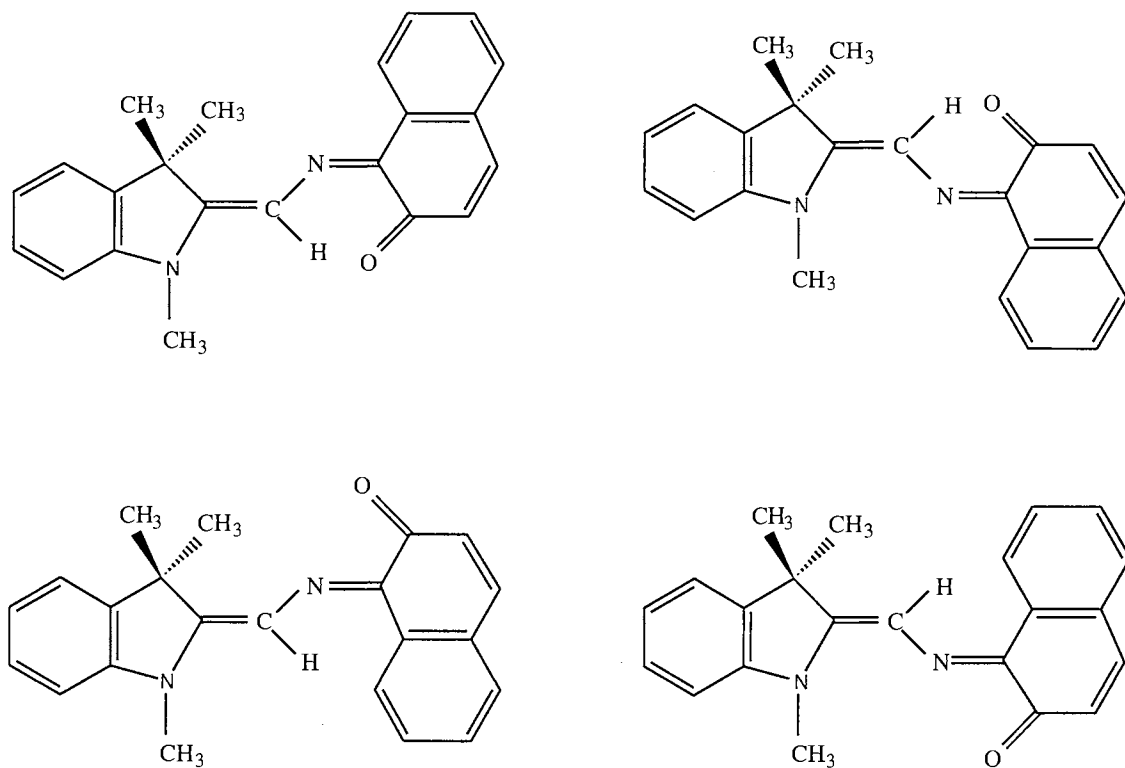


Figure 1-2. Four isomers of photomerocyanine form.

This research project was conducted in order to gain new understanding of the behavior of photochromic spirooxazine compounds and to provide a novel route for the preparation of solid state photonicly-active media. The previously described structural

transformations detailed in this section were used to interpret experimental results of the research in this dissertation. Effects included the characterization of photochromic and non-photochromic spirooxazine compounds using X-ray structure analysis and NMR methods. Subsequently, the behavior of photochromic spirooxazine compounds was investigated by absorption and luminescence spectroscopies. Finally, background information pertaining to known photochromic effects and the assessment of new optical properties found for spirooxazine compounds were used to promote the preparation and characterization of novel sol-gel derived photochromic media.

References

- 1.1 *Photochromism*, Edited by G. H. Brown, Wiley-Interscience, New York, 1971.
- 1.2 *Photochromism: Molecules and Systems.*, Edited by H. Durr and H. Bouas-Laurent, Elsevier, Amsterdam, 1990.
- 1.3 Y. Hirshberg, *Comp. Rend.* **231** (1950) 903.
- 1.4 Y. Hirshberg, *J. Am. Chem. Soc.* **68** (1956) 2304.
- 1.5 J. H. Day, *Chem. Rev.* **63** (1963) 65.
- 1.6 R. C. Bertelson, *Mol. Cryst. Liq. Cryst. Sci. and Technol. Sec. A* **246** (1994) 1.
- 1.7 M. Fritsche, *Comp. Rend.* **69** (1867) 1035.
- 1.8 E. J. Houston, *Chem. News* **24** (1871) 177, 188.
- 1.9 C. Bohne, M. G. Fan, Z. J. Li, Y. C. Liang, J. Lusztyk and J. C. Scaiano, *J. Photochem. Photobiol. A: Chem.* **66** (1992) 79.
- 1.10 A. Zelichenok, F. Buchholtz, J. Ratner, E. Fischer and V. Krongauz, *J. Photochem. Photobiol. A: Chem.* **77** (1994) 201.
- 1.11 S. Schneider, F. Baumann, U. Kluter and M. Melzig, *Ber. Bunsenges. Phys. Chem.* **91** (1987) 1225.

CHAPTER 2

CRYSTAL STRUCTURE ANALYSIS OF PHOTOCROMIC SPIROOXAZINE COMPOUNDS AND NON-PHOTOCROMIC THIAZOLINOSPIROOXAZINE COMPOUNDS

2.1. Introduction

The fundamental relationship between chemical structure and photochromic behavior is of interest to researchers in the field.^{2.1,2.2} Figure 2-1 shows the mechanism of photochromism in spirooxazine compounds in more detail. Spirooxazine compounds (spiro form *A* shown in Figure 2-1) in appropriate solutions undergo a reversible color change under the influence of UV irradiation, as shown in Figure 1-1. NMR evidence^{2.3} supports the thesis that photochromism in these systems involves UV-induced dissociation of the oxazine's spiro C–O bond, to form the planar PMC structure, which occurs in at least four isomeric forms. Form (*B*) is stabilized by electron pair donation from the adjacent nitrogen atom (as shown in form *C*). Electron delocalization over an extended range occurs when the structural framework is planar as shown in form *D*. Return to the colorless spiro form (*A*) is driven by heat or photon excitation.

The crystal structures of photochromic spirooxazine compounds have been studied by many researchers.^{2.4-2.6} These investigators have analyzed structures of spirooxazines and its derivatives, and have identified specific details which might presage the photochromic *vs.* non-photochromic behavior found in simple solutions. Although extensions to solution behavior from solid state structural detail is questionable (due to the unclear role solvation might play in the mechanism of C–O bond breaking), it is useful to assess bond lengths and bond angles in the terms of their fundamental molecular influences on photochromic behavior. In Figure 2-1, electron withdrawing substituents are often

present at R4 and R6 in spirooxazines, which act to stabilize the molecule. R1 is normally a methyl group. According to the literature,^{2,5} there appears to be no special requirement for R3 and R5. When R2 is a bulky alkyl group, the lifetime of the colored PMC form has been reported to diminish significantly.^{2,4,2.5} The comparison of photochromic behavior of three spirooxazine compounds ($Z = (\text{CH}_3)_2\text{C}$, $X = \text{N}$) in which $R_2 = \text{H}$ with their non-photochromic counterparts in which $R_2 = \text{CH}_3$ suggests that steric strain in the planar state (conformation *C* in Figure 2-1) arising from group R2 generally increases the rate of return to the twisted form (*A* in Figure 2-1).^{2.7} Thiazo derivatives, however, do not necessarily follow this trend. 3-Ethyl-8-methyl-6-nitro-2H-1-benzopyran-2-spiro-2'-(3'-methylthiazolidine), for example, is photochromic even though there exists an ethyl substituent at the R2-equivalent position.^{2.8} This compound (represented as example *E* in Figure 2-2) represents the only previously reported structure of a spirooxazine-type compound with $Z = \text{S}$ ($R_1 = \text{CH}_3$, $R_4 = \text{NO}_2$, $R_6 = \text{OCH}_3$, $R_3, R_5 = \text{H}$, $X = \text{CH}$, unsubstituted aromatic ring labeled # not present).

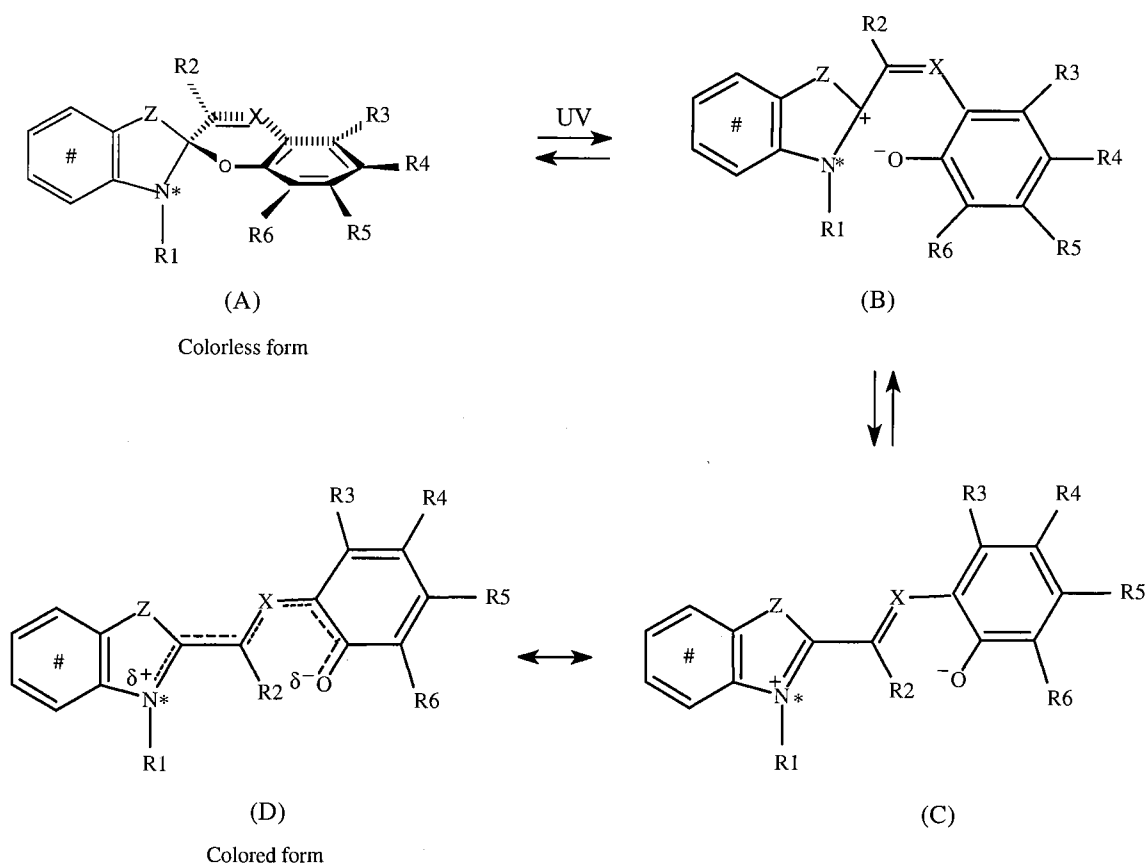
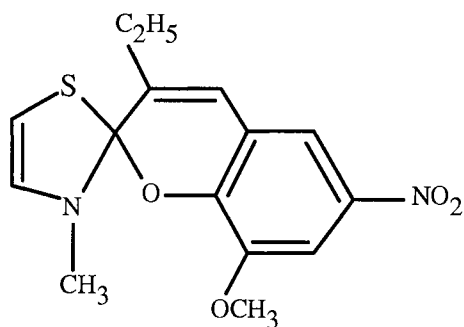


Figure 2-1. The mechanism of photochromism in spirooxazine compounds.



Example E: photochromic

Figure 2-2. Example of photochromic thiazo compound

The crystallographic structures of five previously uncharacterized spirooxazine derivatives, including three thiazo-types, have been determined. The bond lengths and

bond angles in these compounds have been probed in relation to the fundamental influence of bond nature on photochromism in spirooxazines. This work represents a logical extension of that performed by other researchers, who have examined bond lengths, especially those at the spiro carbon position. It has been reported that photochromic spirooxazine compounds have longer and thus weaker C–O bonds and shorter C(9)–N(8) distances, an omen of donation of the unshared pair on nitrogen towards the spiro carbon atom.^{2.9} These observations reflect facilitation of C–O bond breakage^{2.10} In general, photochromic spirooxazine compounds possess C(9)–O(22) bond lengths of 1.46 Å or greater, and C(9)–N(8) bond lengths of 1.425(6)–1.434(3) Å or shorter.^{2.9} Similarly, the sum of the bond angles at *N*(*) has been examined for evidence that an *sp*³ hybridized (angle total 3 × 109° or 327°) nitrogen atom tends towards a more stable tetrahedral orientation, whereas planar or *sp*² hybridized (angle total 360°) geometry promotes electron pair donation with inherent stabilization of the cationic species seen in structure *C* of Figure 2-1. Thus, bond angle totals approach 360° at *N*(*) suggest potential photochromism. Although photochromic spirooxazine compounds have previously been characterized by X-ray analysis, there is no reported description of the relationship between crystal structure and photochromism for thiazolinospirooxazine compounds (where Z = S in Figure 2-1).

The research presented in this chapter includes structural analysis of three benzothiazolinospirooxazines which do not display photochromism; 1-methylbenzothiazolinospiro-2,3'-(2'-methyl-[3H]phenanthro[9,10-*b*][1,4]oxazine) (Structure I, Figure 2-3), 1-methylbenzothiazolinospiro-2,3'-(2'-methyl-[3H]naphth [2,1-*b*][1,4]oxazine) (II, Figure 2-4) and 1-methylbenzothiazolinospiro-2,3'-(2'-methyl-9'-methoxy-[3H]naphth [2,1-*b*][1,4]oxazine) (III, Figure 2-5). Two previously uncharacterized photochromic spirooxazine compounds, spiro(1,3,3-trimethyl-2'-methylindolo-2,3'-naphth[1,2-*b*]-1,4-oxazine) (IV, Figure 2-6) and spiro(1,3,3-trimethyl-indolo-9'-methoxy-2,3'-naphth[1,2-*b*]-1,4-oxazine) (V, Figure 2-7) have also been

studied. Each compound was characterized using single crystal X-ray methods. The purpose of these studies was: (1) to report the single crystal structures, including bond angles and lengths, for the previously uncharacterized spirooxazine analogues, and (2) to examine the influences of selected substitutions on bond angles and bond lengths, two key parameters which determine photochromic behavior in such compounds. This work represents the first known discussion pertaining to the influence of heteroatomic substitution in the spiro ring on the photochromic behavior of spirooxazine analogues.

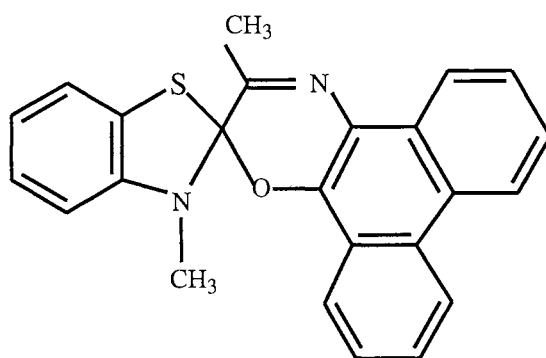


Figure 2-3. Chemical structure of 1-methylbenzothiazolinospiro-2,3'-(2'-methyl-[3H]phenanthro [9,10-*b*][1,4]oxazine) (Structure I).

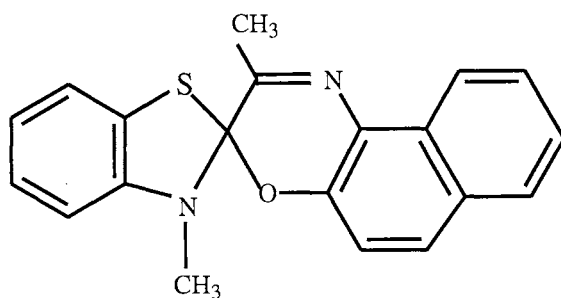


Figure 2-4. Chemical structure of 1-methylbenzothiazolinospiro-2,3'-(2'-methyl-[3H]naphth [2,1-*b*][1,4]oxazine) (Structure II).

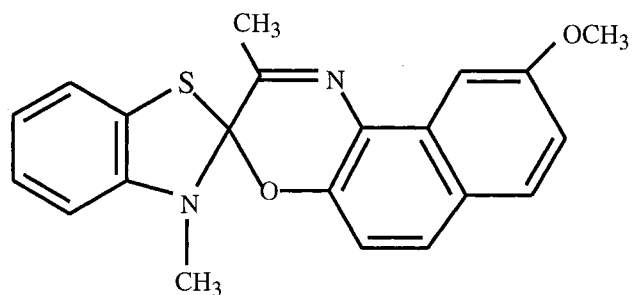


Figure 2-5. Chemical structure of 1-methylbenzothiazolinospiro-2,3'-(2'-methyl-9'-methoxy-[3H]naphth [2,1-*b*][1,4]oxazine) (Structure III).

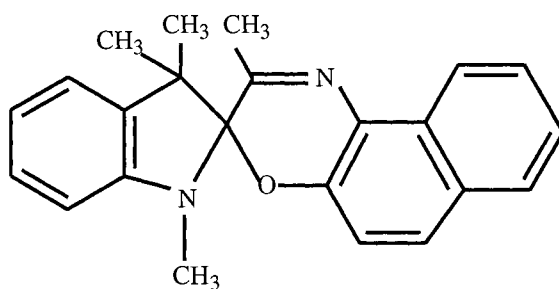


Figure 2-6. Chemical structure of spiro(1,3,3-trimethyl-2'-methylindolo-2,3'-naphth[1,2-*b*]-1,4-oxazine) (Structure IV)

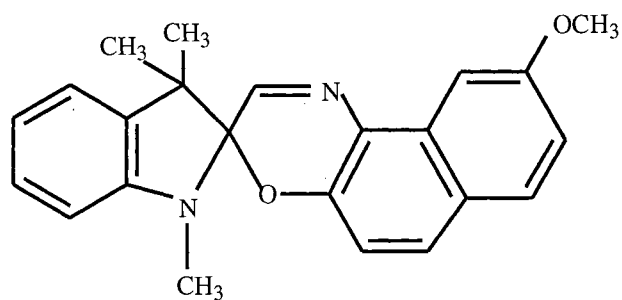


Figure 2-7. Chemical structure of spiro(1,3,3-trimethyl-indolo-9'-methoxy-2,3'-naphth[1,2-*b*]-1,4-oxazine) (Structure V).

2.II. Experimental Methods

2.II.A. *Synthesis of Title Compounds*

The title compounds were generously supplied by Prof. Meigong Fan, Institute of Photographic Chemistry, Chinese Academy of Sciences. The synthetic approach to the preparation of substituted spirooxazine compounds has been fully described elsewhere.^{2.11} The synthesis and IR characterization of compound II, 1-methylbenzothiazolinospiro-2,3'-(2'-methyl-[3H]naphth [2,1-*b*][1,4]oxazine), have previously been reported.^{2.12} The general synthesis of the thiazolinospirooxazine compounds has also been summarized elsewhere.^{2.13}

2.II.B. *Preparation of Single Crystals*

The solid sample was dissolved in a 1:1 mixture of chloroform and petroleum ether in a covered container at room temperature. The covers were perforated to allow solvent evaporation in the fume hood. Single crystals were subsequently obtained after a few days. Crystals with appropriate dimensions (approximately 0.2×0.2×0.2 mm) were mounted on a glass fiber for use in structural analysis by X-ray diffraction.

2.II.C. *Crystallography*

Single crystal specimens with appropriate dimensions were mounted on a Siemens P4 automated four-circle diffractometer equipped with a IBM-486DX computer using molybdenum radiation ($\lambda = 0.71073 \text{ \AA}$). Unit cell dimensions were determined using the centered angles for up to 100 independent strong reflections which were refined using least-squares methods by the automated procedure in XSCANS.^{2.14} The intensity data were collected at room temperature using a variable scan rate, a θ - 2θ scan mode and a scan

range of 0.6° below $K\alpha_1$ and 0.6° above $K\alpha_2$ to a maximum 2θ value (normally 50.0°). Backgrounds were measured at each end of the scan range for a combined time equal to the total scan time. The intensities of three standard reflections were remeasured after every 107 reflections.

2.III. Results and Discussion

Thiazolinospirooxazine compounds (I, II and III) are found to lack photochromic properties in solution, while substituent spirooxazine compounds IV and V are found to exhibit photochromic properties. All five compounds crystallize with two relatively planar moieties (atoms 1-9 and atoms 10-24) which display interplanar angles close to 90° . Table 2-1 shows the interplanar angle for all of the five compounds. It can be seen from the table that the interplanar angle for photochromic compounds (IV: 77.2° and V: 80.9°) is much smaller than that for non-photochromic compounds (I: 103.3° , II: 105.0° and III: 103.1°).

Table 2-1
Interplanar Angle ($^\circ$) of Compounds

Structure	Interplanar angle ($^\circ$)
I	93.3
II	105.0
III	103.1
IV	77.2
V	80.9

Since the mechanism of photochromism in spirooxazines involves cleavage of the spiro C–O bond, bond length to the spiro carbon (*C9* in all compounds) is of great importance. The measured bond length of the spiro carbon (*C9*) to sulfur *SI* (I, II and III) or to corresponding *CI*(IV and V), spiro C–O and spiro C–N of the five compounds is shown in Table 2-2. The C(9)–O(22) bond lengths of the non-photochromic thiazolinospirooxazine compounds I, II and III [1.422(6) Å to 1.437(5) Å] are significantly shorter than those characteristic of photochromic counterpart (1.463(3) Å, structure *E* in Figure 2-2), which is postulated to be a contributing factor in the loss of photochromic properties by the thiazolinospirooxazine compounds. Photochromic spirooxazine compounds (*e.g.* SP1) normally display long C–O at the spiro carbon (*C9*) atom; 1.454(3) Å for the C–O bond, and 1.436(3) Å for the C–N bond.^{2,9} For the two photochromic compounds characterized herein, the C–O and C–N bonds are longer than those for SP1, 1.459(11) Å to 1.504(12) Å for the C–O bond and 1.439(10) to 1.462(13) Å for the C–N bond (indicated in Table 2-2). The shorter C–N bond has also been found for non-photochromic thiazolinospirooxazine compounds comparing photochromic spirooxazine compounds (Table 2-2). The C–N bond shortening in non-photochromic compounds may be attributed to the presence of the sulfur and the contribution of its two lone pairs to the ring on the other side.

Table 2-2
Bond Length (Å) Related to Spiro C
vs. Photochromic Behavior

Structure	S(1)–C(9)	C(1)–C(9)	C(9)–O(22)	C(9)–N(8)	Photochromic
I	1.838(5)		1.422(6)	1.402(6)	No
II	1.829(3)		1.430(4)	1.409(4)	No
III	1.845(4)		1.437(5)	1.429(5)	No
Example E	1.852(3)		1.469(3)	1.421(4)	Yes ^{2.7}
IV		1.510(15)	1.459(11)	1.439(10)	Yes
V		1.590(2)	1.504(12)	1.462(13)	Yes
SP1		1.548(3)	1.454(3)	1.436(3)	yes ^{2.6}

Table 2-3 shows the bond angle totals at nitrogen (*N8*) in the indoline ring. Non-photochromic compounds (I), (II) and (III) display considerable flattening at *N8*, 350.9(4)° for (I), 349.2(2)° for (II) and 350.9(2)° for (III) compared to 338.4° total reported for the photochromic counterpart (structure *E* in Figure 2-2). Photochromism is correlated with more *sp*³ hybridized (angle total 3 × 109° or 327°), while non-photochromic compounds exhibit more *sp*² type (angle total 360°). These results for thiazolino compounds do not agree with the previous report on spirooxazine compounds.^{2.9} Smaller bond angle totals are seen for the photochromic compounds, 347.9(2)° for (IV) and 345.3(2)° for (V) compared for photochromic SP1 [349.0(2)°].

Table 2-3
Bond Angle Totals at *N8* (°) vs. Photochromic Behavior

Structure	Bond Angle Totals (°)	Photochromic
I	350.9(4)	No
II	349.2(2)	No
III	350.9(2)	No
Example E	338.4	Yes ^{2.8}
IV	347.9(2)	Yes
V	345.3(2)	Yes
SP1	349.0(2)	yes ^{2.6}

Table 2-4 shows the bond lengths related to *S1* and *N8* atoms for thiazolino spirooxazine compounds (I), (II) and (III). Compounds (I) and (II) are bright red in color, suggesting significant amounts of bond delocalization involving sulfur, nitrogen and the adjacent aromatic ring. The bonds between the hetero atoms and this ring [S(1)–C(2) and N(8)–C(7)] are much shorter than those of the corresponding photochromic compound (example *E* in Figure 2-2), S(1)–C(2): 1.817, N(8)–C(7): 1.464. The shortness coupled with the relative planarity of bonds at *N8* suggests a degree of rehybridization at *S1* and *N8* to facilitate delocalization of their lone pairs. Thus, the ability of either hetero atom to stabilize a cation developing at the spirocarbon atom is severely reduced. In the corresponding thiazolino photochromic compound (structure *E* in Figure 2-2), which lacks

the aromatic ring adjacent to the hetero atoms, unshared pairs on *N* and *S* are available to stabilize the cation developing at the spiro carbon in the photochromic mechanism.

Table 2-4
Bond Length (Å) Related to *S1* and *N8* for Thiazolino Compounds

Structure	S(1)–C(2)	N(8)–C(7)	S(1)–C(9)	N(8)–C(9)
I	1.743(5)	1.385(7)	1.838(5)	1.402(6)
II	1.740(3)	1.388(4)	1.829(3)	1.409(4)
III	1.742(5)	1.398(6)	1.845(4)	1.429(5)
Example E	1.817(3)	1.464	1.852(3)	1.421(4) ^{2,8}

2.IV. Summary and Conclusions

The single crystal X-ray structures of three non-photochromic thiazolinospirooxazine derivatives and two photochromic spirooxazine derivatives have been determined. A fundamental correlation of the molecular structure and photochromic behavior has been obtained. The results suggest that thiazolinospiro derivatives' lack of photochromic behavior is due to hetero atom electron pair delocalization which reduces potential stabilization of a cationic intermediate. The accurate molecular and crystal structure given here could be used for theoretical studies which may give further information on the mechanism of photochromism.

2.V. References

- 2.1 *Photochromism*, Edited by G. H. Brown, Wiley-Interscience, New York, 1971.
- 2.2 *Photochromism: Molecules and Systems.*, Edited by H. Durr and H. Bouas-Laurent, Elsevier, Amsterdam, 1990.
- 2.3 A. Samat, J. Kister, F. Garnier, J. Metzger and R. Guglielmetti, *Bull. Soc. Chim. France* **T11-12** (1975) 2627.
- 2.4 R. Guglielmetti, M. Mosse, J. C. Metras and J. Metzger, *J. Chim. Phys.* **65** (1968) 454.
- 2.5 F. Mientienne, A. Samat, R. Guglielmetti, F. Garnier, J. E. Dubois and J. Metzger, *J. Chim. Phys.* **70(3)** (1973) 544.
- 2.6 R. Millini, G. Del Piero, P. Allegrini and L. Crisci, *Acta Cryst.* **C47** (1991) 2567.
- 2.7 W. Clegg, N. C. Norman, T. Flood, L. Sallans, W. S. Kwak, P. L. Kwiatowski and J. G. Lasch, *Acta Cryst.* **C47** (1991) 817.
- 2.8 E. Miler-Srenger, R. Guglielmetti, *Acta Cryst.* **C40** (1984) 2050.
- 2.9 Y. T. Osano, K. Mitsuhashi, S. Maeda and T. Matsuzaki, *Acta Cryst.* **C47** (1991) 2137.
- 2.10 R. Millini, G. Del Piero, P. Allegrini, V. Malatesta and G. Castaldi, *Acta Cryst.* **C49** (1993) 1205.
- 2.11 X. Y. Zhang, S. Jin, Y. F. Ming, Y. C. Liang, L. H. Yu, M. G. Fan, J. Luo, Z. H. Zuo and S. D. Yao, *J. Photochem. Photobiol. A: Chem.* **80** (1994) 221.
- 2.12 G. Arnold and G. Paal, *Tetrahedron* **27** (1971) 1699.
- 2.13 X. D. Sun, Y. C. Liang, M. G. Fan, E. T. Knobbe and E. M. Holt *Acta Cryst.* **C** (in press).
- 2.14 XSCANS Users Manual, Siemens Analytical X-ray Instruments, Inc., Madison, Wisc., (1991).

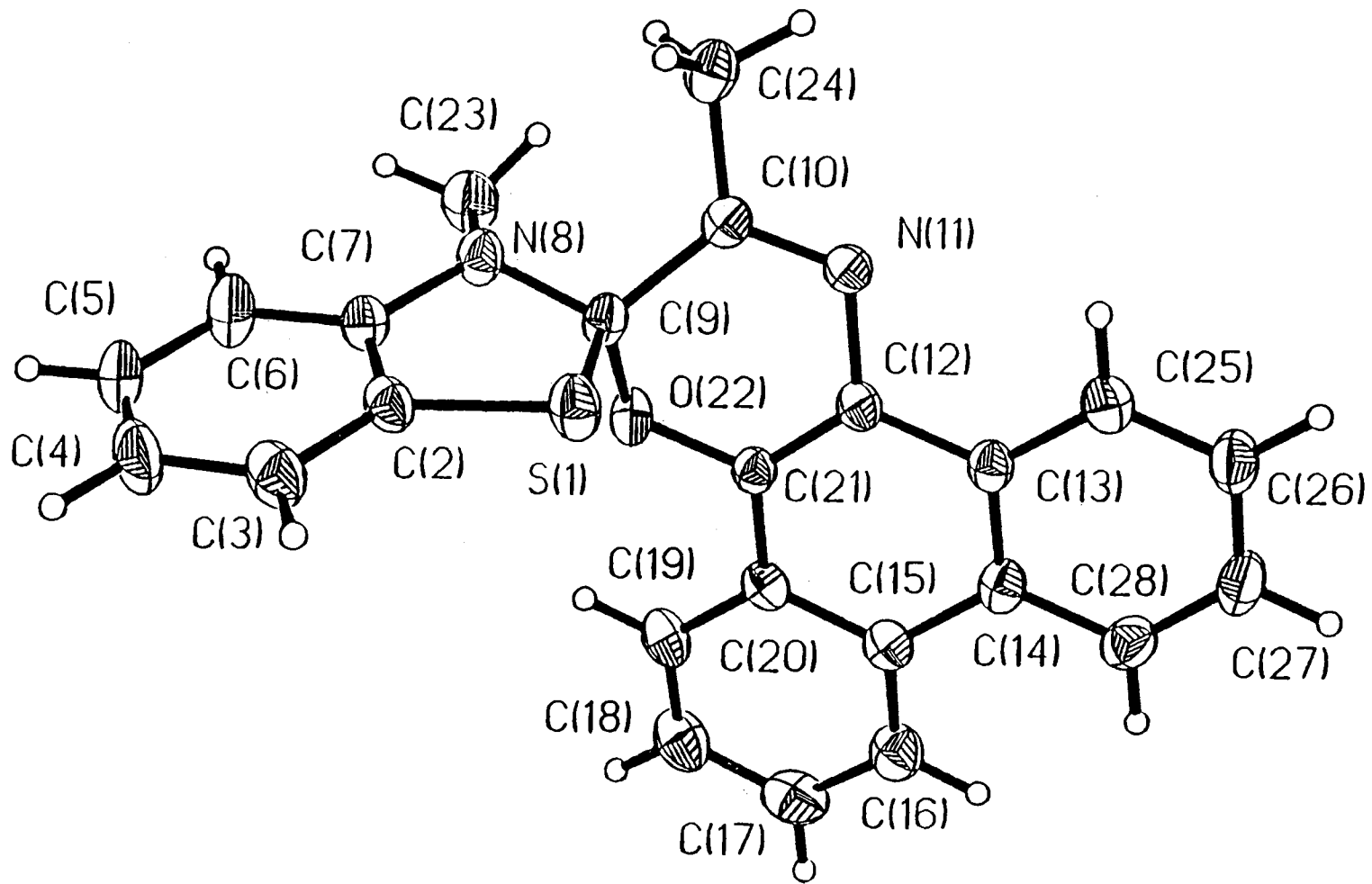


Figure 2-8 Projection View of I

Table 2-5
Crystal Data for Compound I

Empirical Formula	C ₂₄ H ₁₈ N ₂ O S
Color; Habit	red cube
Crystal size (mm)	0.2 x 0.2 x 0.2
Crystal System	Monoclinic
Space Group	P2 ₁ /n
Unit Cell Dimensions	$a = 6.286(3) \text{ \AA}$ $b = 12.033(5) \text{ \AA}$ $c = 24.523(14) \text{ \AA}$ $\beta = 95.31(4)$
Volume	1846.9(16) \AA^3
Z	4
Formula weight	382.5
Density (calc.)	1.375 Mg/m ³
Absorption Coefficient	0.193 mm ⁻¹
F(000)	800

Table 2-6

Atomic Coordinates ($\times 10^4$) and Equivalent Isotropic
Displacement Coefficients ($\text{\AA}^2 \times 10^3$) for Compound I

Atom	x	y	z	U(eq)
S(1)	2752(2)	2757(1)	1109(1)	51(1)
C(2)	1293(9)	3979(4)	992(2)	44(2)
C(3)	1718(10)	5005(5)	1225(3)	59(2)
C(4)	344(12)	5856(5)	1072(3)	73(3)
C(5)	-1386(13)	5687(5)	711(3)	75(3)
C(6)	-1823(11)	4664(5)	479(3)	66(3)
C(7)	-428(9)	3802(4)	619(2)	45(2)
N(8)	-541(7)	2743(3)	397(2)	46(2)
C(9)	630(8)	1956(4)	721(2)	37(2)
C(10)	1717(8)	1067(4)	419(2)	40(2)
N(11)	2291(7)	166(3)	660(2)	39(2)
C(12)	1620(8)	-28(4)	1180(2)	38(2)
C(13)	2515(8)	-947(4)	1491(2)	39(2)
C(14)	1634(8)	-1249(4)	1969(2)	42(2)
C(15)	-190(8)	-650(4)	2141(2)	41(2)
C(16)	-1193(10)	-941(5)	2596(3)	56(2)
C(17)	-2943(11)	-392(6)	2738(3)	66(3)
C(18)	-3779(10)	478(5)	2421(3)	64(3)
C(19)	-2812(9)	794(4)	1976(3)	50(2)
C(20)	-1020(8)	249(4)	1824(2)	38(2)

Table 2-6 (Continued)

C(21)	30(8)	555(4)	1361(2)	36(2)
O(22)	-765(5)	1457(3)	1074(2)	45(1)
C(23)	-2478(9)	2387(5)	85(3)	61(2)
C(24)	2247(9)	1267(4)	-151(2)	53(2)
C(25)	4251(9)	-1538(4)	1330(3)	50(2)
C(26)	5107(9)	-2407(5)	1624(3)	58(2)
C(27)	4237(10)	-2703(5)	2095(3)	61(2)
C(28)	2551(9)	-2145(5)	2270(2)	53(2)

* Equivalent isotropic U defined as one third of the trace of the orthogonalized U_{ij} tensor

Table 2-7
Bond Lengths (Å) for Compound I

S(1)-C(2)	1.743 (5)	S(1)-C(9)	1.838 (5)
C(2)-C(3)	1.376 (8)	C(2)-C(7)	1.367 (8)
C(3)-C(4)	1.369 (9)	C(4)-C(5)	1.354 (11)
C(5)-C(6)	1.372 (9)	C(6)-C(7)	1.380 (8)
C(7)-N(8)	1.385 (7)	N(8)-C(9)	1.402 (6)
N(8)-C(23)	1.441 (7)	C(9)-C(10)	1.501 (7)
C(9)-O(22)	1.422 (6)	C(10)-N(11)	1.272 (7)
C(10)-C(24)	1.487 (8)	N(11)-C(12)	1.399 (7)
C(12)-C(13)	1.429 (7)	C(12)-C(21)	1.331 (7)
C(13)-C(14)	1.388 (8)	C(13)-C(25)	1.391 (8)
C(14)-C(15)	1.450 (8)	C(14)-C(28)	1.400 (8)
C(15)-C(16)	1.377 (9)	C(15)-C(20)	1.405 (7)
C(16)-C(17)	1.356 (9)	C(17)-C(18)	1.380 (9)
C(18)-C(19)	1.350 (10)	C(19)-C(20)	1.384 (8)
C(20)-C(21)	1.413 (8)	C(21)-O(22)	1.363 (6)
C(25)-C(26)	1.353 (8)	C(26)-C(27)	1.370 (9)
C(27)-C(28)	1.356 (9)		

Table 2-8
Bond Angles (°) for Compound I

C(2)-S(1)-C(9)	90.7(2)	S(1)-C(2)-C(3)	127.5(4)
S(1)-C(2)-C(7)	110.5(4)	C(3)-C(2)-C(7)	121.9(5)
C(2)-C(3)-C(4)	117.6(6)	C(3)-C(4)-C(5)	121.0(6)
C(4)-C(5)-C(6)	121.6(6)	C(5)-C(6)-C(7)	118.2(6)
C(2)-C(7)-C(6)	119.6(5)	C(2)-C(7)-N(8)	114.5(5)
C(6)-C(7)-N(8)	125.8(5)	C(7)-N(8)-C(9)	113.1(4)
C(7)-N(8)-C(23)	119.5(4)	C(9)-N(8)-C(23)	118.3(4)
S(1)-C(9)-N(8)	104.9(3)	S(1)-C(9)-C(10)	106.7(3)
N(8)-C(9)-C(10)	116.1(4)	S(1)-C(9)-O(22)	111.4(3)
N(8)-C(9)-O(22)	108.1(4)	C(10)-C(9)-O(22)	109.5(4)
C(9)-C(10)-N(11)	120.0(5)	C(9)-C(10)-C(24)	120.0(4)
N(11)-C(10)-C(24)	119.8(5)	C(10)-N(11)-C(12)	118.0(4)
N(11)-C(12)-C(13)	118.6(5)	N(11)-C(12)-C(21)	121.0(5)
C(13)-C(12)-C(21)	120.0(5)	C(12)-C(13)-C(14)	119.0(5)
C(12)-C(13)-C(25)	121.6(5)	C(14)-C(13)-C(25)	119.4(5)
C(13)-C(14)-C(15)	120.2(5)	C(13)-C(14)-C(28)	118.0(5)
C(15)-C(14)-C(28)	121.8(5)	C(14)-C(15)-C(16)	123.0(5)
C(14)-C(15)-C(20)	119.0(5)	C(16)-C(15)-C(20)	118.0(5)
C(15)-C(16)-C(17)	121.9(6)	C(16)-C(17)-C(18)	120.0(7)
C(17)-C(18)-C(19)	119.5(6)	C(18)-C(19)-C(20)	121.5(5)
C(15)-C(20)-C(19)	119.0(5)	C(15)-C(20)-C(21)	117.9(5)
C(19)-C(20)-C(21)	123.0(5)	C(12)-C(21)-C(20)	123.4(5)
C(12)-C(21)-O(22)	119.9(5)	C(20)-C(21)-O(22)	116.5(4)

Table 2-8 (Continued)

C(9)-O(22)-C(21)	115.7(4)	C(13)-C(25)-C(26)	121.8(6)
C(25)-C(26)-C(27)	118.7(6)	C(26)-C(27)-C(28)	121.4(6)
C(14)-C(28)-C(27)	120.7(6)		

Table 2-9

Anisotropic Displacement Coefficients ($\text{\AA}^2 \times 10^3$) for Compound I

Atom	U ₁₁	U ₂₂	U ₃₃	U ₁₂	U ₁₃	U ₂₃
S(1)	49(1)	36(1)	66(1)	-1(1)	-11(1)	-9(1)
C(2)	51(3)	31(3)	53(4)	-5(3)	15(3)	-5(3)
C(3)	69(4)	38(3)	70(5)	-11(3)	11(4)	-12(3)
C(4)	103(6)	28(3)	90(6)	1(4)	25(5)	-5(3)
C(5)	106(6)	38(4)	81(6)	25(4)	12(5)	8(4)
C(6)	73(5)	42(3)	82(5)	13(3)	2(4)	6(3)
C(7)	54(3)	34(3)	47(4)	0(3)	6(3)	-1(3)
N(8)	53(3)	31(2)	51(3)	-2(2)	-9(2)	-3(2)
C(9)	38(3)	30(3)	42(3)	0(2)	-3(2)	2(2)
C(10)	42(3)	35(3)	42(3)	-7(2)	-2(2)	-1(3)
N(11)	46(3)	32(2)	38(3)	-3(2)	-1(2)	-5(2)
C(12)	41(3)	28(3)	44(4)	-3(2)	5(3)	-4(2)
C(13)	42(3)	29(3)	46(4)	-2(2)	1(3)	-2(2)
C(14)	42(3)	29(3)	53(4)	-8(2)	-4(3)	-1(3)
C(15)	42(3)	34(3)	48(4)	-10(2)	2(3)	-5(3)
C(16)	62(4)	46(3)	62(5)	-5(3)	10(4)	2(3)
C(17)	73(5)	68(4)	63(5)	-20(4)	30(4)	-3(4)
C(18)	55(4)	58(4)	82(6)	-2(3)	27(4)	-9(4)
C(19)	43(3)	39(3)	70(4)	-3(3)	11(3)	-11(3)
C(20)	33(3)	34(3)	48(4)	-7(2)	5(3)	-9(3)
C(21)	39(3)	29(3)	39(3)	-1(2)	0(3)	-3(2)

Table 2-9 (Continued)

O(22)	43(2)	34(2)	60(3)	6(2)	6(2)	5(2)
C(23)	64(4)	51(4)	65(4)	-3(3)	-14(3)	-12(3)
C(24)	56(4)	39(3)	62(4)	-5(3)	2(3)	3(3)
C(25)	50(4)	43(3)	57(4)	1(3)	4(3)	-4(3)
C(26)	51(4)	54(4)	67(4)	16(3)	-2(3)	0(3)
C(27)	65(4)	48(3)	69(5)	14(3)	-5(3)	11(4)
C(28)	63(4)	47(3)	48(4)	-4(3)	2(3)	7(3)

The anisotropic displacement exponent takes the form:

$$-2\pi^2 (h^2a^2U_{11} + \dots + 2hka^*b^* U_{12})$$

Table 2-10

Hydrogen Atom Coordinates ($\times 10^4$) and Isotropic
Displacement Coefficients ($\text{\AA}^2 \times 10^3$) for Compound I

Atom	x	y	z	U
H(3A)	2957	5119	1478	80
H(4A)	599	6580	1230	80
H(5A)	-2331	6298	617	80
H(6A)	-3061	4546	226	80
H(16A)	-636	-1553	2817	80
H(17A)	-3581	-598	3065	80
H(18A)	-5055	846	2512	80
H(19A)	-3371	1413	1761	80
H(23A)	-3119	3003	-117	80
H(23B)	-2155	1809	-164	80
H(23C)	-3453	2109	332	80
H(24A)	2936	622	-284	80
H(24B)	961	1416	-382	80
H(24C)	3189	1894	-156	80
H(25A)	4854	-1321	1000	80
H(26A)	6306	-2806	1507	80
H(27A)	4824	-3322	2306	80
H(28A)	1981	-2357	2604	80

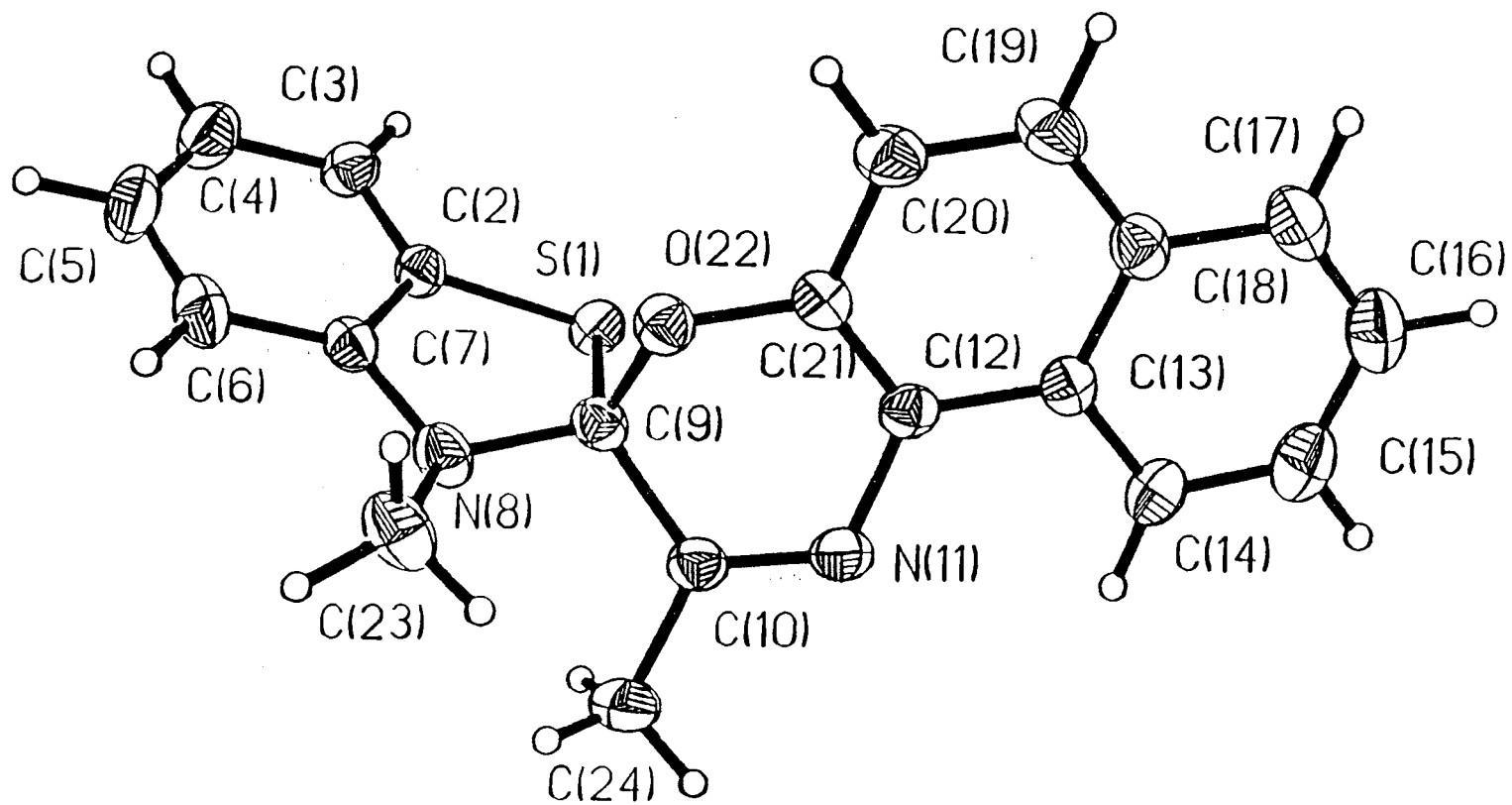


Figure 2-9 Projection View of II

Table 2-11
Crystal Data for Compound II

Empirical Formula	C ₂₀ H ₁₆ N ₂ O S
Color; Habit	red cube
Crystal size (mm)	0.2 x 0.2 x 0.2
Crystal System	Monoclinic
Space Group	P2 ₁ /n
Unit Cell Dimensions	$a = 10.237(3) \text{ \AA}$ $b = 13.364(7) \text{ \AA}$ $c = 12.296(14) \text{ \AA}$ $\beta = 102.16(3)$
Volume	1646.6(14) \AA^3
Z	4
Formula weight	332.4
Density (calc.)	1.341 Mg/m ³
Absorption Coefficient	0.205 mm ⁻¹
F(000)	696

Table 2-12
Atomic Coordinates ($\times 10^4$) and Equivalent Isotropic
Displacement Coefficients ($\text{\AA}^2 \times 10^3$) for Compound II

Atom	x	y	z	U(eq)
S(1)	9730(1)	677(1)	1132(1)	45(1)
C(2)	8491(3)	1436(2)	361(2)	40(1)
C(3)	7618(3)	1201(3)	-609(2)	49(1)
C(4)	6716(3)	1912(3)	-1103(3)	66(1)
C(5)	6708(4)	2838(3)	-629(3)	69(2)
C(6)	7574(3)	3074(3)	346(3)	59(1)
C(7)	8474(3)	2366(2)	848(3)	43(1)
N(8)	9404(2)	2457(2)	1844(2)	48(1)
C(9)	10461(3)	1767(2)	1933(2)	41(1)
C(10)	11081(3)	1416(2)	3091(2)	46(1)
N(11)	12263(3)	1064(2)	3319(2)	47(1)
C(12)	13007(3)	1087(2)	2486(2)	41(1)
C(13)	14198(3)	536(2)	2621(2)	42(1)
C(14)	14650(3)	-90(2)	3534(3)	53(1)
C(15)	15809(4)	-601(3)	3628(3)	68(1)
C(16)	16580(4)	-519(3)	2843(4)	77(2)
C(17)	16171(3)	76(3)	1952(3)	68(1)
C(18)	14983(3)	623(2)	1808(3)	50(1)
C(19)	14548(3)	1251(3)	895(3)	58(1)
C(20)	13380(3)	1764(3)	759(3)	54(1)

Table 2-12 (Continued)

C(21)	12622(3)	1675(2)	1564(2)	41(1)
O(22)	11464(2)	2206(2)	1430(2)	47(1)
C(23)	9718(4)	3443(2)	2314(3)	65(1)
C(24)	10246(3)	1390(3)	3938(3)	70(1)

* Equivalent isotropic U defined as one third of the trace of the orthogonalized U_{ij} tensor

Table 2-13
Bond Lengths (Å) for Compound II

S(1)-C(2)	1.740 (3)	S(1)-C(9)	1.829 (3)
C(2)-C(3)	1.368 (4)	C(2)-C(7)	1.381 (4)
C(3)-C(4)	1.374 (5)	C(4)-C(5)	1.369 (6)
C(5)-C(6)	1.369 (5)	C(6)-C(7)	1.373 (4)
C(7)-N(8)	1.388 (4)	N(8)-C(9)	1.409 (4)
N(8)-C(23)	1.447 (4)	C(9)-C(10)	1.507 (4)
C(9)-O(22)	1.430 (4)	C(10)-N(11)	1.273 (4)
C(10)-C(24)	1.480 (5)	N(11)-C(12)	1.400 (4)
C(12)-C(13)	1.404 (4)	C(12)-C(21)	1.366 (4)
C(13)-C(14)	1.398 (4)	C(13)-C(18)	1.413 (5)
C(14)-C(15)	1.352 (5)	C(15)-C(16)	1.375 (7)
C(16)-C(17)	1.347 (6)	C(17)-C(18)	1.398 (5)
C(18)-C(19)	1.398 (5)	C(19)-C(20)	1.358 (5)
C(20)-C(21)	1.385 (5)	C(21)-O(22)	1.362 (4)

Table 2-14
Bond Angles (°) for Compound II

C(2)-S(1)-C(9)	89.8(1)	S(1)-C(2)-C(3)	127.5(2)
S(1)-C(2)-C(7)	111.3(2)	C(3)-C(2)-C(7)	121.2(3)
C(2)-C(3)-C(4)	118.8(3)	C(3)-C(4)-C(5)	120.1(3)
C(4)-C(5)-C(6)	121.3(3)	C(5)-C(6)-C(7)	119.0(3)
C(2)-C(7)-C(6)	119.6(3)	C(2)-C(7)-N(8)	113.1(2)
C(6)-C(7)-N(8)	127.3(3)	C(7)-N(8)-C(9)	112.6(2)
C(7)-N(8)-C(23)	119.1(2)	C(9)-N(8)-C(23)	117.5(2)
S(1)-C(9)-N(8)	105.0(2)	S(1)-C(9)-C(10)	107.7(2)
N(8)-C(9)-C(10)	116.2(3)	S(1)-C(9)-O(22)	110.1(2)
N(8)-C(9)-O(22)	107.9(2)	C(10)-C(9)-O(22)	109.8(2)
C(9)-C(10)-N(11)	121.0(3)	C(9)-C(10)-C(24)	118.8(3)
N(11)-C(10)-C(24)	120.0(3)	C(10)-N(11)-C(12)	117.9(2)
N(11)-C(12)-C(13)	119.6(2)	N(11)-C(12)-C(21)	120.9(3)
C(13)-C(12)-C(21)	119.5(3)	C(12)-C(13)-C(14)	122.8(3)
C(12)-C(13)-C(18)	118.8(3)	C(14)-C(13)-C(18)	118.4(3)
C(13)-C(14)-C(15)	120.5(3)	C(14)-C(15)-C(16)	121.5(4)
C(15)-C(16)-C(17)	119.5(4)	C(16)-C(17)-C(18)	121.6(4)
C(13)-C(18)-C(17)	118.5(3)	C(13)-C(18)-C(19)	119.1(3)
C(17)-C(18)-C(19)	122.4(3)	C(18)-C(19)-C(20)	121.7(3)
C(19)-C(20)-C(21)	118.7(3)	C(12)-C(21)-C(20)	122.3(3)
C(12)-C(21)-O(22)	119.5(3)	C(20)-C(21)-O(22)	118.2(3)
C(9)-O(22)-C(21)	114.8(2)		

Table 2-15

Anisotropic Displacement Coefficients ($\text{\AA}^2 \times 10^3$) for Compound II

Atom	U ₁₁	U ₂₂	U ₃₃	U ₁₂	U ₁₃	U ₂₃
S(1)	54(1)	32(1)	45(1)	4(1)	3(1)	-5(1)
C(2)	43(2)	35(1)	42(2)	4(1)	11(1)	4(1)
C(3)	50(2)	53(2)	44(2)	-1(2)	8(2)	-2(2)
C(4)	54(2)	84(3)	57(2)	4(2)	2(2)	10(2)
C(5)	57(2)	70(3)	77(3)	19(2)	7(2)	24(2)
C(6)	55(2)	44(2)	81(2)	12(2)	23(2)	6(2)
C(7)	44(2)	39(2)	48(2)	4(1)	16(1)	-1(1)
N(8)	50(2)	39(1)	55(2)	4(1)	13(1)	-14(1)
C(9)	42(2)	41(2)	41(2)	0(1)	11(1)	-9(1)
C(10)	46(2)	56(2)	37(2)	-3(2)	9(1)	-10(1)
N(11)	48(2)	58(2)	37(1)	-5(1)	11(1)	-4(1)
C(12)	42(2)	43(2)	38(2)	-7(2)	7(1)	-5(1)
C(13)	38(2)	39(2)	48(2)	-6(1)	6(1)	-8(1)
C(14)	51(2)	50(2)	53(2)	-4(2)	1(2)	2(2)
C(15)	65(2)	59(2)	72(2)	6(2)	-3(2)	4(2)
C(16)	55(2)	75(3)	101(3)	19(2)	11(2)	-2(3)
C(17)	52(2)	77(3)	80(3)	8(2)	25(2)	-6(2)
C(18)	40(2)	52(2)	57(2)	-6(2)	12(1)	-7(2)
C(19)	57(2)	62(2)	63(2)	-1(2)	32(2)	5(2)
C(20)	60(2)	55(2)	52(2)	-5(2)	23(2)	8(2)
C(21)	40(2)	37(2)	49(2)	-4(1)	13(1)	-4(1)

Table 2-15 (Continued)

O(22)	49(1)	42(1)	52(1)	3(1)	14(1)	2(1)
C(23)	69(2)	45(2)	84(2)	2(2)	23(2)	-25(2)
C(24)	65(2)	106(3)	44(2)	5(2)	20(2)	-5(2)

The anisotropic displacement exponent takes the form:

$$-2\pi^2 (h^2a^2U_{11} + \dots + 2hka^*b^*U_{12})$$

Table 2-16

Hydrogen Atom Coordinates ($\times 10^4$) and Isotropic
Displacement Coefficients ($\text{\AA}^2 \times 10^3$) for Compound II

Atom	x	y	z	U
H(3A)	7628	551	-940	80
H(4A)	6104	1759	-1787	80
H(5A)	6057	3320	-975	80
H(6A)	7574	3729	666	80
H(14A)	14144	-160	4104	80
H(15A)	16108	-1014	4271	80
H(16A)	17409	-877	2930	80
H(17A)	16680	111	1380	80
H(19A)	15068	1311	333	80
H(20A)	13106	2191	125	80
H(23A)	10375	3368	2992	80
H(23D)	10072	3857	1807	80
H(23B)	8930	3749	2472	80
H(24D)	10720	1152	4648	80
H(24A)	9933	2058	4016	80
H(24B)	9499	960	3663	80

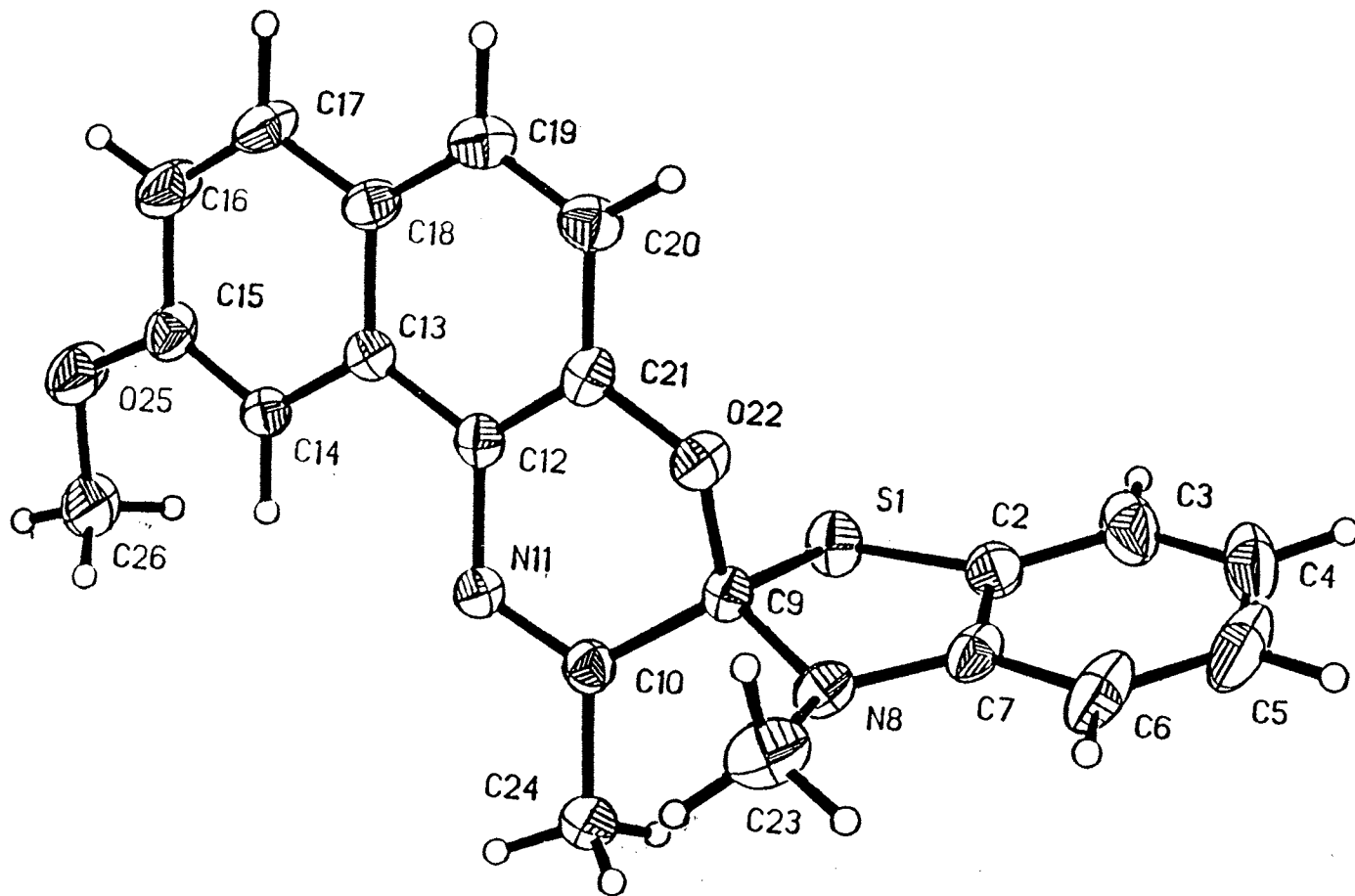


Figure 2-10 Projection View of III

Table 2-17
Crystal Data for Compound III

Empirical Formula	C ₂₁ H ₁₈ N ₂ O ₂ S
Color; Habit	colorless chunk
Crystal size (mm)	0.2 x 0.2 x 0.2
Crystal System	Orthorhombic
Space Group	Pccn
Unit Cell Dimensions	$a = 26.769(9) \text{ \AA}$ $b = 10.889(6) \text{ \AA}$ $c = 12.748(5) \text{ \AA}$
Volume	3713(3) \AA^3
Z	8
Formula weight	362.4
Density (calc.)	1.297 Mg/m ³
Absorption Coefficient	0.192 mm ⁻¹
F(000)	1520

Table 2-18

Atomic Coordinates ($\times 10^4$) and Equivalent Isotropic
Displacement Coefficients ($\text{\AA}^2 \times 10^3$) for Compound III

Atom	x	y	z	U(eq)
S(1)	5468(1)	182(1)	2551(1)	52(1)
C(2)	5967(2)	769(5)	1830(4)	49(2)
C(3)	6244(2)	191(6)	1056(4)	74(2)
C(4)	6630(3)	846(8)	600(5)	98(3)
C(5)	6746(2)	1996(8)	924(6)	96(4)
C(6)	6474(2)	2582(6)	1683(5)	73(2)
C(7)	6086(2)	1951(5)	2148(4)	47(2)
N(8)	5774(1)	2384(3)	2945(3)	44(1)
C(9)	5310(2)	1740(4)	3013(4)	36(2)
C(10)	5088(2)	1657(4)	4101(4)	42(2)
N(11)	4619(1)	1559(3)	4233(3)	42(1)
C(12)	4298(2)	1619(4)	3355(4)	36(2)
C(13)	3785(2)	1325(4)	3462(3)	36(2)
C(14)	3578(2)	907(4)	4419(4)	41(2)
C(15)	3089(2)	626(5)	4489(4)	53(2)
C(16)	2775(2)	797(5)	3616(4)	67(2)
C(17)	2962(2)	1185(5)	2690(4)	57(2)
C(18)	3471(2)	1467(4)	2572(4)	43(2)
C(19)	3676(2)	1891(4)	1621(4)	49(2)
C(20)	4167(2)	2161(4)	1530(4)	48(2)

Table 2-18 (Continued)

C(21)	4480(2)	2006(3)	2403(4)	40(2)
O(22)	4970(1)	2314(3)	2289(2)	44(1)
C(23)	5768(2)	3701(4)	3221(5)	69(2)
C(24)	5432(2)	1599(5)	5014(4)	59(2)
O(25)	2850(1)	189(4)	5358(3)	72(2)
C(26)	3154(2)	-192(5)	6215(4)	72(2)

* Equivalent isotropic U defined as one third of the trace of the orthogonalized U_{ij} tensor

Table 2-19

Bond Lengths (Å) for Compound III

S(1)-C(2)	1.742 (5)	S(1)-C(9)	1.845(4)
C(2)-C(3)	1.386 (8)	C(2)-C(7)	1.386 (7)
C(3)-C(4)	1.384 (10)	C(4)-C(5)	1.355 (12)
C(5)-C(6)	1.368 (9)	C(6)-C(7)	1.380 (7)
C(7)-N(8)	1.398 (6)	N(8)-C(9)	1.429 (5)
N(8)-C(23)	1.477 (6)	C(9)-C(10)	1.511 (7)
C(9)-O(22)	1.437 (5)	C(10)-N(11)	1.273 (6)
C(10)-C(24)	1.485 (7)	N(11)-C(12)	1.411 (6)
C(12)-C(13)	1.418 (6)	C(12)-C(21)	1.373 (7)
C(13)-C(14)	1.414 (6)	C(13)-C(18)	1.421 (7)
C(14)-C(15)	1.348 (6)	C(15)-C(16)	1.408 (7)
C(15)-O(25)	1.364 (6)	C(16)-C(17)	1.351 (8)
C(17)-C(18)	1.403 (6)	C(18)-C(19)	1.410 (7)
C(19)-C(20)	1.350 (7)	C(20)-C(21)	1.403 (7)
C(21)-O(22)	1.363 (5)	O(25)-C(26)	1.424 (6)

Table 2-20

Bond Angles (°) for Compound III

C(2)-S(1)-C(9)	90.4(2)	S(1)-C(2)-C(3)	128.2(4)
S(1)-C(2)-C(7)	111.3(4)	C(3)-C(2)-C(7)	120.5(5)
C(2)-C(3)-C(4)	117.7(6)	C(3)-C(4)-C(5)	121.3(6)
C(4)-C(5)-C(6)	121.7(6)	C(5)-C(6)-C(7)	118.2(6)
C(2)-C(7)-C(6)	120.7(5)	C(2)-C(7)-N(8)	112.8(4)
C(6)-C(7)-N(8)	126.5(5)	C(7)-N(8)-C(9)	113.5(4)
C(7)-N(8)-C(23)	120.4(4)	C(9)-N(8)-C(23)	117.0(3)
S(1)-C(9)-N(8)	103.4(3)	S(1)-C(9)-C(10)	109.2(3)
N(8)-C(9)-C(10)	115.1(4)	S(1)-C(9)-O(22)	109.9(3)
N(8)-C(9)-O(22)	107.3(3)	C(10)-C(9)-O(22)	111.5(3)
C(9)-C(10)-N(11)	120.9(4)	C(9)-C(10)-C(24)	118.6(4)
N(11)-C(10)-C(24)	120.4(4)	C(10)-N(11)-C(12)	119.4(4)
N(11)-C(12)-C(13)	120.1(4)	N(11)-C(12)-C(21)	120.0(4)
C(13)-C(12)-C(21)	119.8(4)	C(12)-C(13)-C(14)	122.4(4)
C(12)-C(13)-C(18)	118.2(4)	C(14)-C(13)-C(18)	119.5(4)
C(13)-C(14)-C(15)	120.7(4)	C(14)-C(15)-C(16)	119.8(5)
C(14)-C(15)-O(25)	126.1(4)	C(16)-C(15)-O(25)	114.0(4)
C(15)-C(16)-C(17)	120.7(4)	C(16)-C(17)-C(18)	121.5(5)
C(13)-C(18)-C(17)	117.7(4)	C(13)-C(18)-C(19)	119.4(4)
C(17)-C(18)-C(19)	122.9(4)	C(18)-C(19)-C(20)	121.7(4)
C(19)-C(20)-C(21)	119.1(4)	C(12)-C(21)-C(20)	121.8(4)
C(12)-C(21)-O(22)	120.6(4)	C(20)-C(21)-O(22)	117.5(4)
C(9)-O(22)-C(21)	115.7(3)	C(15)-O(25)-C(26)	117.1(4)

Table 2-21

Anisotropic Displacement Coefficients ($\text{\AA}^2 \times 10^3$) for Compound III

Atom	U_{11}	U_{22}	U_{33}	U_{12}	U_{13}	U_{23}
S (1)	59(1)	35(1)	63(1)	1(1)	9(1)	-4(1)
C (2)	48(3)	57(3)	44(3)	12(3)	-3(3)	4(3)
C (3)	73(4)	92(5)	56(4)	40(4)	11(3)	2(4)
C (4)	66(5)	173(8)	54(4)	57(6)	18(4)	29(6)
C (5)	37(3)	153(8)	98(6)	6(5)	8(4)	64(6)
C (6)	37(3)	85(4)	96(5)	1(3)	5(3)	42(4)
C (7)	32(2)	59(3)	49(3)	3(3)	-3(3)	24(3)
N (8)	41(2)	35(2)	56(3)	-5(2)	-3(2)	3(2)
C (9)	37(2)	29(3)	44(3)	1(2)	3(2)	-1(2)
C (10)	41(3)	40(3)	45(3)	1(2)	3(3)	-6(3)
N (11)	40(2)	45(2)	41(2)	3(2)	-2(2)	-3(2)
C (12)	39(3)	29(3)	41(3)	-3(2)	4(2)	-4(2)
C (13)	44(3)	25(2)	40(3)	-3(2)	2(2)	-1(2)
C (14)	38(3)	46(3)	40(3)	-2(2)	0(2)	-4(3)
C (15)	44(3)	60(4)	53(3)	2(3)	8(3)	13(3)
C (16)	37(3)	93(4)	70(4)	-14(3)	-1(3)	20(4)
C (17)	38(3)	71(4)	63(4)	-5(3)	-12(3)	11(3)
C (18)	43(2)	39(3)	48(3)	0(2)	-7(3)	4(3)
C (19)	54(3)	45(3)	49(4)	-9(3)	-9(3)	11(3)
C (20)	57(3)	47(3)	41(3)	-6(3)	-2(3)	10(3)

Table 2-21 (Continued)

C(21)	37(2)	29(2)	56(3)	-1(2)	4(3)	0(3)
O(22)	40(2)	44(2)	48(2)	-3(1)	-2(2)	12(2)
C(23)	68(4)	50(3)	89(5)	-6(3)	-15(3)	3(3)
C(24)	52(3)	83(4)	43(3)	0(3)	-2(3)	-2(3)
O(25)	47(2)	108(3)	63(2)	-4(2)	5(2)	26(2)
C(26)	62(3)	100(5)	54(4)	-3(4)	11(3)	18(4)

The anisotropic displacement exponent takes the form:

$$-2\pi^2 (h^2a^2U_{11} + \dots + 2hka*b*U_{12})$$

Table 2-22

Hydrogen Atom Coordinates ($\times 10^4$) and Isotropic
Displacement Coefficients ($\text{\AA}^2 \times 10^3$) for Compound III

Atom	x	y	z	U
H(3A)	6167	-638	857	80
H(4A)	6814	477	36	80
H(5A)	7026	2402	606	80
H(6A)	6553	3407	1893	80
H(14A)	3789	814	5023	80
H(16A)	2424	643	3692	80
H(17A)	2747	1259	2091	80
H(19A)	3460	1974	1024	80
H(20A)	4302	2461	881	80
H(23A)	6098	4035	3143	80
H(23B)	5542	4130	2768	80
H(23C)	5662	3792	3936	80
H(23D)	5783	4003	2531	80
H(23E)	5391	3905	3636	80
H(23F)	6135	3738	3616	80
H(24E)	5767	1634	4743	80
H(24F)	5392	802	5324	80
H(24A)	5245	1550	5655	80
H(24B)	5641	886	4948	80
H(24C)	5637	2323	5023	80

Table 2-22 (Continued)

H(24D)	5410	2251	5632	80
H(26A)	2946	-483	6775	80
H(26B)	3370	-843	5983	80
H(26C)	3353	484	6459	80

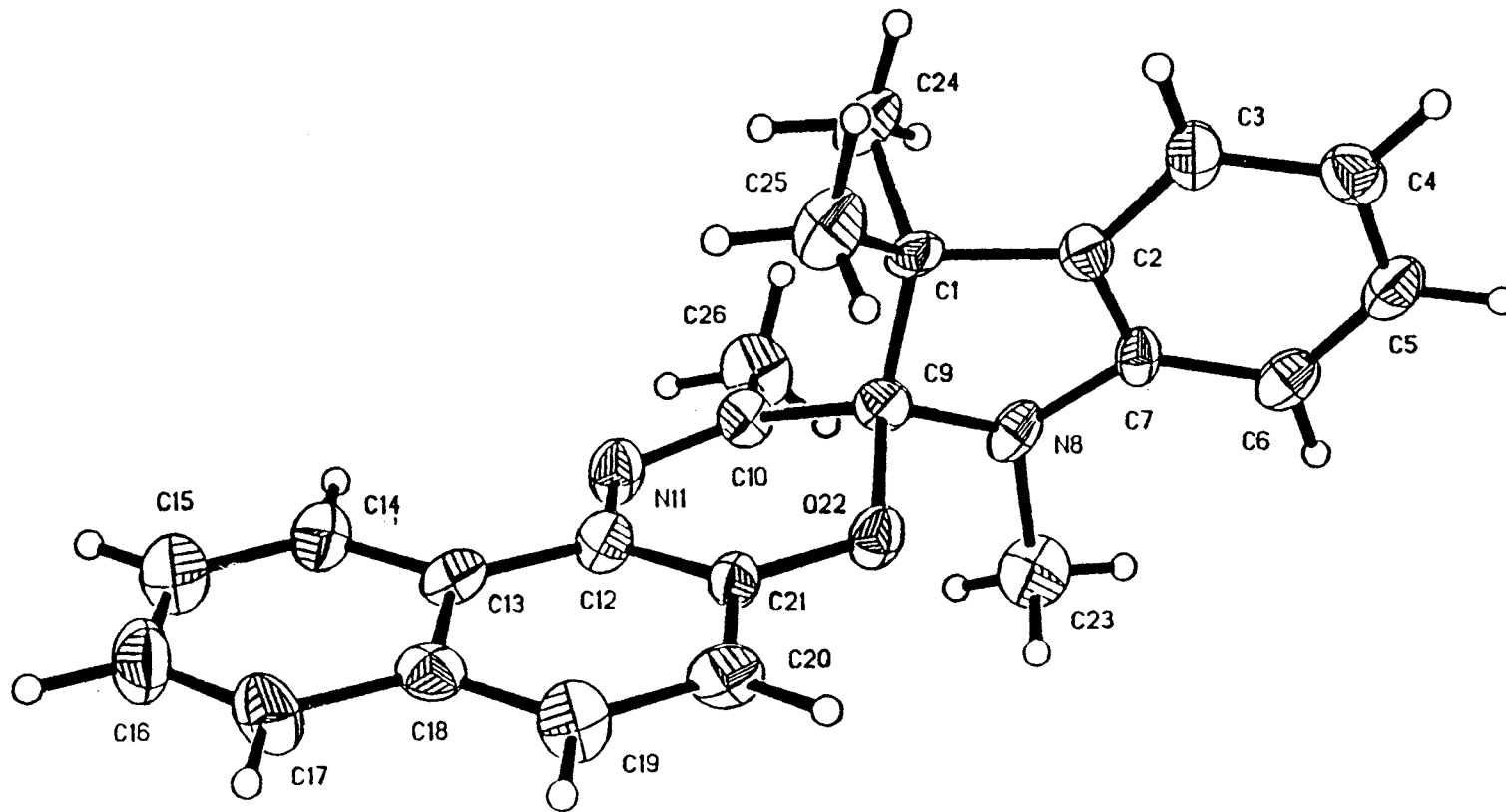


Figure 2-11 Projection View of IV

Table 2-23
Crystal Data for Compound IV

Empirical Formula	C ₂₃ H ₂₂ N ₂ O
Color; Habit	yellow plate
Crystal size (mm)	0.2 x 0.2 x 0.1
Crystal System	Monoclinic
Space Group	C2/c
Unit Cell Dimensions	$a = 26.564(16) \text{ \AA}$ $b = 8.321(5) \text{ \AA}$ $c = 16.222(10) \text{ \AA}$ $\beta = 97.47(4)^\circ$
Volume	3556(4) \AA^3
Z	8
Formula weight	342.4
Density (calc.)	1.279 Mg/m ³
Absorption Coefficient	0.079 mm ⁻¹
F(000)	1456

Table 2-24

Atomic Coordinates ($\times 10^4$) and Equivalent Isotropic
Displacement Coefficients ($\text{\AA}^2 \times 10^3$) for Compound IV

Atom	x	y	z	U(eq)
C(1)	3889(3)	4546(13)	-371(5)	40(3)
C(2)	3907(3)	5569(14)	376(5)	39(4)
C(3)	3712(3)	7032(14)	494(5)	49(4)
C(4)	3813(3)	7777(13)	1260(6)	54(4)
C(5)	4114(4)	7024(15)	1886(6)	56(4)
C(6)	4330(3)	5537(14)	1789(5)	49(4)
C(7)	4221(3)	4866(12)	1013(5)	36(4)
N(8)	4402(3)	3388(12)	749(4)	43(3)
C(9)	4078(3)	2959(13)	0(5)	43(4)
C(10)	4337(3)	1842(13)	-542(5)	39(4)
N(11)	4113(3)	712(11)	-995(4)	50(3)
C(12)	3602(3)	417(14)	-893(6)	45(4)
C(13)	3320(3)	-561(13)	-1470(5)	45(4)
C(14)	3499(4)	-1194(13)	-2174(6)	54(4)
C(15)	3213(4)	-2131(15)	-2713(6)	68(5)
C(16)	2725(5)	-2543(14)	-2588(6)	74(5)
C(17)	2533(3)	-2015(14)	-1900(7)	67(5)
C(18)	2827(4)	-1032(12)	-1325(5)	48(4)
C(19)	2637(3)	-428(14)	-616(6)	57(4)
C(20)	2908(3)	566(13)	-80(6)	54(4)

Table 2-24 (Continued)

C(21)	3392(3)	1031(12)	-242(5)	40(4)
O(22)	3667(2)	2047(9)	293(3)	44(2)
C(23)	4591(3)	2178(13)	1342(5)	66(4)
C(24)	4253(3)	5245(13)	-939(5)	61(4)
C(25)	3358(3)	4488(13)	-888(5)	61(4)
C(26)	4899(3)	2018(13)	-566(5)	68(5)

* Equivalent isotropic U defined as one third of the trace of the orthogonalized U_{ij} tensor

Table 2-25

Bond Lengths (Å) for Compound IV

C(1)-C(2)	1.476 (13)	C(1)-C(9)	1.510 (15)
C(1)-C(24)	1.534 (13)	C(1)-C(25)	1.545 (11)
C(2)-C(3)	1.346 (16)	C(2)-C(7)	1.372 (12)
C(3)-C(4)	1.384 (13)	C(4)-C(5)	1.361 (13)
C(5)-C(6)	1.381 (17)	C(6)-C(7)	1.372 (12)
C(7)-N(8)	1.407 (13)	N(8)-C(9)	1.439 (10)
N(8)-C(23)	1.438 (12)	C(9)-C(10)	1.505 (14)
C(9)-O(22)	1.459 (11)	C(10)-N(11)	1.291 (12)
C(10)-C(26)	1.505 (12)	N(11)-C(12)	1.409 (12)
C(12)-C(13)	1.386 (13)	C(12)-C(21)	1.358 (14)
C(13)-C(14)	1.396 (14)	C(13)-C(18)	1.415 (14)
C(14)-C(15)	1.333 (14)	C(15)-C(16)	1.381 (17)
C(16)-C(17)	1.360 (16)	C(17)-C(18)	1.401 (14)
C(18)-C(19)	1.409 (14)	C(19)-C(20)	1.340 (14)
C(20)-C(21)	1.400 (13)	C(21)-O(22)	1.355 (11)

Table 2-26

Bond Angles (°) for Compound IV

C(2)-C(1)-C(9)	101.8(7)	C(2)-C(1)-C(24)	108.6(8)
C(9)-C(1)-C(24)	111.6(8)	C(2)-C(1)-C(25)	113.2(8)
C(9)-C(1)-C(25)	114.9(8)	C(24)-C(1)-C(25)	106.7(6)
C(1)-C(2)-C(3)	131.7(8)	C(1)-C(2)-C(7)	108.9(9)
C(3)-C(2)-C(7)	119.1(8)	C(2)-C(3)-C(4)	120.0(8)
C(3)-C(4)-C(5)	119.3(10)	C(4)-C(5)-C(6)	122.7(9)
C(5)-C(6)-C(7)	115.3(8)	C(2)-C(7)-C(6)	123.6(9)
C(2)-C(7)-N(8)	110.0(8)	C(6)-C(7)-N(8)	126.5(8)
C(7)-N(8)-C(9)	106.5(7)	C(7)-N(8)-C(23)	120.8(7)
C(9)-N(8)-C(23)	120.6(9)	C(1)-C(9)-N(8)	104.5(8)
C(1)-C(9)-C(10)	117.4(7)	N(8)-C(9)-C(10)	112.2(7)
C(1)-C(9)-O(22)	111.1(7)	N(8)-C(9)-O(22)	104.2(6)
C(10)-C(9)-O(22)	106.7(8)	C(9)-C(10)-N(11)	124.8(8)
C(9)-C(10)-C(26)	119.0(8)	N(11)-C(10)-C(26)	116.2(9)
C(10)-N(11)-C(12)	116.0(8)	N(11)-C(12)-C(13)	117.9(9)
N(11)-C(12)-C(21)	121.8(8)	C(13)-C(12)-C(21)	120.3(9)
C(12)-C(13)-C(14)	124.2(9)	C(12)-C(13)-C(18)	118.8(9)
C(14)-C(13)-C(18)	116.9(9)	C(13)-C(14)-C(15)	122.2(10)
C(14)-C(15)-C(16)	120.9(10)	C(15)-C(16)-C(17)	120.1(10)
C(16)-C(17)-C(18)	119.9(10)	C(13)-C(18)-C(17)	120.0(9)
C(13)-C(18)-C(19)	118.4(9)	C(17)-C(18)-C(19)	121.6(9)
C(18)-C(19)-C(20)	122.0(9)	C(19)-C(20)-C(21)	118.6(9)
C(12)-C(21)-C(20)	121.5(9)	C(12)-C(21)-O(22)	119.3(8)

Table 2-26 (Continued)

C(20)-C(21)-O(22)	119.0(8)	C(9)-O(22)-C(21)	118.8(6)
-------------------	----------	------------------	----------

Table 2-27

Anisotropic Displacement Coefficients ($\text{\AA}^2 \times 10^3$) for Compound IV

Atom	U_{11}	U_{22}	U_{33}	U_{12}	U_{13}	U_{23}
C(1)	43(6)	45(7)	33(5)	-14(6)	13(4)	7(6)
C(2)	35(6)	42(8)	38(6)	-6(6)	-1(5)	-3(6)
C(3)	51(7)	51(9)	46(6)	-7(7)	11(5)	-11(6)
C(4)	60(7)	40(8)	67(7)	-6(7)	29(6)	0(7)
C(5)	57(7)	74(9)	38(6)	-16(8)	12(5)	-1(7)
C(6)	40(6)	67(9)	39(6)	-2(7)	3(5)	7(7)
C(7)	29(6)	45(8)	36(6)	-4(6)	11(5)	-12(6)
N(8)	31(5)	67(7)	29(4)	-4(5)	3(4)	1(5)
C(9)	37(6)	49(8)	41(6)	-26(6)	2(5)	0(6)
C(10)	29(6)	44(7)	47(6)	4(6)	13(5)	-2(6)
N(11)	46(5)	61(7)	46(5)	-6(5)	15(4)	-10(5)
C(12)	38(6)	56(8)	42(6)	-5(7)	6(5)	-2(6)
C(13)	43(6)	53(8)	39(6)	3(7)	6(5)	12(7)
C(14)	54(7)	58(9)	47(6)	0(6)	1(6)	-4(6)
C(15)	66(9)	71(10)	68(8)	-3(8)	8(7)	-11(7)
C(16)	86(10)	70(10)	57(8)	-6(8)	-18(7)	-15(7)
C(17)	50(7)	68(9)	78(7)	-27(7)	-7(6)	-11(8)
C(18)	50(8)	37(8)	55(7)	7(6)	-4(6)	11(6)
C(19)	36(6)	68(9)	70(7)	-2(7)	17(6)	-13(7)
C(20)	37(7)	64(9)	64(7)	-11(7)	24(5)	4(7)
C(21)	46(7)	40(8)	35(6)	-9(6)	11(5)	-5(5)

Table 2-27 (Continued)

O(22)	40(4)	58(5)	37(3)	-11(4)	11(3)	-6(4)
C(23)	51(7)	75(9)	71(7)	16(7)	-1(5)	5(8)
C(24)	64(7)	85(10)	36(5)	0(7)	15(5)	9(6)
C(25)	37(5)	89(9)	51(5)	0(7)	-17(4)	1(7)
C(26)	36(6)	80(9)	92(8)	-8(7)	22(5)	-11(8)

The anisotropic displacement exponent takes the form:

$$-2\pi^2 (h^2 a^2 U_{11} + \dots + 2hka^* b^* U_{12})$$

Table 2-28

Hydrogen Atom Coordinates ($\times 10^4$) and Isotropic
Displacement Coefficients ($\text{\AA}^2 \times 10^3$) for Compound IV

Atom	x	y	z	U
H(3A)	3508	7557	40	80
H(4A)	3671	8812	1353	80
H(5A)	4181	7531	2421	80
H(6A)	4546	5011	2228	80
H(14A)	3838	-927	-2271	80
H(15A)	3348	-2542	-3193	80
H(16A)	2521	-3207	-2984	80
H(17A)	2195	-2309	-1807	80
H(19A)	2306	-763	-509	80
H(20A)	2775	963	404	80
H(23A)	4797	2684	1800	80
H(23B)	4312	1635	1542	80
H(23C)	4792	1414	1085	80
H(24A)	4586	5313	-631	80
H(24B)	4261	4544	-1408	80
H(24C)	4144	6296	-1131	80
H(25A)	3262	5530	-1109	80
H(25B)	3365	3739	-1336	80
H(25C)	3117	4134	-535	80
H(26A)	5011	1227	-933	80

Table 2-28 (Continued)

H(26B)	4962	3073	-769	80
H(26C)	5081	1884	-19	80

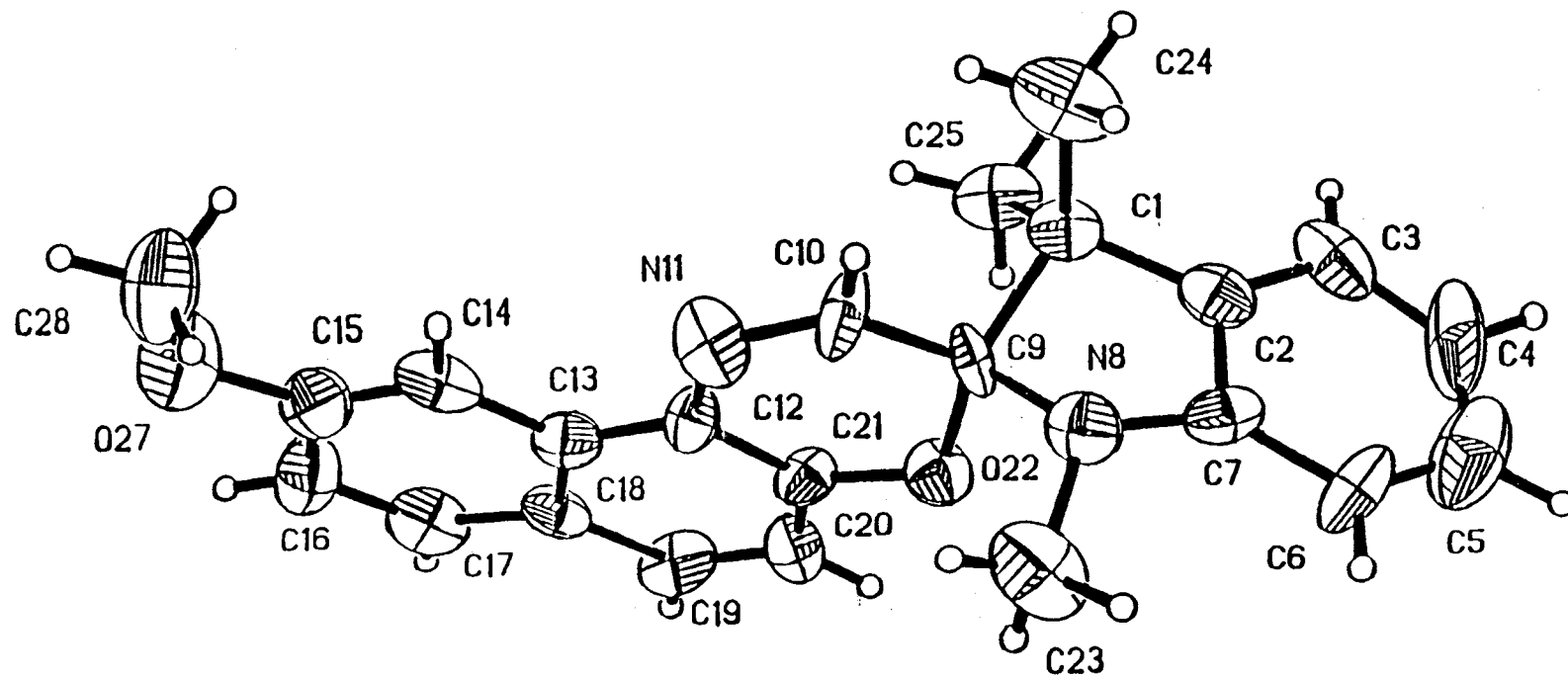


Figure 2-12 Projection View of V

Table 2-29

Crystal Data for Compound V

Empirical Formula	C ₂₃ H ₂₂ N ₂ O ₂
Color; Habit	red cube
Crystal size (mm)	0.1 x 0.1 x 0.1
Crystal System	Monoclinic
Space Group	P2 ₁ /a
Unit Cell Dimensions	$a = 6.286(3) \text{ \AA}, \alpha = 90^\circ$ $b = 12.033(5) \text{ \AA}, \beta = 95.31(4)^\circ$ $c = 24.523(14) \text{ \AA}, \gamma = 90^\circ$
Volume	1964(3) \AA^3
Z	4
Formula weight	358.43
Density (calc.)	1.212 Mg/m ³
Absorption Coefficient	0.078 mm ⁻¹
F(000)	760

Table 2-30

Atomic Coordinates ($\times 10^4$) and Equivalent Isotropic
Displacement Coefficients ($\text{\AA}^2 \times 10^3$) for Compound V

Atom	x	y	z	U(eq)
C(1)	5809(22)	5914(5)	1924(12)	62(4)
C(2)	7233(25)	6365(6)	1987(15)	75(5)
C(3)	7374(25)	6737(6)	1137(13)	86(6)
C(4)	8798(32)	7095(7)	1492(19)	127(9)
C(5)	10030(33)	7109(8)	2660(18)	138(9)
C(6)	9842(24)	6749(6)	3470(14)	90(6)
C(7)	8491(23)	6361(6)	3168(15)	69(4)
N(8)	8008(18)	5956(5)	3822(10)	72(4)
C(9)	7041(23)	5587(5)	2972(12)	55(4)
C(10)	5804(20)	5262(5)	3614(11)	76(5)
N(11)	5834(17)	4783(4)	3477(8)	77(4)
C(12)	7136(21)	4558(5)	2698(10)	51(4)
C(13)	7098(24)	4075(5)	2469(12)	61(4)
C(14)	5633(24)	3756(5)	2961(12)	77(5)
C(15)	5619(27)	3275(7)	2748(14)	80(5)
C(16)	6944(25)	3045(5)	2008(13)	92(6)
C(17)	8347(24)	3361(6)	1514(11)	88(6)
C(18)	8484(23)	3868(5)	1744(12)	66(4)
C(19)	9969(21)	4179(6)	1302(10)	78(5)
C(20)	9957(22)	4654(5)	1563(11)	74(5)

Table 2-30 (Continued)

C(21)	8515(21)	4851(5)	2231(11)	57(4)
O(22)	8778(13)	5334(3)	2474(7)	68(3)
C(23)	9520(21)	5780(4)	4865(11)	125(6)
C(24)	3752(19)	6052(4)	2252(10)	101(5)
C(25)	5475(16)	5629(4)	702(10)	94(5)
O(27)	4428(18)	2918(3)	3233(10)	111(4)
C(28)	3127(23)	3096(5)	4039(12)	131(7)

* Equivalent isotropic U defined as one third of the
trace of the orthogonalized U_{ij} tensor

Table 2-31
Bond Lengths (Å) for Compound V

C(1)-C(24)	1.495(14)	C(1)-C(25)	1.539(13)
C(1)-C(2)	1.55(2)	C(1)-C(9)	1.59(2)
C(2)-C(3)	1.40(2)	C(2)-C(7)	1.43(2)
C(3)-C(4)	1.38(2)	C(4)-C(5)	1.41(2)
C(5)-C(6)	1.35(2)	C(6)-C(7)	1.40(2)
C(7)-N(8)	1.389(14)	N(8)-C(9)	1.462(13)
N(8)-C(23)	1.483(13)	C(9)-C(10)	1.458(13)
C(9)-O(22)	1.504(12)	C(10)-N(11)	1.330(12)
N(11)-C(12)	1.433(12)	C(12)-C(13)	1.356(13)
C(12)-C(21)	1.366(14)	C(13)-C(18)	1.412(14)
C(13)-C(14)	1.46(2)	C(14)-C(15)	1.35(2)
C(15)-C(16)	1.42(2)	C(15)-O(27)	1.41(2)
C(16)-C(17)	1.43(2)	C(17)-C(18)	1.42(2)
C(18)-C(19)	1.43(2)	C(19)-C(20)	1.343(14)
C(20)-C(21)	1.39(2)	C(21)-O(22)	1.367(12)
O(27)-C(28)	1.401(12)		

Table 2-32

Bond Angles (°) for Compound V

C(24)-C(1)-C(25)	108.5(12)	C(24)-C(1)-C(2)	110.1(11)
C(25)-C(1)-C(2)	117.2(12)	C(24)-C(1)-C(9)	110.9(11)
C(25)-C(1)-C(9)	109.4(11)	C(2)-C(1)-C(9)	100.5(12)
C(3)-C(2)-C(7)	121(2)	C(3)-C(2)-C(1)	131(2)
C(7)-C(2)-C(1)	108(2)	C(4)-C(3)-C(2)	117(2)
C(3)-C(4)-C(5)	124(2)	C(6)-C(5)-C(4)	119(2)
C(5)-C(6)-C(7)	122(2)	C(6)-C(7)-N(8)	133(2)
C(6)-C(7)-C(2)	118(2)	N(8)-C(7)-C(2)	109(2)
C(7)-N(8)-C(9)	110.1(11)	C(7)-N(8)-C(23)	118.9(14)
C(9)-N(8)-C(23)	116.3(12)	N(8)-C(9)-C(10)	110.1(11)
N(8)-C(9)-O(22)	105.7(12)	C(10)-C(9)-O(22)	113.1(10)
N(8)-C(9)-C(1)	101.2(10)	C(10)-C(9)-C(1)	115.9(13)
O(22)-C(9)-C(1)	109.7(10)	N(11)-C(10)-C(9)	122.7(13)
C(10)-N(11)-C(12)	121.2(12)	C(13)-C(12)-C(21)	120.6(14)
C(13)-C(12)-N(11)	122.6(13)	C(21)-C(12)-N(11)	116.7(12)
C(12)-C(13)-C(18)	120(2)	C(12)-C(13)-C(14)	121.4(14)
C(18)-C(13)-C(14)	118.2(14)	C(15)-C(14)-C(13)	121(2)
C(14)-C(15)-C(16)	123(2)	C(14)-C(15)-O(27)	128(2)
C(16)-C(15)-O(27)	109(2)	C(17)-C(16)-C(15)	115(2)
C(16)-C(17)-C(18)	124(2)	C(13)-C(18)-C(17)	118(2)
C(13)-C(18)-C(19)	118.1(14)	C(17)-C(18)-C(19)	124(2)
C(20)-C(19)-C(18)	119.2(14)	C(19)-C(20)-C(21)	121.3(14)
O(22)-C(21)-C(20)	114.1(13)	O(22)-C(21)-C(12)	125.2(13)

Table 2-32 (Continued)

C(20)-C(21)-C(12)	120.3(13)	C(21)-O(22)-C(9)	116.3(10)
C(28)-O(27)-C(15)	114.5(12)		

Table 2-33

Anisotropic Displacement Coefficients ($\text{\AA}^2 \times 10^3$) for Compound V

Atom	U_{11}	U_{22}	U_{33}	U_{12}	U_{13}	U_{23}
C(1)	61(12)	72(10)	56(9)	-18(9)	24(9)	9(10)
C(2)	68(13)	79(13)	82(12)	5(11)	22(11)	32(11)
C(3)	96(16)	90(12)	79(11)	19(11)	41(11)	36(12)
C(4)	151(25)	62(13)	196(22)	15(17)	120(19)	-16(15)
C(5)	146(23)	109(17)	179(22)	-46(20)	94(18)	-55(16)
C(6)	88(14)	100(13)	87(12)	-24(11)	25(10)	-53(12)
C(7)	39(11)	87(13)	81(13)	-14(11)	9(10)	1(11)
N(8)	74(10)	81(10)	62(8)	16(8)	14(7)	-4(9)
C(9)	77(12)	33(8)	56(9)	18(8)	18(9)	13(9)
C(10)	85(13)	55(9)	93(11)	-19(9)	31(9)	-37(10)
N(11)	97(10)	85(9)	55(7)	4(7)	36(7)	18(9)
C(12)	57(11)	55(9)	45(8)	0(7)	19(7)	-1(10)
C(13)	57(12)	73(11)	52(9)	1(9)	6(8)	6(11)
C(14)	95(15)	71(11)	58(10)	-30(9)	-11(9)	31(12)
C(15)	83(15)	96(15)	60(11)	22(11)	7(10)	-3(13)
C(16)	104(17)	86(13)	84(12)	10(11)	3(11)	-9(12)
C(17)	112(17)	107(14)	44(9)	-21(9)	3(9)	30(13)
C(18)	66(13)	65(11)	66(10)	-11(9)	9(9)	17(10)
C(19)	80(13)	109(13)	56(9)	2(10)	50(9)	-10(12)
C(20)	91(14)	66(11)	64(10)	11(9)	5(9)	0(11)
C(21)	48(11)	67(10)	61(9)	-10(9)	22(8)	-4(9)

Table 2-33 (Continued)

O(22)	66(8)	71(6)	71(6)	3(5)	25(5)	7(6)
C(23)	201(19)	95(12)	75(11)	-21(9)	7(12)	45(13)
C(24)	101(15)	153(13)	47(9)	-6(9)	1(9)	42(12)
C(25)	77(12)	134(12)	71(10)	13(9)	15(9)	-3(10)
O(27)	130(11)	91(8)	116(9)	-16(7)	34(8)	-11(8)
C(28)	183(20)	93(12)	128(14)	-25(10)	62(13)	-28(12)

The anisotropic displacement exponent takes the form:

$$-2\pi^2 (h^2 a^2 U_{11} + \dots + 2hka^*b^* U_{12})$$

Table 2-34

Hydrogen Atom Coordinates ($\times 10^4$) and Isotropic
Displacement Coefficients ($\text{\AA}^2 \times 10^3$) for Compound V

Atom	x	y	z	U
H(3 A)	6559(25)	6740(6)	336(13)	80
H(4 A)	8893(32)	7355(7)	920(19)	80
H(5 A)	10946(33)	7378(8)	2860(18)	80
H(6 A)	10682(24)	6750(6)	4264(14)	80
H(10 A)	4909(20)	5400(5)	4143(11)	80
H(14 A)	4701(24)	3887(5)	3476(12)	80
H(16 A)	6910(25)	2702(5)	1867(13)	80
H(17 A)	9250(24)	3229(6)	983(11)	80
H(19 A)	10932(21)	4047(6)	810(10)	80
H(20 A)	10974(22)	4864(5)	1299(11)	80
H(23 A)	10047(21)	6049(4)	5370(11)	80
H(23 B)	8873(21)	5555(4)	5356(11)	80
H(23 C)	10629(21)	5623(4)	4540(11)	80
H(24 A)	2994(19)	6245(4)	1614(10)	80
H(24 B)	2979(19)	5766(4)	2378(10)	80
H(24 C)	3987(19)	6235(4)	3004(10)	80
H(25 A)	4710(16)	5818(4)	58(10)	80
H(25 B)	6806(16)	5555(4)	485(10)	80
H(25 C)	4750(16)	5334(4)	808(10)	80

Table 2-34 (Continued)

H(28A)	2353(23)	2833(5)	4316(12)	80
H(28B)	3919(23)	3250(5)	4737(12)	80
H(28C)	2201(23)	3328(5)	3604(12)	80

CHAPTER 3

ACIDIC CHROMIC EFFECTS IN PHOTOCROMIC SPIRO(1,3,3-TRIMETHYLINDOLO-2,3'-NAPHTH[1,2-B]-1,4-OXAZINE): ABSORPTION CHARACTERISTICS

3.1. Introduction

Photochromic spirooxazines have been of much interest in the field of materials chemistry.^{3.1,3.2} Most studies of spirooxazines have emphasized the synthesis of new photochromic analogues and potential device applications.

Recently, Rys *et al.*^{3.3} found that the absorption bands of protonated spironaphthoxazines were shifted to shorter wavelengths when the alcoholic solution pH was decreased from 4.52 to 1.28. They concluded that protonation of the nitrogen of the indoline moiety caused the hypsochromic shift.

The research presented in this chapter focuses on photochromic effects in alcoholic solutions containing spiro(1,3,3-trimethylindolo-2,3'-naphth[1,2-*b*]-1,4-oxazine) (referred to as SP1 hereinafter). Among the findings, SP1 has been observed to be quite sensitive to proton activity in solution. When an alcoholic SP1 solution is made acidic by addition of HCl, absorption and photochromic characteristics were found to be substantially changed. The phrase "acidichromic" has been coined to indicate such phenomenon, wherein the spectral characteristics of a photochromic species are reversibly changed by proton activity in solution.^{3.4} It is believed that research in the area of acidichromic systems will become quite active, as the absorption and emission characteristics of such chromophoric species may be tuned by adjusting proton activity.

Results described herein focus on activity-dependent acidichromic and photochromic processes in solution. Discussion of the observed acidichromic photoproduct decay kinetics is also included.

3.II. Experimental Methods

SP1 was synthesized from 2-methylene-1,3,3-trimethylindoline and 1-nitroso-2-naphthol; the synthetic approach has been fully described elsewhere.^{3,5} SP1 solutions for acidichromic studies were prepared by dissolving SP1 in anhydrous reagent grade isopropanol (Fisher Scientific Company). Proton activity (or concentration of H⁺) in the solution was adjusted by dropwise addition of 0.01 M HCl in isopropanol. The UV irradiation source was a B-100SP 160-W (Fisher Scientific Company) UV Lamp with peak emission at 365 nm and a manufacturer-specified irradiation intensity of 11,600 μW/cm². The distance between the lamp and samples was 15 cm. Absorbance spectra were determined using a Cary 5E spectrophotometer (2.0 nm spectral band pass) and 1.0 × 10⁻⁵ M SP1 solution in quartz cuvettes with 1 cm pathlength. All spectral measurements were conducted at room temperature.

3.III. Results and Discussion

Figure 3-1 shows the acidichromic effect in a 0.01 mM SP1 isopropanol solution. Curve A represents the absorption spectrum of SP1 dissolved in pure isopropanol. An intense peak centered at 320 nm and exhibiting a shoulder at 350 nm was observed. [As an aside, this absorption band structure was found to be comparatively insensitive to the presence of water. Isopropyl alcohol solutions containing SP1 and up to 20 vol. % H₂O were found to have absorption spectra which were indiscernible from that shown in Curve

A of Figure 3-1.] Upon acidification by addition of alcoholic HCl, the optical density at wavelengths less than the region below 360 nm was noticeably perturbed. The HCl/SP1 ratio in isopropanol solution was increased from 0 (Curve A) to 1 (Curve H) and 2 (Curve B). Similarly, a proton activity increased from 0 to 2, a new absorption band appeared in the visible region ($\lambda_{\max} = 430$ nm) with steady growth in intensity upon acid addition. Over this range, an isosbestic point was observed, indicating that only two distinct species are involved in the acidichromic process associated with Curves A, H, B and J in Figure 3-1. The indicated acidichromic reaction is hypothesized to result in the protonation of SP1, *i.e.*:



where SP1•HCl represents the acidichromic product. HCl activity-dependent equilibria between the SP1 and SP1•HCl species are readily noted by comparison of Curves H, B and J in Figure 3-1.

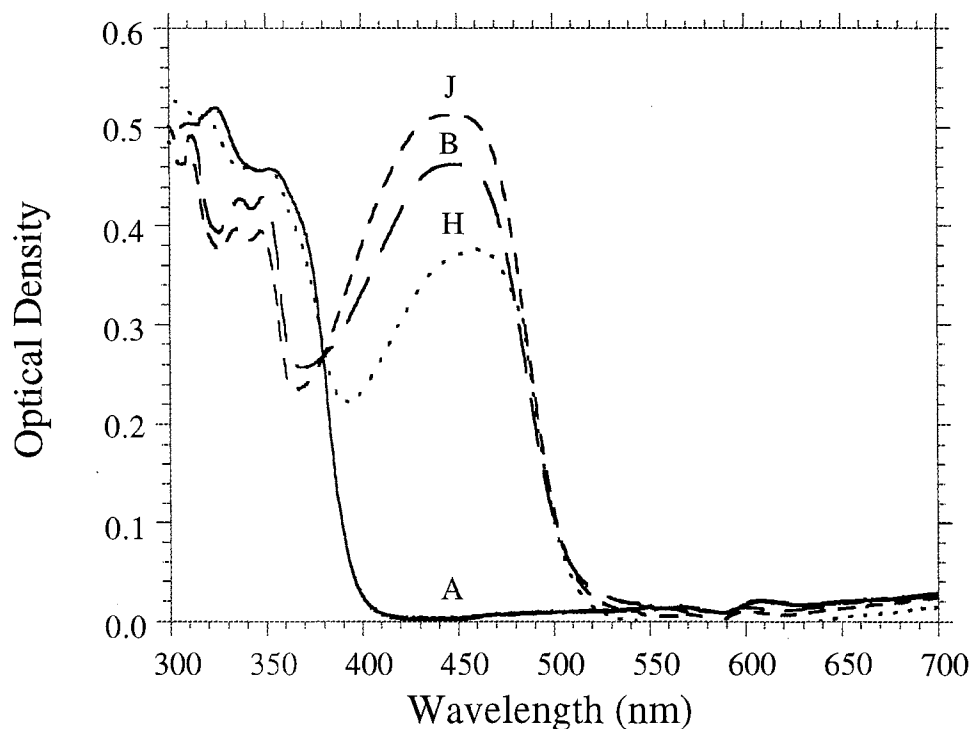


Figure 3-1. Absorption spectra of alcoholic spirooxazine solutions ($1.0 \times 10^{-5} M$) as a function of proton activities. HCl:SP1: (A) 0; (H) 1:1; (B) 2:1; (J) 4:1.

Further spectral investigation was focused on the assessment of photochromic products in alcoholic solutions. Figure 3-2 represents the absorption characteristics of four readily distinguished species which result from acidification and/or UV irradiation. Curves A and B are associated with the absorption spectra of SP1 in anhydrous isopropanol and acidified alcoholic solutions, respectively (also shown as Curves A and B in Figure 3-1). Irradiation of the acidichromic product (B) with UV light yielded the measured absorption spectrum indicated as Curve C in Figure 3-2. The photoproduct (C) shown was found to be long-lived in solution, as indicated later in this Chapter (Figure 3-6). Curve D is taken from the work by Bohne *et al.*, indicating the corresponding absorption band of PMCl

(species D, shown in Figure 3-2), which reportedly peaks near 600 nm in acetonitrile. 3.6 The indicated peak was obtained by a high speed laser photolysis method; the 600 nm peak reportedly does not change its position significantly in different organic solutions. 3.7 Because of the comparatively short-lived nature of the PMC1 (D) species, it is difficult to observe its absorption spectrum by conventional methods.

The photochromic product of the SP1•HCl complex, (C), exhibits a new absorption band centered at 526 nm. This represents a hypsochromic shift of some 74 nm compared with Curve D, the reported absorption spectrum of UV-irradiated SP1. Thus, photochromic effects which are observed in SP1 solutions are also observed for solutions containing the acidichromic product, SP1•HCl. The unique aspect of this work, however, is that the peak position of the photochromic band is dependent upon proton activity. Photochromic effects in the SP1•HCl solutions were found to be completely reversible, an effect that is particularly useful for colorometric applications. The reversible tuning of photochromic absorption bands using acid/base, *i.e.*, acidichromism, has not been previously reported for any photochromic compound. An interesting aspect of this work is that similar effects may be found in other photochromic systems, thereby marking the initiation of a new research area.

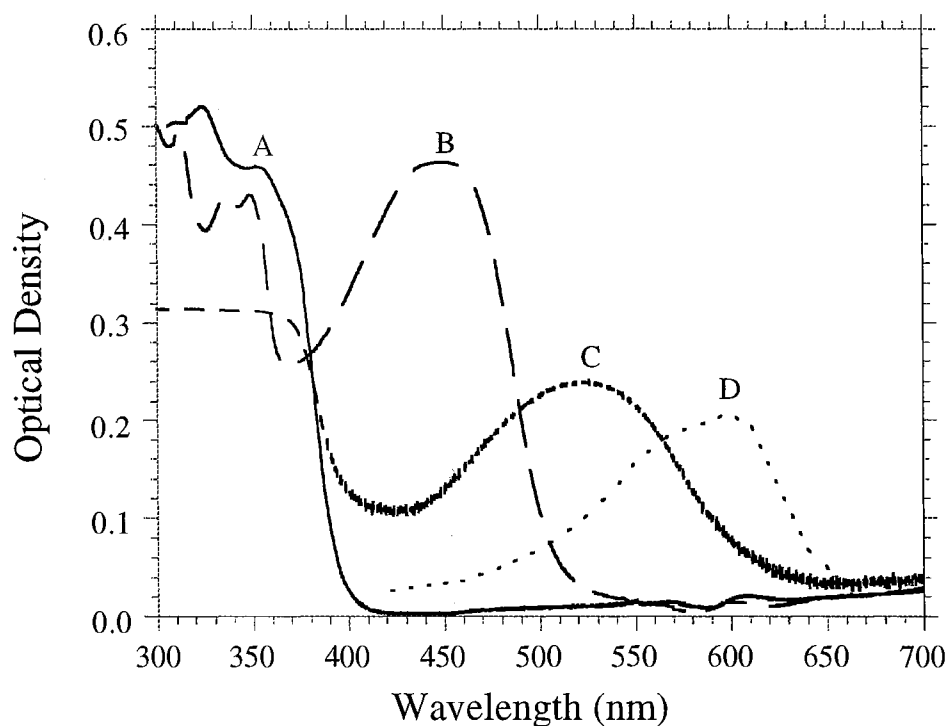


Figure 3-2. Absorption spectra of four species. (A). alcoholic SP1 solutions; (B). acidichromic product $SP1 \bullet HCl$ formed at $HCl/SP1 = 2$; (C). photochromic product of $SP1 \bullet HCl$, $PMC1 \bullet HCl$; (D). photochromic product of SP1 in acetonitrile, data from Ref. [6].

A proposed molecular model, given in Figure 3-3, suggests a chemical mechanism associated with the observed acidichromic and photochromic processes. Transformation of SP1 (A) to $SP1 \bullet HCl$ (B) represents the protonation process which is evidenced by the spectral shifts observed in Figure 3-1. Conversion of the $SP1 \bullet HCl$ (B) form to the protonated photomerocyanine form, $PMC1 \bullet HCl$ (C), is the UV-induced photochromic process evidenced by the shift associated with Curve C in Figure 3-2. It is known that $PMC1$ (D), the photochromic product of SP1 (A) generated by UV irradiation under neutral

conditions, is a blue species with a conformational lifetime of approximately one-half second in common solvent.^{3.6} Photomerocyanine products are postulated to undergo reversible protonation/deprotonation process, similar to SP1, as indicated by the dashed arrow in Figure 3-3, although this has not been observed.

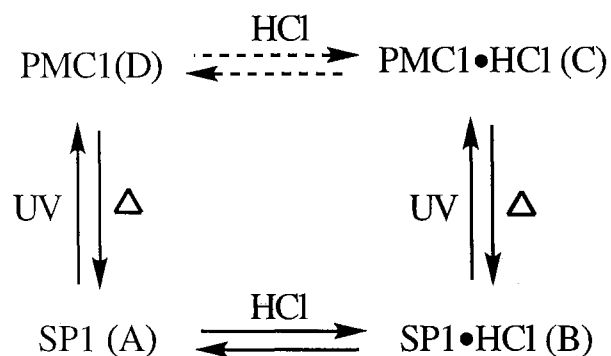


Figure 3-3. Proposed transformation among A, B, C and D forms.

Although the structures of SP1•HCl (B) and PMC1•HCl (C) are not reported in the literature, it is possible to conjecture on conformational changes induced by protonation through interpretation of spectroscopic data. SP1 (A) is known to have a twist arrangement between the two ring systems as described in Chapter 2, section 2.III.^{3.6} In the absence of substantial molecular rearrangements, bathochromic shifts such as the one observed (Curves A and B, Figure 3-1) are associated with the formation of a more planar molecular conformation, resulting in resonance forms having increased effective conjugation lengths. Conversely, PMC1•HCl (C) was found to exhibit a large hypsochromic shift compared to the spectrum reported for the PMC1 (D) form. This result has been interpreted as follows: In PMC1 (D), the indolino-nitrogen acts as an electron-donor, while the oxygen atom bound to the naphthyl ring serves as an electron-withdrawing species. PMC1 (D) may exist as a planar, fully conjugated structure having an extensive delocalized π -electron system which results from the donor-acceptor resonance structure shown as structure

PMC1 (D) in Figure 3-4. This is consistent with the large bathochromic shift compared to the SP1 (A) form. When hydrogen chloride begins to react with the conjugated photomerocyanine system, the donor-acceptor system is destroyed through the formation of an internal salt, *i.e.*, structure PMC1•HCl (C) in Figure 3-4. The loss of the donor-acceptor system is associated with reduced π -system delocalization and is consistent with the hypsochromic-shift observed in the absorption spectrum found in going from the PMC1•HCl (C) to the PMC1 (D) band.

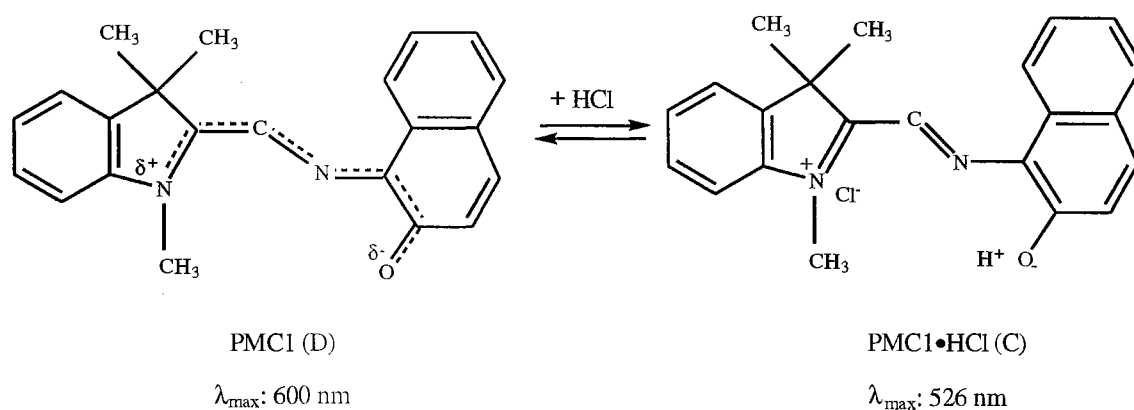


Figure 3-4. Proposed acidichromic process of the photomerocyanine form.

Results reported by Rys *et al.*^{3.3} indicated that protonation of the indolino-nitrogen heteroatom was the dominant structure for spirooxazine-type molecular forms under mildly acidic conditions. These authors, however, did not indicate an absorption peak for spirooxazine in the visible region; instead, the maximum absorption wavelength for the base spirooxazine compound was below 250 nm. Conversely, it appears from the spectroscopic data gathered on the spirooxazine compound presently studied that substantial conjugation results from the protonation. This suggests ligation of the Cl^- anion to the protonated indoline nitrogen atom, with donation of π -electron density from Cl^- into

the indoline ring. Such donation would serve to yield the more conjugated ring system needed to account for the observed absorption band in the blue region.

The proposed chemical structure SP1•HCl product may be represented as indicated in Figure 3-5.

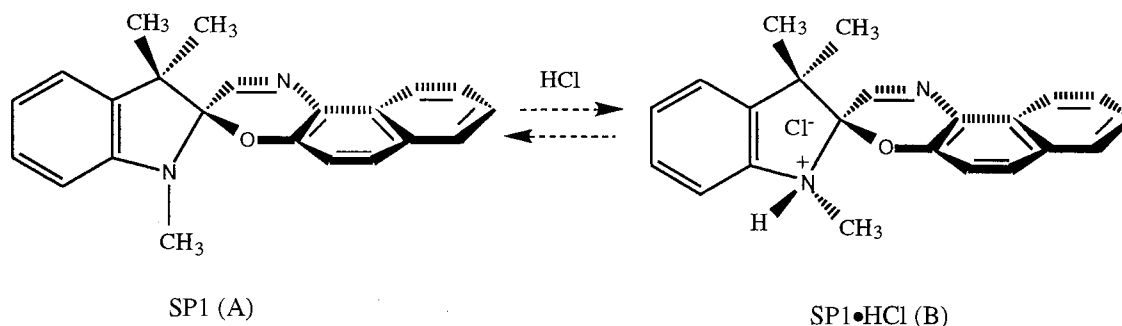


Figure 3-5. Proposed acidichromic process between SP1(A) and SP1•HCl (B).

The photochromic product PMC1•HCl (C), which is generated upon UV excitation of SP1•HCl (B), spontaneously decays back to the SP1•HCl (B) form at room temperature. This transformation is apparently thermally activated. Decay kinetic data associated with the PMC1•HCl (C) to SP1•HCl (B) transition are shown in Figure 3-6. The change in optical density (absorption $\lambda = 526$ nm) was measured as a function of time immediately following a two-minute irradiation exposure at 365 nm (estimated to be 14 mJ/cm²). A plot of the natural logarithm of relative absorbance (A/A_0) versus decay time was found to be of first order, with a correlation coefficient of 0.999 (over nearly three lifetime periods as indicated in the Figure 3-6 inset). The thermally-induced relaxation lifetime of the acidichromic product (C) was found to be 115 seconds. Thus, the protonation product of PMC1, PMC1•HCl (C), was found to have a much longer conformational lifetime (by more than 2 orders of magnitude) than that of the free PMC1 form, which has been reported to be about one-half seconds.^{3,6} HCl induced

acidichromism, therefore, is noted to have unique effects on both the absorption spectrum and on the UV-photoproduct lifetimes. Such changes are of potential interest in various device applications, such as optical information storage and/or opto-chemical transducers.

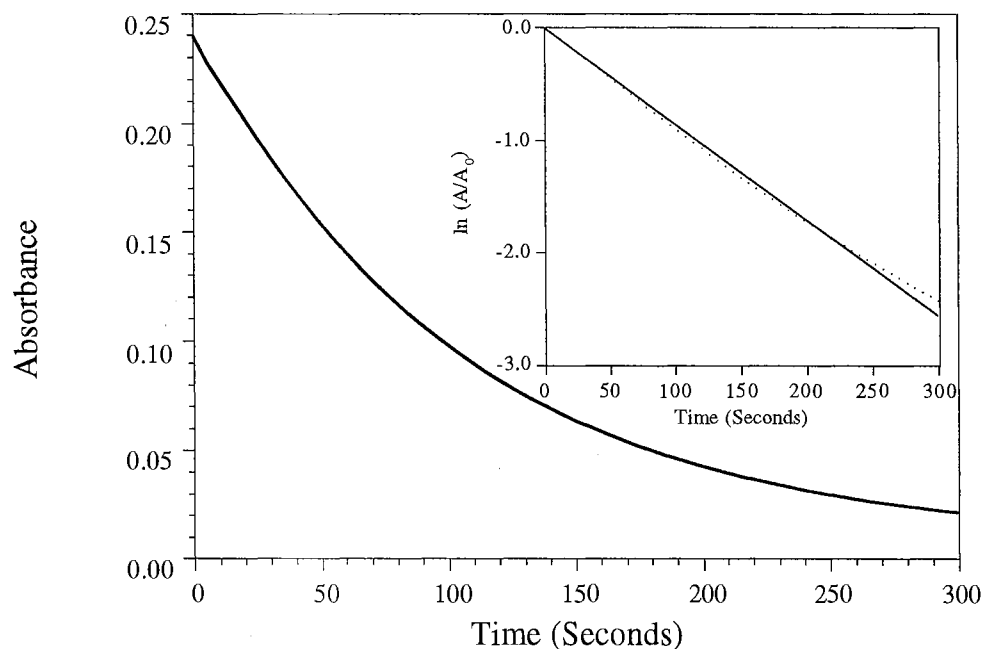


Figure 3-6. Time evolution of alcoholic SP1•HCl solution absorbance at 526 nm, following UV irradiation.

Inset: $\ln(A/A_0)$, versus decay time ($\lambda = 526$ nm); (...) = actual data, (—) = single exponential fit.

3.IV. Summary and Conclusions

HCl activity-dependent photochromic effects in alcoholic spirooxazine solutions were investigated. A new term, acidichromism, was coined to describe the reversible effects observed for spirooxazine under conditions of varying HCl activity. Spirooxazine

(SP1) and its acidichromic product (SP1•HCl) exhibit dramatically different spectral characteristics; a new absorption peak at 430 nm for SP1•HCl was observed. In addition, the absorption band of PMC1•HCl was found to have undergone a substantive hypsochromic shift, by 74 nm, with respect to the peak reported for PMC1. This hypsochromic shift is hypothesized to be due to changes in the donor-acceptor character of the PMC1 form, resulting in a perturbation to the conjugated π -electron system of photomerocyanine. Thermally-initiated relaxation kinetics of PMC1•HCl to SP1•HCl were found to be first order at room temperature, with a computed relaxation time of 115 seconds compared to approximately 0.5 seconds for the PMC1 form. A model for acidichromic and photochromic processes in these systems has been proposed. Preliminary results indicate that spirooxazine compounds are potentially useful in a variety of device applications.

3.V. References

- 3-1 *Photochromism*, Edited by G. H. Brown, Wiley-Interscience, New York, 1971.
- 3-2 *Photochromism: Molecules and Systems.*, Edited by H. Durr and H. Bouas-Laurent, Elsevier, Amsterdam, 1990.
- 3-3 P. Rys, R. Weber and Q. Wu, *Can. J. Chem.* **71** (1993) 1828.
- 3-4 X. D. Sun, M. G. Fan, X. J. Meng and E. T. Knobbe, *J. Photochem. Photobiol. A: Chem.* (in press).
- 3-5 X. Y. Zhang, S. Jin, Y. F. Ming, Y. C. Liang, L. H. Yu, M. G. Fan, J. Luo, Z. H. Zuo and S. D. Yao, *J. Photochem. Photobiol. A: Chem.* **80** (1994) 221.
- 3-6 C. Bohne, M. G. Fan, Z. J. Li, Y. C. Liang, J. Lusztyk and J. C. Scaiano, *J. Photochem. Photobiol. A: Chem.* **66** (1992) 79.
- 3-7 M. G. Fan, Personal communication.

CHAPTER 4

ACIDICHRROMISM IN PHOTOCROMIC SPIROOXAZINES: STRUCTURAL EFFECTS

4.1. Introduction

In Chapter 3, it was stated and demonstrated that acidichromism in spirooxazine compounds is a unique phenomenon wherein the spectral characteristics of a photochromic species are reversibly changed by varying solution proton activity.^{4.1} The research in the area of acidichromic systems is believed to be one which will become quite active as similar effects are likely to be found in other photochromic systems.^{4.2}

The ideas presented in this chapter focus on achieving a better understanding of the mechanism of photochromism and acidichromic behavior through the study of representative spirooxazine compounds and the effects of moiety substitution and proton activity dependence on absorption characteristics. Discussion of the potential mechanisms associated with acidichromic and photochromic reactions of various spirooxazine compounds is included.

Title compounds are given in Figure 4-1. The abbreviated names are designated as SP1, SP2, SP3 and SP4, respectively, according to the R¹ and R² substituents as indicated.

addition to the SP3 solution, an intense new absorption band appeared in the visible region ($\lambda_{\text{max}} = 490 \text{ nm}$) with steady growth in intensity as shown in Curves 2, 3 and 4 in Figure 4-2.

In Chapter 3, it was stated that addition of HCl into an isopropanol solution of SP1 gave rise to a new absorption band centered at 436 nm. The absorption intensity of the new peak was found to increase as a function of HCl activity. Subsequent measurements have shown that SP2 and SP4 exhibit inherently comparable behavior, with the onset of an HCl-induced absorption band in isopropanol solution centered around 436 and 492 nm, respectively. ^{4.1,4.2} By analogous reasoning to the ideas presented in Chapter 3, the new peaks have been assigned as the protonated product of SP4 (*i.e.* SP2•HCl, SP3•HCl and SP4•HCl).

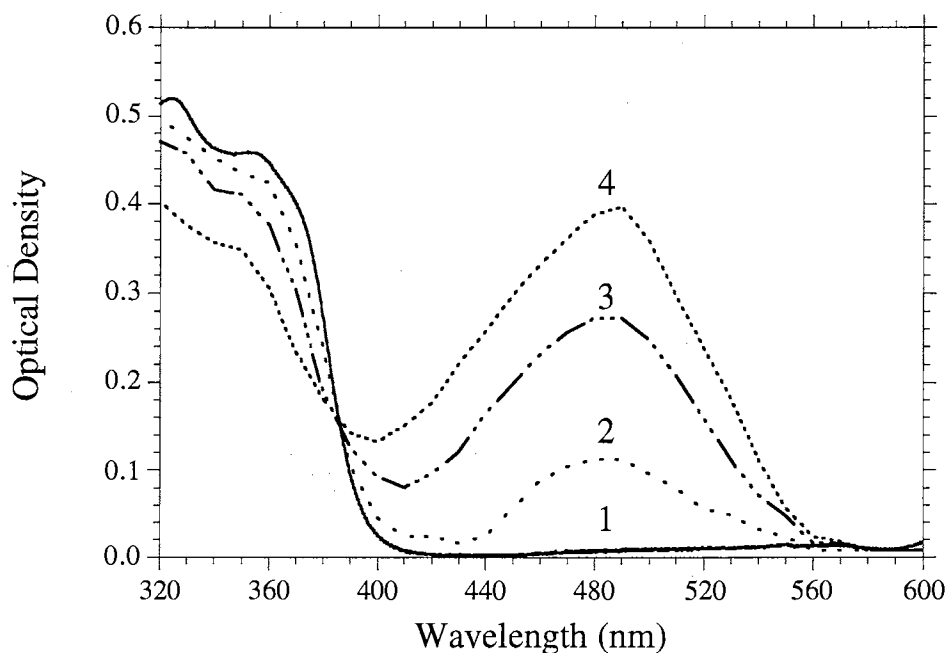


Figure 4-2. The absorption spectra changes of SP3 in acidic isopropanol solutions at low (Curve 1, HCl: SP3 = 1:3), moderate (Curves 2 and 3, HCl: SP3 = 2:3 and 1:1), and high (Curve 4, HCl: SP3 = 3:2) HCl activities.

SP3 and SP4 each have a hydroxyl group attached at the 9'-position of naphthooxazine moiety, creating a β -naphthol (abbreviated SPOH) functionality which is known to behave as a weak acid.^{4,5} When isopropanol solutions of SP3 and SP4 were made basic by addition of sodium hydroxide, new absorption bands centered at 404 and 405 nm, respectively, were found to result (see Figure 4-3 for SP3 results; SP4 similar). Base-induced products formed in the isopropanol solution are proposed to have a salt-like structure of the type SPO^-Na^+ . It should be noted that the postulated conjugated base SPO^-Na^+ , which is formed in basic solution, is not very stable. The intensity of the absorption bands centered at 404 and 405 nm were found to decrease slowly when solutions were stored in the dark.

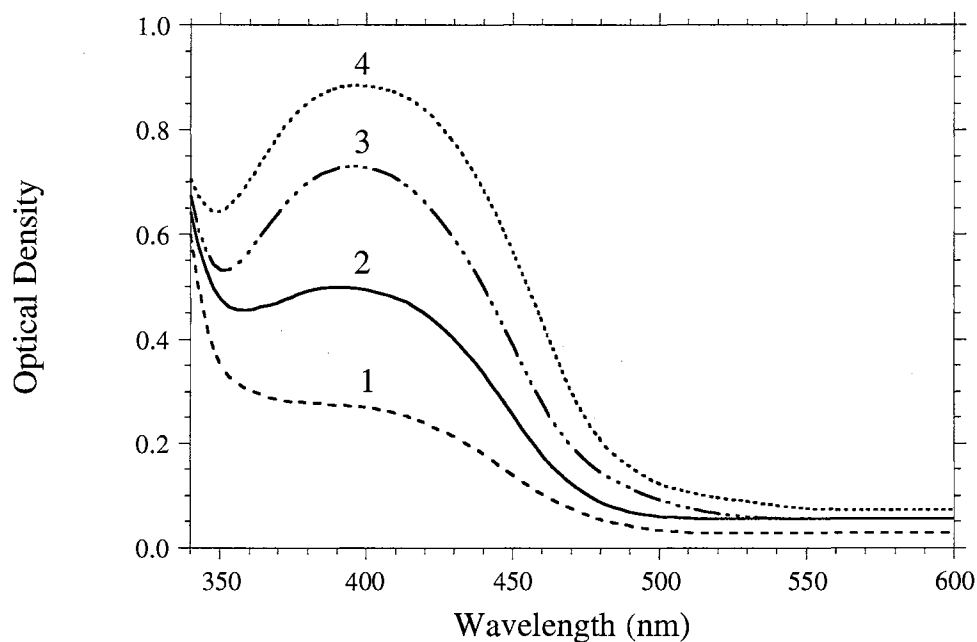


Figure 4-3. The absorption spectra changes of SP3 in basic isopropanol solutions at low (Curve 1, NaOH: SP3 = 1:3), moderate (Curves 2 and 3, NaOH: SP3 = 2:3 and 1:1), and high (Curve 4, NaOH: SP3 = 3:2) sodium hydroxide concentrations.

The acid and base-induced peaks were found to be completely reversible. When sodium hydroxide was added into the acidic solution containing SP3•HCl, the absorption band centered at 490 nm gradually disappeared. This is consistent with regeneration of SP3 in the alcoholic solution. Addition of sodium hydroxide in excess of HCl equivalence gave rise to the 404 nm absorption band which is characteristic of the SPO⁻Na⁺ conjugate base. Conversely, when hydrogen chloride was added to the basic solution, the 404 nm band was replaced by a 490 nm peak.

4.III.B. *Photochromic Character of the Acidichromic Compounds*

Photochromism of acidichromic compounds of SP1 has been previously addressed in Section 3 of Chapter 3. As discussed in Section 1 in this chapter, the acidichromic products associated with SP3 and SP4 compounds are readily distinguishable in both acidic and basic solutions. SP1 and SP2, by comparison, did not show base-induced chromophoric modifications.

The acidichromic products were found to be sensitive to blue light. The acidichromic product SP3•HCl is used as an example; all others were comparable. 450 nm irradiation of SP3•HCl in isopropanol leads to a smooth decrease in absorption intensity of the 490 nm peak, as shown in Figure 4-4. There was a concomitant increase in absorption intensity at 340 nm. The increasing 340 nm band is consistent with elevated activities of the free SP3 form. Thus, 450 nm irradiation provides a secondary path for formation of SP3 from SP3•HCl.

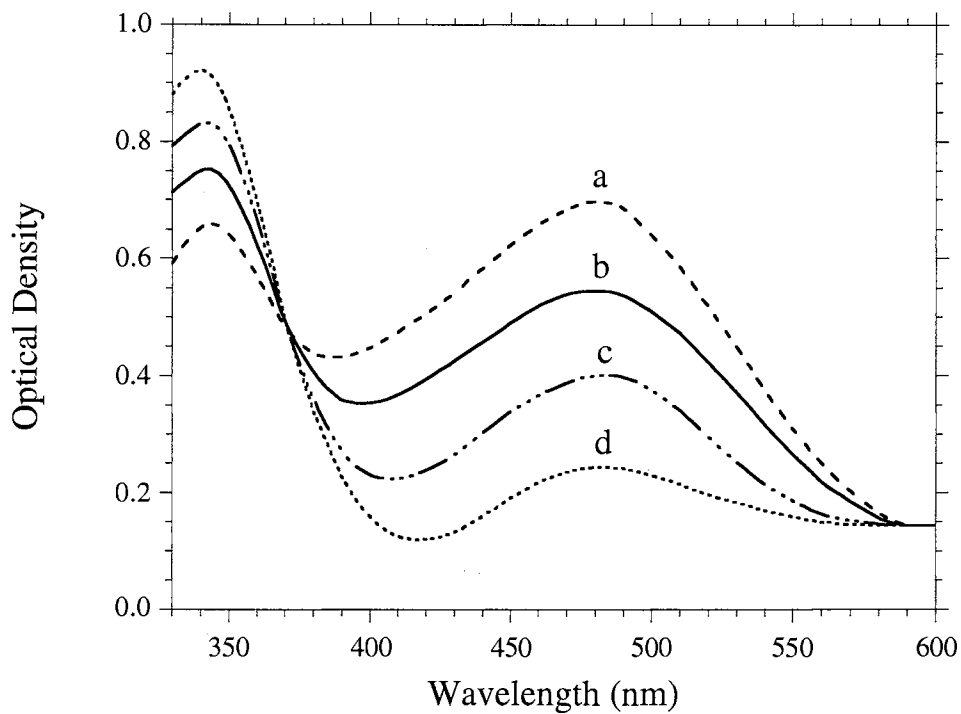


Figure 4-4. Absorption intensity changes of SP3•HCl with various 450 nm irradiation times.

Curves a = unirradiated, b = 10 min. irradiation, c = 20 min. irradiation, d = 25 min. irradiation.

The base-induced acidichromic products were found to be sensitive to UV light. Curve a of Figure 4-5 represents the absorption spectrum of base-induced acidichromic SP3 product (SPO-Na⁺), centered at 404 nm. When the specimens were irradiated with

365 nm light, the 404 nm-centered band decreased in intensity as a function of irradiation time (Curves b and c of Figure 4-5). At the same time, the 340 nm absorption band intensity increased, again consistent with a secondary photochemical path for regeneration of free SP3 in solution. Thus, SP3 can be produced by both thermal and photochemical routes.

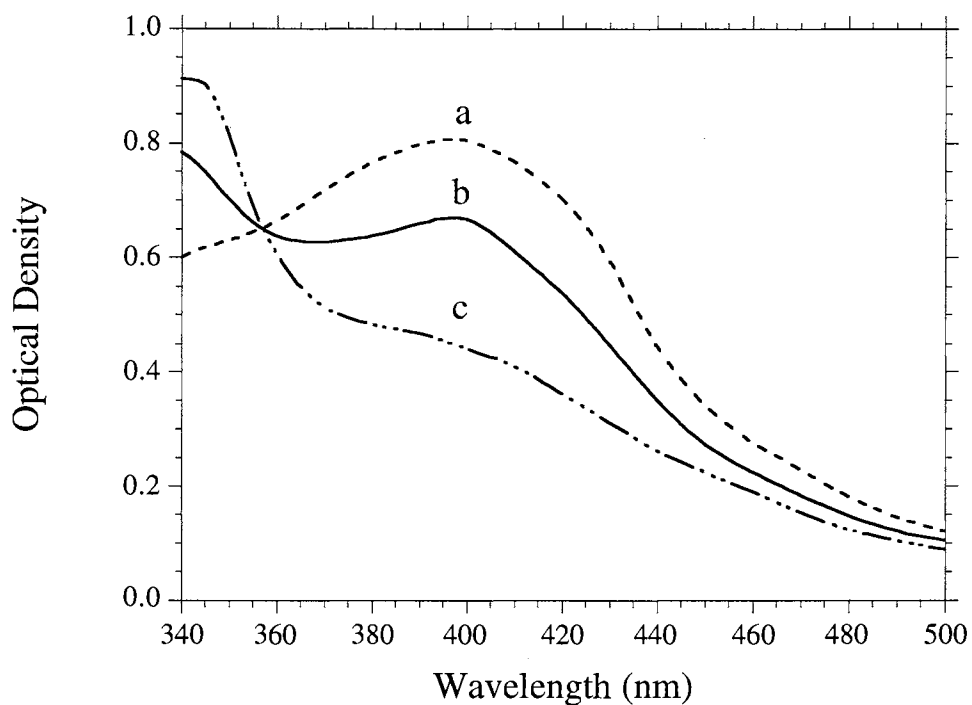


Figure 4-5. The absorption spectra change of basic isopropanol solution of SP3 with various irradiation time by 365 nm light.
Curves a = unirradiated; b = 5 min. irradiation;
c = 10 min. irradiation.

4.III.C. *Substituent Effects on the Absorption Maxima of Acidichromic Products*

The absorption maxima (λ_{\max}) of four protonated products (SP•HCl) in acidic isopropanol are summarized in Table 4-1. The difference of absorption maxima of four

acidichromic products is probably due to the 9'-position substituent (see Figure 4-1) electron donating effect. The electron donating groups are believed to favor the more planar structure, which results in the shift of absorption spectra to longer wavelengths. Thus, SP3•HCl and SP4•HCl exhibit bathochromic shift, owing to the electron donating nature of the hydroxyl group placed at the 9'-position.

Table 4-1

λ_{\max} of protonated product in isopropanol solutions

Protonation product	9'-position substituent	λ/nm
SP1•HCl	-H	436
SP2•HCl	-OCH ₃	460
SP3•HCl	-OH	490
SP4•HCl	-OH	492

4.III.D. *Discussion of the Acidichromic Mechanism for the Hydroxylated Spirooxazine Compounds*

It was noted that sodium hydroxide addition to isopropanol solutions of SP1 and SP2 did not result in any changes to the absorption spectra.^{4.1,4.2} The preparation of SP3 and SP4 compounds, introducing a hydroxyl group at the 9'-position, gives rise to fundamentally different acid-base chemistry. In the case of SP3 and SP4 solutions, acidichromic effects were observed. A proposed acidichromic conversion mechanism

diagram is given in Figure 4-6, based on the available data. In the figure, SPOH represents the shorthand notation for the hydroxylated (β -naphthol) SP3 and SP4 compounds. Reversible conversions which were directly observed are shown as solid arrows, while those which remain conjectural are shown as dashed arrows.

The open photomerocyanine form of SPO^- and SPO^-Na^+ were not be observed using steady state spectroscopic methods. These species are expected to have a very short lifetime, precluding their observation by classical steady state methods.

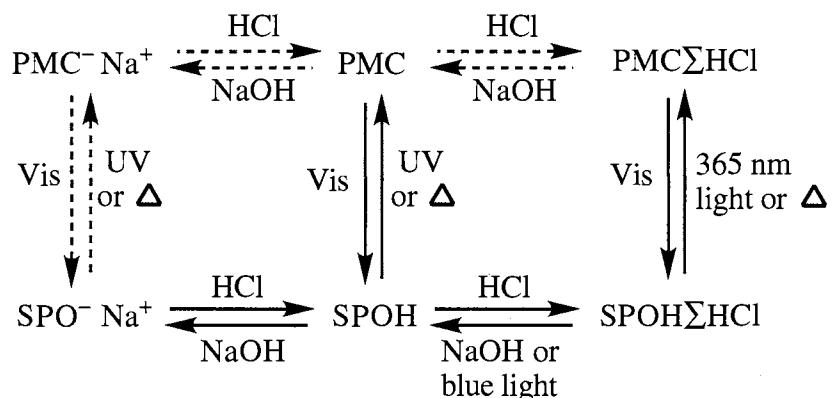


Figure 4-6. The proposed mechanistic scheme of acidichromism for SP3 and SP4 behavior in isopropanol solutions.

The indicated mechanism is supported by the following observations. (1) All of the photon and acid/base induced processes were found to be reversible, a characteristic of acidichromic and photochromic reactions. (2) Hydroxylation of the parent spirooxazine molecule leads to acidichromism effects in both acidic and basic solutions. The protonation product $\text{SPOH}\cdot\text{HCl}$ is thermally stable in acidic solutions, while the conjugate base SPO^-Na^+ was found to be unstable in basic solutions. Decomposition of the SPO^-Na^+ species is hypothesized to occur by a thermally-initiated mechanism, yielding the parent species through a solvation process. (3) The protonation product $\text{SPOH}\cdot\text{HCl}$ was found to exhibit two photochromic pathways. When irradiated using

blue light, ($\lambda_{\text{ex}} = 450 \text{ nm}$), it bleached to form SPOH and HCl. The protonation product SPOH•HCl was slowly reproduced after the irradiating source was turned off. Alternatively, when this protonated product was irradiated with UV light ($\lambda_{\text{ex}} = 365 \text{ nm}$), another photochromic reaction was observed, leading to the indicated protonated product photomerocyanine•HCl (PMC•HCl). (4) The acidichromic product SPO-Na⁺ salt, formed under basic conditions, is a newly observed conjugate base which exhibits unique photochemical behavior and could be induced to reproduce the parent SPOH compound by photochemical means.

While many of the suggested mechanistic processes remain to be substantiated, it is clear these compounds display highly unusual optical properties which may occur due to chemical conditions. This work represents the first documentation of acid- and base-induced colorimetric shifts associated with photochromic compounds.

4.IV. Summary and Conclusions

Four photochromic spirooxazine compounds were studied by absorption spectra. Acidichromic effects were found in both acidic and basic solutions when an OH group was added at the 9'-position of the parent spirooxazine. The absorption spectra of acidichromic product in both acidic and basic solutions are bathochromic compared with that of parent spirooxazine. Proton activity and substituents effects of structures on acidichromism were systematically studied.

4.V. References

- 4-1 X. D. Sun, M. G. Fan, X. J. Meng and E. T. Knobbe, *J. Photochem. Photobiol. A: Chem.* (in press).
- 4-2 Y. C. Liang, Y. F. Ming and M. G. Fan, *Science in China, B: Chem.* (in press).
- 4-3 N. Y. C. Chu, "Spirooxazines" in *Photochromism: Molecules and Systems*, Edited by H. Durr and H. Bouas-Laurent, Elsevier, Amsterdam, 1990, p493.
- 4-4 X. Y. Zhang, S. Jin, Y. F. Ming, Y. C. Liang, L. H. Yu, M. G. Fan, J. Luo, Z. H. Zuo and S. D. Yao, *J. Photochem. Photobiol. A: Chem.* **80** (1994) 221.
- 4-5 T. W. G. Solomons, *Organic Chemistry*, 5th ed., John Wiley & Sons, Inc, 1992, p94.

CHAPTER 5

ACIDIC CHROMIC EFFECTS IN SPIRO(1,3,3-TRIMETHYLINDOLO-2,3'-NAPHTH[1,2-B]-1,4-OXAZINE): FLUORESCENCE STUDIES

5.1. Introduction

Photophysical and photochemical processes result from the interaction of light and matter. The jump of an electron from one orbital to another is a transition between two energy states. Such transition requires an input of energy, in the form of a photon of light for example. This is the absorption of light energy by the atom. A reverse transition is accompanied by the release of energy, typically by photon and/or phonon emission. Radiative decay is the process of emission or luminescence. The luminescence of photochromic compounds comprises part of this work because of the information which may be acquired pertaining to the ground state and excited states.

Photochromism has been characterized mainly through the use of steady state and transient time-resolved absorption spectroscopy. ^{5.1,5.2} Literature references to luminescence studies on photochromic spirooxazine compounds are sparse. ^{5.3-5.5} To date, no fluorescence studies associated with the molecular conformers of photochromic SP1 have been reported.

Spirooxazine compounds have been found to be quite sensitive to proton activity in alcoholic solutions as described in Chapter 3 and 4. The acidichromic effect provides a novel route for tuning the optical properties of the spirooxazines. ^{5.6} A better understanding of this tunable acidichromism is of great importance for the utilization of the photochromic spirooxazine in a liquid solution or a solid matrix. Research described in this chapter focuses on photophysical and photochemistry aspects of spirooxazine.

Acidichromic and photochromic products are probed using conventional *cw* fluorescence methods.

5.II. *Experimental Methods*

SP1 was synthesized from 2-methylene-1,3,3-trimethylindoline and 1-nitroso-2-naphthol by Prof. Meigong Fan, Institute of Photographic Chemistry, Chinese Academy of Sciences. His synthetic approach has been described elsewhere in detail.^{5.7} SP1 solutions for luminescent studies were prepared by dissolution of SP1 into anhydrous reagent grade isopropanol (Fisher Scientific Company). The concentration of SP1 for all luminescent studies was $1.0 \times 10^{-5} M$ in alcoholic solution. The proton activity of the solution was adjusted by the dropwise addition of 0.01 *M* HCl in isopropanol. The UV irradiation source was a B-100SP 160-W UV Lamp (Fisher Scientific Company) with peak emission at 365 nm and a manufacturer-specified irradiation intensity of 11,600 $\mu\text{W}/\text{cm}^2$. Continuous wave front face excitation and emission spectra were measured at room temperature using a Spex Industries Model F112A spectrofluorimeter. Excitation and emission band passes of 5.55 nm and 2.58 nm, respectively, were used. All luminescence spectra were corrected for instrument response.

5.III. *Results and Discussion*

5.III.A. *Fluorescence Emission and Excitation Spectra of SP1*

Figure 5-1 shows the fluorescence excitation and emission spectra of SP1 in isopropanol solution. A pair of excitation bands, centered at 310 nm and 350 nm, were observed (Curve 1 of Figure 5-1) for an emission wavelength of 450 nm. This is a previously described characteristic of the SP1 molecule (Chapter 3, section 3.III). Curve

2 shows the emission spectrum of SP1 under 350 nm excitation. The intense band centered at 435 nm is attributed to radiative relaxation from the first excited singlet state of SP1.

This result may be interpreted as follows: the SP1 molecule can be divided into functional regions by the spirocarbon atom: an indoline and a naphthooxazine moiety. In general, conjugation effects do not extend over the two moieties, due to their nearly orthogonal relationship. The two excitation bands centered at 310 and 350 nm are postulated to correspond to selective excitation of the two constituent moieties of the SP1 molecule. 350 nm excitation gave rise to a fluorescence band centered at 435 nm, which is postulated to represent the excited naphthooxazine moiety. Such results are qualitatively similar to that found for a monomeric analog, naphth[1,2-*d*]oxazol.^{5,8} The intense emission band was observed to remain essentially unchanged over excitation wavelengths ranging from 310 to 350 nm, indicating that intramolecular energy transfer between two orthogonal parts may occur in the SP1 molecule. As discussed by Becker *et al.*^{5,9} in a similar photochromic naphthospiropyran compound, the results indicate that the emissions are localized or originate from a particularly efficient fluorochromic portion of the molecule. Based on the characteristics of SP1 emission and the image relationship of emission and absorption, the fluorescence of the SP1 molecule is assigned as originating from its first excited singlet state.

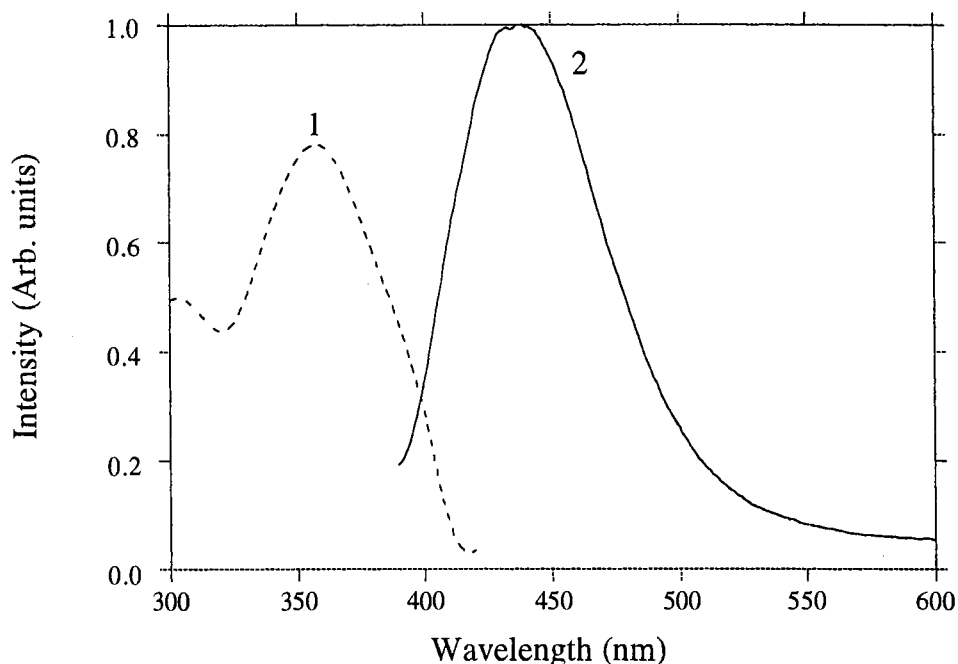


Figure 5-1. Fluorescence emission and excitation spectra of alcoholic SP1 solution.

(1). excitation spectrum ($\lambda_{em} = 450$ nm);

(2). emission spectrum ($\lambda_{ex} = 350$ nm).

5.III.B. Fluorescence Emission and Excitation Spectra of $SP1 \bullet HCl$

When hydrogen chloride was added to make a 1:1 SP1/HCl molar ratio solution, a new fluorescence band centered at 560 nm appeared (Curve 2 of Figure 5-2). The onset of this band is consistent with the formation of the protonated product $SP1 \bullet HCl$ as described in Section III of Chapter 3. The new fluorescence emission band is attributed to radiative relaxation from the first excited singlet state of acidichromic product, ${}^1(SP1 \bullet HCl)^*$. The excitation spectrum of $SP1 \bullet HCl$ is shown in Curve 1 of Figure 5-2 with a peak centered around 450 nm, indicating the acidichromic product has an excitation spectrum which is dramatically different from the excitation spectrum of the

free SP1 form (Curve 1, Figure 5-1). Similarly, the emission spectrum of the excited state singlet has a substantially different energy (Curve 2, Figure 5-2), λ_{em} peaked at 560 nm, compared to the free SP1 form (Curve 2, Figure 5-1), λ_{em} which peaked at 440 nm.

It was stated in Chapter 3 that SP1 is very sensitive to proton activity in alcoholic solutions, and the photochromic characteristics are substantially changed as a result. The results presented herein indicate that the luminescence spectra of SP1 are also quite sensitive to proton activity in solution. This is believed to be the first report on the luminescence spectra change for photochromic spirooxazine as a function of proton activity.

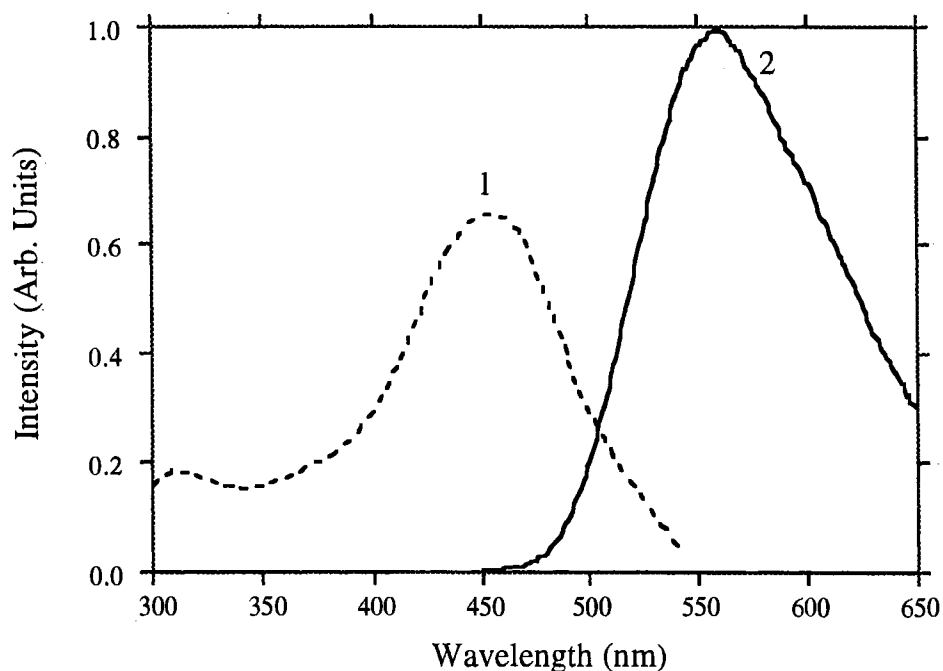


Figure 5-2. Fluorescence emission and excitation spectra in acidified SP1 solution (HCl:SP1 = 1:1).
(1). excitation spectrum ($\lambda_{em} = 560$ nm);
(2). emission spectrum ($\lambda_{em} = 435$ nm).

5.III.C. Proton Activity Dependence of Fluorescence Spectra

Figure 5-3 shows the fluorescence emission spectra of SP1 and SP1•HCl, at different proton activities in solution, using the same excitation sources. Curve 1 of Figure 5-3 shows the fluorescence spectrum of SP1 in isopropanol solution (*i.e.* HCl/SP1 = 0) with $\lambda_{\text{ex}} = 370$ nm. Only one emission band, centered at 435 nm, was observed. Upon the addition of hydrogen chloride to the solution, an acidichromic process occurred as previously described in Chapter 3, section 3.III. Curve 2 of Figure 5-3 was generated when HCl/SP1 = 1 ($\lambda_{\text{ex}} = 370$ nm). The emission spectrum shows two bands, one centered at 440 nm and the second at 560 nm. The fluorescence spectrum for a solution containing an elevated proton activity (HCl/SP1 = 3) appears as Curve 3 in Figure 5-3. The intense 560 nm exists as the major emission feature. High proton activity is believed to have significant influences on the equilibrium between SP1 and SP1•HCl. Thus, the fluorescence intensity of SP1•HCl ($\lambda_{\text{max}} = 560$ nm) is much stronger than that of SP1 ($\lambda_{\text{max}} = 440$ nm). The fluorescence studies strongly correlated with the earlier absorption spectroscopy findings in the sense, that proton activity in solution plays an extremely important role in the establishment of the equilibrium condition between SP1 and SP1•HCl, as indicated in equation 3-1 and Figure 3-1 in Chapter 3. Elevated HCl activities produce more of the acidichromic product, resulting in an increase of the intensity of the green emission band centered at 560 nm.

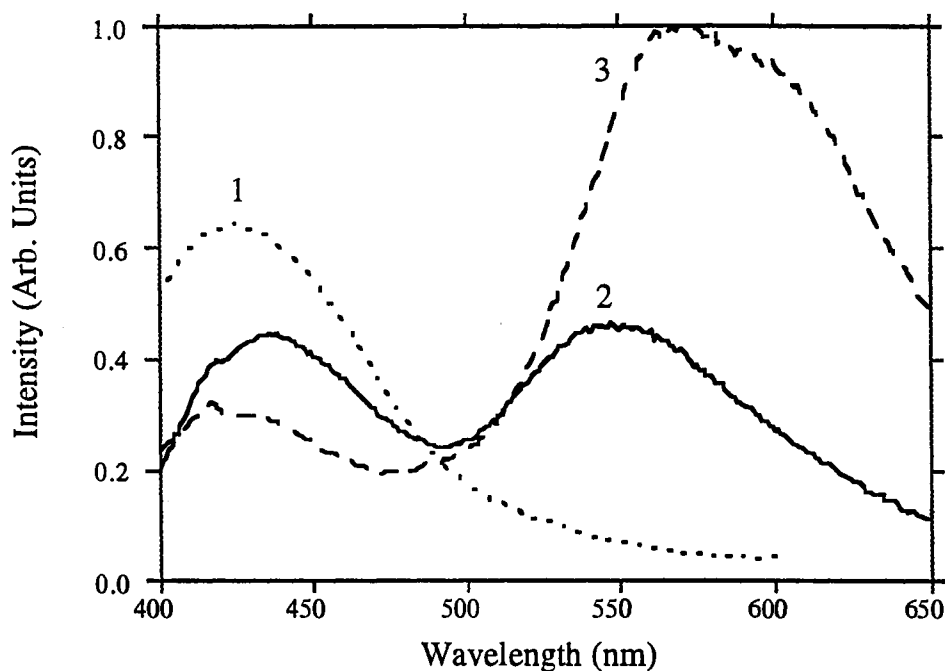


Figure 5-3. Fluorescence emission spectra of SP1 in isopropanol solution at different HCl:SP1 value ($\lambda_{\text{ex}} = 370 \text{ nm}$).
 (1). HCl:SP1 = 0; (2). HCl:SP1 = 1:1; (3). HCl/SP1 = 3:1.

5.III.D. Fluorescence Emission of $\text{PMC1} \cdot \text{HCl}$

When the acidified SP1 solution was irradiated with UV light for 2 minutes, (yielding the protonated product $\text{PMC1} \cdot \text{HCl}$) with subsequent irradiation at 525 nm light, another fluorescence band appeared (Curve 3 of Figure 5-4). The appearance of the new band was accompanied by a pronounced decrease in the intensity of the 560 nm band. The band ($\lambda_{\text{max}} = 612 \text{ nm}$) is consistent with the results reported by Schneider *et al.*^{5.3} pertaining to SP1. The 612 nm band is believed to result from radiative relaxation out of the first excited singlet state of the protonated product of photomerocyanine,

¹(PMC1•HCl)*, formed via UV excitation in acidified solution. Curve 1 and 2 in Figure 5-4 were taken from Figure 5-1 and Figure 5-2, respectively, for comparison.

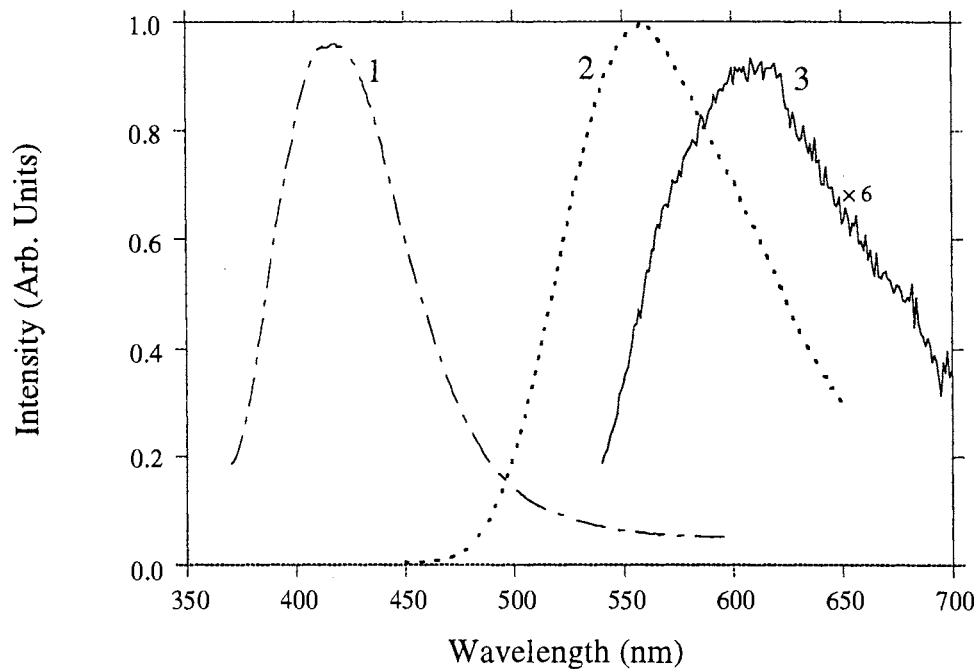


Figure 5-4. The fluorescence emission spectra of SP1, SP1•HCl and PMC1•HCl in isopropanol solution.

- (1) HCl:SP1 = 0, excited at 350 nm, taken from Curve 2 of Figure 5-1;
- (2) HCl:SP1 = 1:1, excited at 435 nm, taken from Curve 2 of Figure 5-2;
- (3) HCl:SP1 = 1:1, excited at 525 nm, after 2-minute UV irradiation of (2).

The three fluorescence bands shown in Figure 5-4 correspond to three distinct chemical species: SP1 (Curve 1), SP1•HCl (Curve 2) and PMC1•HCl (Curve 3). The fluorescence spectrum of PMC1 in solution was not determined, due to the short-lived nature of the photoproduct.

In light of these findings and those reported by other authors, 5.3-5.5 the structure/transition diagram given in Figure 5-5 represents the interconversion of states found for SP1 under the conditions investigated.

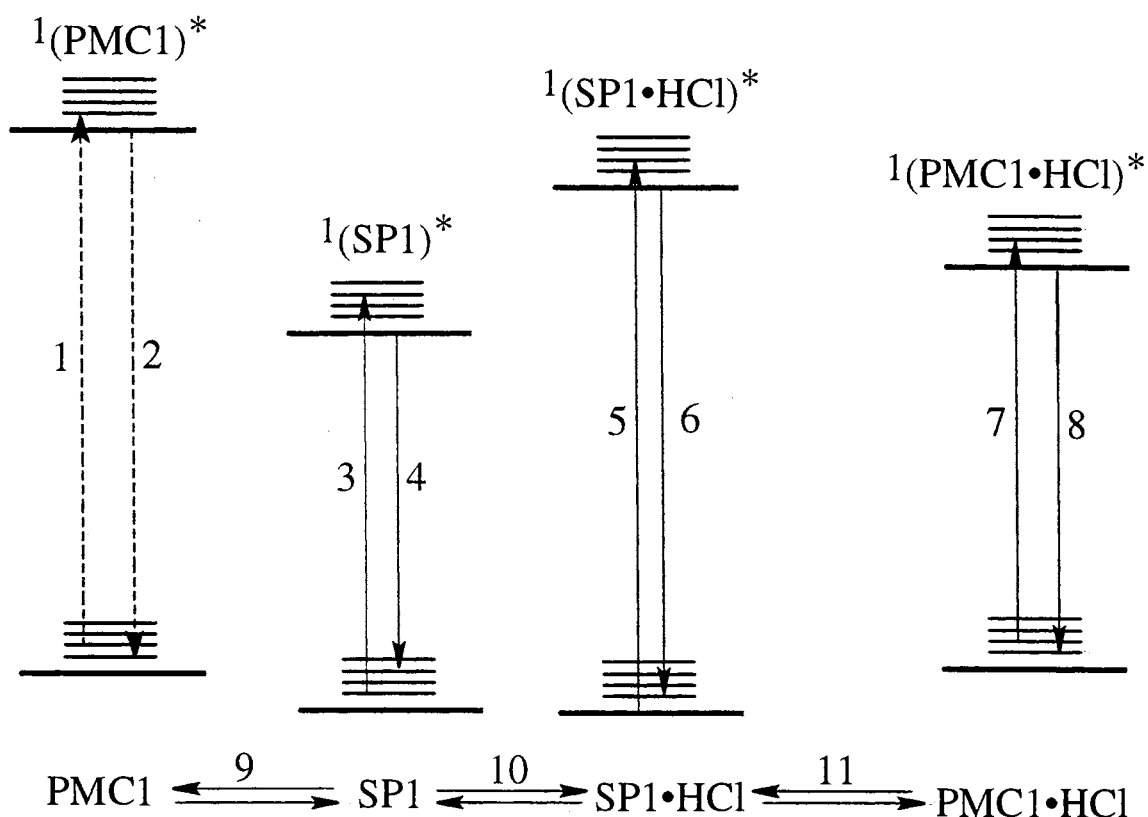


Figure 5-5. Photophysical and photochromic processes of SP1 and its product.

Each process in Figure 5-5 is explained in more details according to the following. Processes 1 to 8 represent absorption and fluorescence decay transition for different species. Among them, the dashed arrows (1 and 2) refer to the processes which were not directly observed in this research. Process 9 indicates the UV-induced photochromic process of SP1 as discussed in Chapter 1. The reverse process is initiated by visible light or heat. Process 10 represents the acidichromic process as discussed in Section 3 of Chapter 3 and earlier in this chapter. This is the reversible HCl-induced

acidichromic process. Process 11 refers to the photochromic process of $SP1 \bullet HCl$. The reverse reaction is found to be thermally activated and $PMC1 \bullet HCl$ has a lifetime of 115 seconds.^{5.6}

It is found in this research that acidichromic product of $SP1$ (*i.e.* $SP1 \bullet HCl$) has a unique fluorescence spectrum and photochromic behavior. This is the first report regarding the fluorescence spectra of photochromic spirooxazine and its acidichromic product. In addition to absorption spectroscopy, luminescence is proved to be a new method to study this tunable photochromism-acidichromism in spirooxazine compounds because it provides more information on the excited states of the molecule.

5.IV. Summary and Conclusions

The photophysical, photochromic, and acidichromic behaviors of $SP1$ and its acidichromic product $SP1 \bullet HCl$ have been investigated. The fluorescence spectra of $SP1$, $SP1 \bullet HCl$, and $PMC1 \bullet HCl$ have been observed. The fluorescence bands found in this work were attributed to radiative relaxation from the first excited singlet state of $SP1$, $SP1 \bullet HCl$, and $PMC1 \bullet HCl$, respectively. The results are believed to be important for understanding of photochromic spirooxazine compounds from the viewpoint of photophysics, photochemistry, and material sciences. The research indicates these photochromic spirooxazine compounds may be potentially useful in a variety of applications, including tunable photochromic and optical storage media based on their unique properties in acid-base conditions.

5.V. References

- 5-1 *Photochromism*, Edited by G. H. Brown, Wiley-Interscience, New York, 1971.
- 5-2 *Photochromism: Molecules and Systems.*, Edited by H. Durr and H. Bouas-Laurent, Elsevier, Amsterdam, 1990.
- 5-3 S. Schneider, A. Mindl, G. Elfinger and M. Melzig, *Ber. Bunsenges. Phys. Chem.* **91** (1987) 1922.
- 5-4 M. G. Fan, Personal communication (1996).
- 5-5 M. J. Preigh, F. -T. Lin, K. Z. Ismail and S. G. Weber, *J. Chem. Soc. Chem. Commun.* **20** (1995) 2091.
- 5-6 X. D. Sun, M. G. Fan, X. J. Meng and E. T. Knobbe, *J. Photochem. Photobiol. A: Chem.* (in press).
- 5-7 X. Y. Zhang, S. Jin, Y. F. Ming, Y. C. Liang, L. H. Yu, M. G. Fan, J. Luo, Z. H. Zuo and S. D. Yao, *J. Photochem. Photobiol. A Chem.* **80** (1994) 221.
- 5-8 J. Biteau, F. Chaput and J. -P. Boilot, *J. Phys. Chem.* **100** (1996) 9026.
- 5-9 N. W. Tyer, Jr. and R. S. Becker, *J. Am. Chem. Soc.* **92** (1970) 1295.

CHAPTER 6

NMR SPECTROSCOPIC STUDIES ON STRUCTURE OF SPIRO(1,3,3-TRIMETHYLINDOLO-2,3'-NAPHTH[1,2-*B*]-1,4-OXAZINE)

6.1. Introduction

NMR spectroscopy has been widely used as a powerful tool for structural determinations. The value of the resonance frequency of a particular nucleus depends upon molecular structure and is influenced by the distribution of electrons in the molecule and its chemical environment. All kinds of organic compounds can be identified by NMR in solution or solid state, in crystalline or non-crystalline forms. ^{6.1-6.4} NMR has been frequently used for structural elucidation of photochromic compounds, but in most cases it has been limited to identification of special functional groups or structural units. ^{6.5,6.6} To date, there are no extensive studies reporting all NMR assignments or conformational structures for a photochromic spirooxazine.

This chapter involves the application of two dimensional Homonuclear Double Quantum Filtered Correlation Spectroscopy (DQFCOSY), Heteronuclear Multiquantum Coherence Spectroscopy (HMQC), and Heteronuclear Multibond Correlation Spectroscopy (HMBC) methods to establish the full resonance assignments of photochromic spirooxazine compound and to derive its conformational structure. Complete interpretation of spiro(1,3,3-trimethylindolo-2,3'-naphth[1,2-*b*]-1,4-oxazine), SP1, is included and the chemical shifts of all proton and carbon atoms have been resolved.

It was indicated in Chapter 3, 4 and 5 that photochromic spirooxazine compounds have shown unique effect in acidified alcoholic solutions. This unique effect, which is coined as acidichromism, is described in early chapters. However, the structure of the

protonated product of SP1 or PMC1 (SP1•HCl or PMC1•HCl) is under investigation. The research described in this chapter also included the use of NMR for the structure identification of the protonated product in alcoholic solution.

6.II. *Experimental Methods*

Spiro(1,3,3-trimethylindolo-2,3'-naphth[1,2-*b*]-1,4-oxazine), SP1, was supplied by Prof. Meigong Fan as described in early chapters. Solvent *d*-chloroform was obtained from Aldrich. SP1 solutions for 2D NMR studies were prepared by dissolution of SP1 into *d*-chloroform. Deuterium chloride (D, 99.5%, DCI 20% w/w solution in D₂O) and CD₃OD were ordered from Cambridge Isotope Laboratories. SP1 solutions for proton NMR studies were prepared by dissolution of SP1 into CD₃OD.

NMR experiments were performed on a Varian UNITY INOVA 400 with a Nalorac 5-mm PFG indirect detection probe. 2D DQFCOSY, HMQC, and HMBC methods were used for resonance assignment. All measurements were taken at 30°C.

6.III. *Results and Discussion*

6.III.A. *¹H Assignments by DQFCOSY*

The chemical structure of spiro(1,3,3-trimethylindolo-2,3'-naphth[1,2-*b*]-1,4-oxazine) (SP1) is shown in Figure 6-1. The molecular formula of the identified compound is C₂₂H₂₀N₂O.

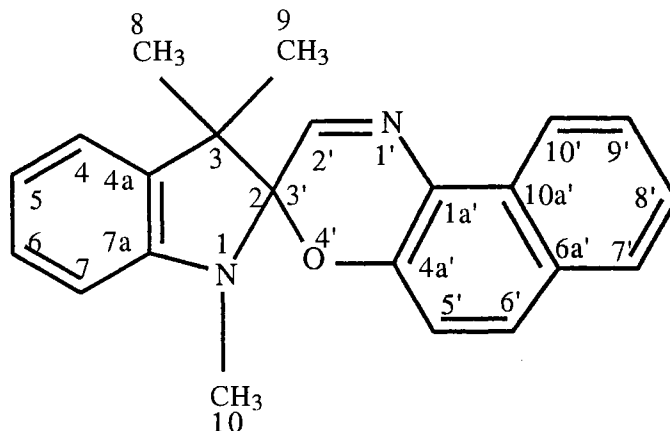


Figure 6-1. Chemical structure of spiro(1,3,3-trimethylindolo-2,3'-naphth[1,2-*b*]-1,4-oxazine) (SP1) (I)

Figure 6-1 illustrates labeled carbon positions for the SP1 molecule. Corresponding hydrogen positions are obtained using these positions. Hydrogen atoms are omitted from the figure for clarity, except in the case of methyl groups. The ^1H and ^{13}C signal assignment and confirmation were carried out by a combined use of 2D DQFCOSY, HMQC, and HMBC methods.

DQFCOSY was used to assign the ^1H spectrum of SP1. The DQFCOSY spectrum of SP1 is shown in Figure 6-2. DQFCOSY shows crosspeaks of all protons which have J coupling magnitude large than ~ 6 Hz. SP1 is expected to have three J_{HH} because of its aromatic rings. They are $J_o \approx 7\text{--}10$ Hz, $J_m \approx 2\text{--}3$ Hz and $J_p \approx 0.1\text{--}1$ Hz.^{6.3}

The only single spin system at 7.747 ppm is found in Figure 6-2. It is assigned to the 2' proton because it has no other protons as its direct neighbor. Two 4-spin systems are also observed. The first is tentatively assigned as proton 4 (7.079 ppm), 5 (6.898 ppm), 6 (7.213 ppm) and 7 (6.569 ppm). The second 4-spin system is tentatively assigned as proton 7' (7.736 ppm), 8' (7.385 ppm), 9' (7.570 ppm) and 10' (8.563 ppm). The only 2-spin system is observed and tentatively assigned as 5' (7.003 ppm) and 6'

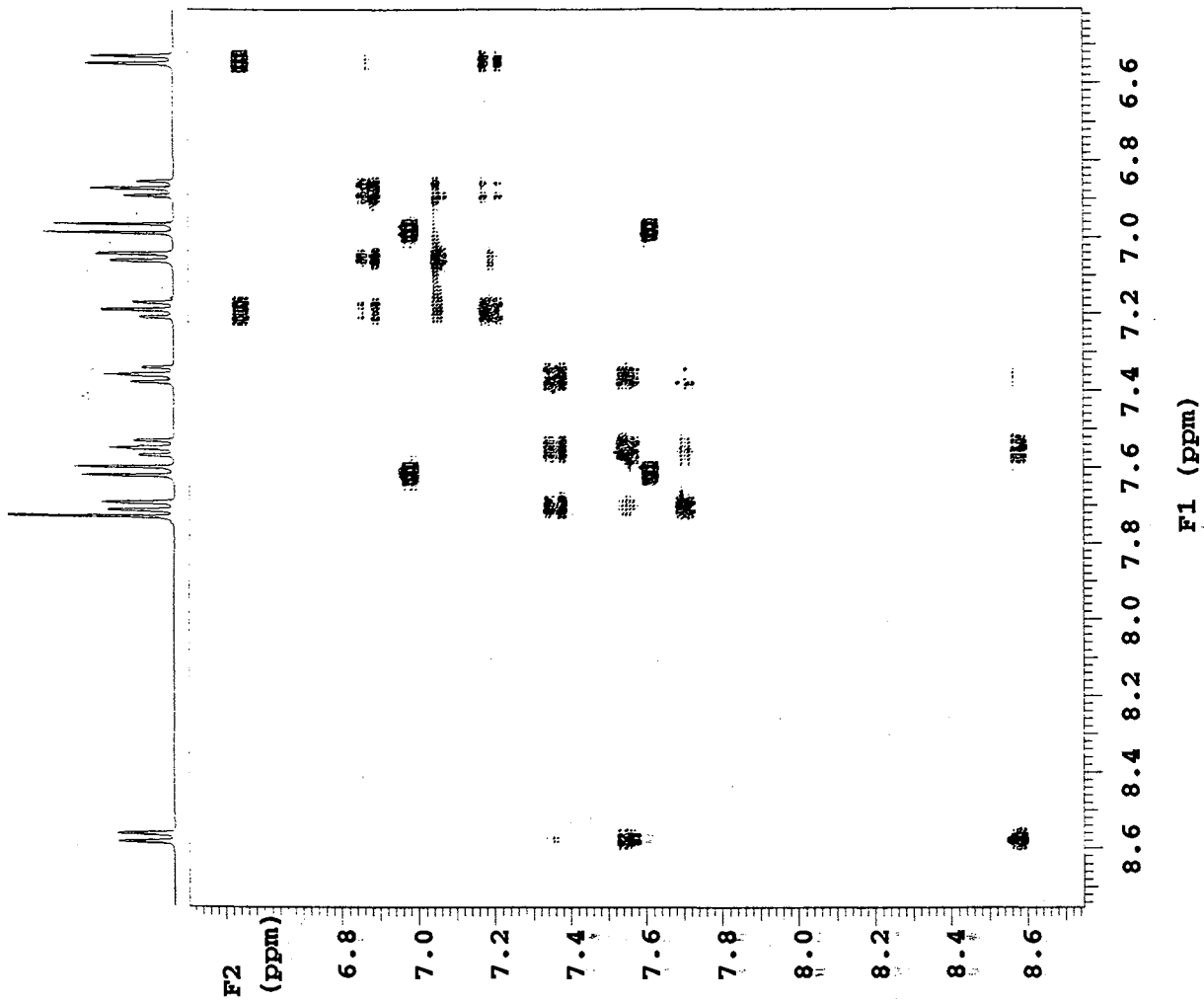


Figure 6-2 The DQF-COSY spectrum of SP1

(7.647 ppm). The tentative assignment is shown in Figure 6-3; it is confirmed by 2D-HMBC experiment as discussed in Section 6.III.B.

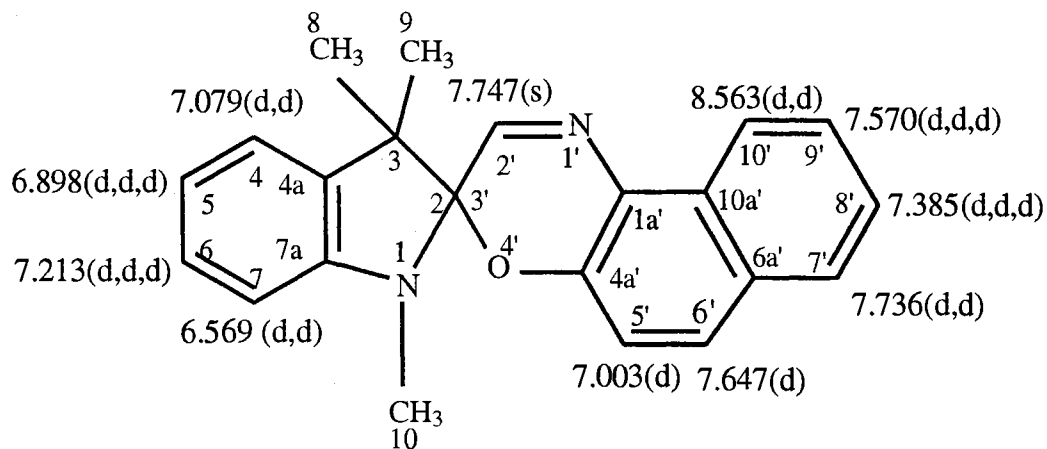


Figure 6-3. Tentative assignment of ^1H by DQFCOSY

6.III.B. ^{13}C Assignment by HMQC and HMBC

The PFG-HMQC experiment was used to assign the protonated ^{13}C resonances. The PFG-HMQC spectrum of SP1 is shown in Figure 6-4, which indicates crosspeaks between direct bonding of ^1H and ^{13}C . From Figure 6-4, one may conclude that carbons at 2(3'), 4a, 7a, 1a', 4a', 6a' and 10a' positions have no direct proton attached. The protonated ^{13}C resonances as methyl 8, 9 (20.6, 25.2 ppm), methyl 10 (29.4 ppm), 3 (51.6 ppm), 4 (121.36 ppm), 5 (119.7 ppm), 6 (127.8 ppm), 7 (107.0 ppm), 7' (127.6 ppm), 8' (124.0 ppm), 9' (126.9 ppm), 10' (121.3 ppm), 5' (116.6 ppm) and 6' (130.1 ppm). The quaternary carbon appeared at high field (51.6 ppm) is assigned to carbon 3. The carbon at low field (150.7 ppm) is associated with the singlet proton (7.747 ppm) and is assigned as carbon 2'. The result of ^{13}C assignment by PFG-HMQC is shown in Figure 6-5.

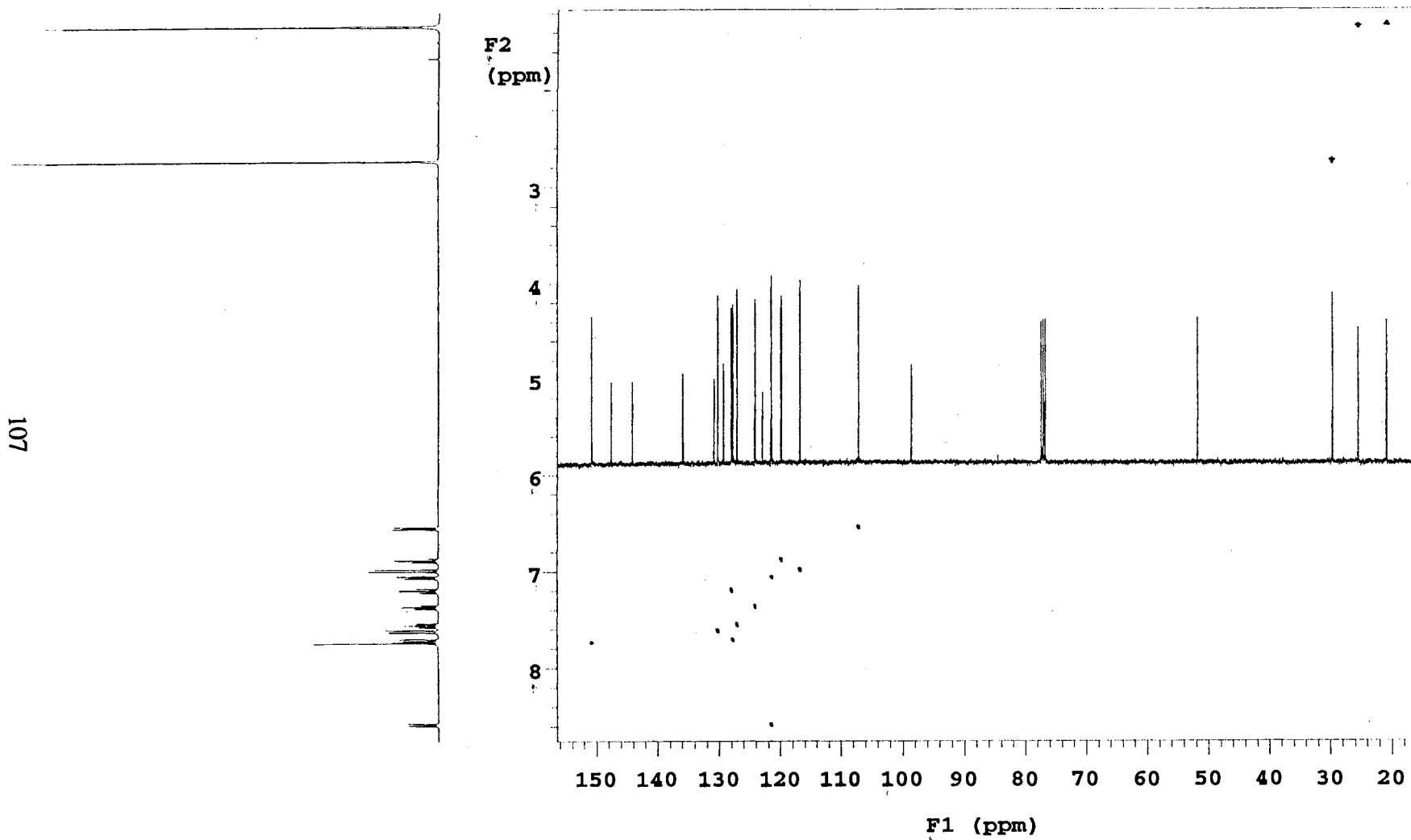


Figure 6-4 The PFG-HMQC spectrum of SP1.

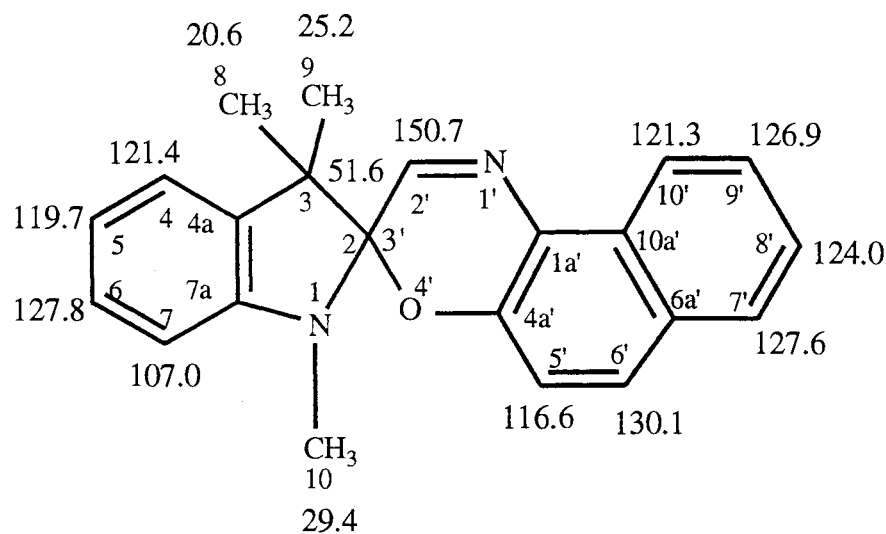


Figure 6-5. ^{13}C assignment by PFG-HMQC

Figure 6-6 shows the HMBC spectrum of SP1. Crosspeaks between ^1H and ^{13}C can be seen in HMBC experiment if their J coupling constants are about ~ 8 Hz. Proton 4 should have a crosspeak with carbon 3, and proton 7 should not have crosspeak with carbon 3. A crosspeak at (7.079 ppm, 51.6 ppm) is observed, indicating 7.079 ppm is for proton 4 instead of proton 7. Thus, the tentative assignment shown in Figure 6-3 from DQFCOSY for protons 4, 5, 6 and 7 is confirmed. For ^1H - ^{13}C long range coupling constant of aromatic compounds, $^2J_{\text{CH}}$ is about 1 Hz, $^3J_{\text{CH}}$ is about 8 Hz and $^4J_{\text{CH}}$ is about -1.2 Hz. Thus, only $^3J_{\text{CH}}$ is expected to yield crosspeaks in HMBC experiment. For hetero-aromatic ring, $^2J_{\text{CH}}$ will be about 8 Hz if proton is on the *o*-position of heteronucleus, which will also have crosspeaks in HMBC spectrum.

The assignment of carbons in the spiro ring can be made as follows. The crosspeaks related with proton 4 can be found in HMBC spectrum in Figure 6-6. *Meta* Carbons 3, 7a, and 6 are assigned because of their crosspeaks at (7.079 ppm, 51.6 ppm), (7.079 ppm, 147.4 ppm) and (7.079 ppm, 127.8 ppm), respectively. In the same way, proton 5 will have crosspeaks with *meta* carbon 4a and 7. They are at (6.893 ppm, 135.7

109

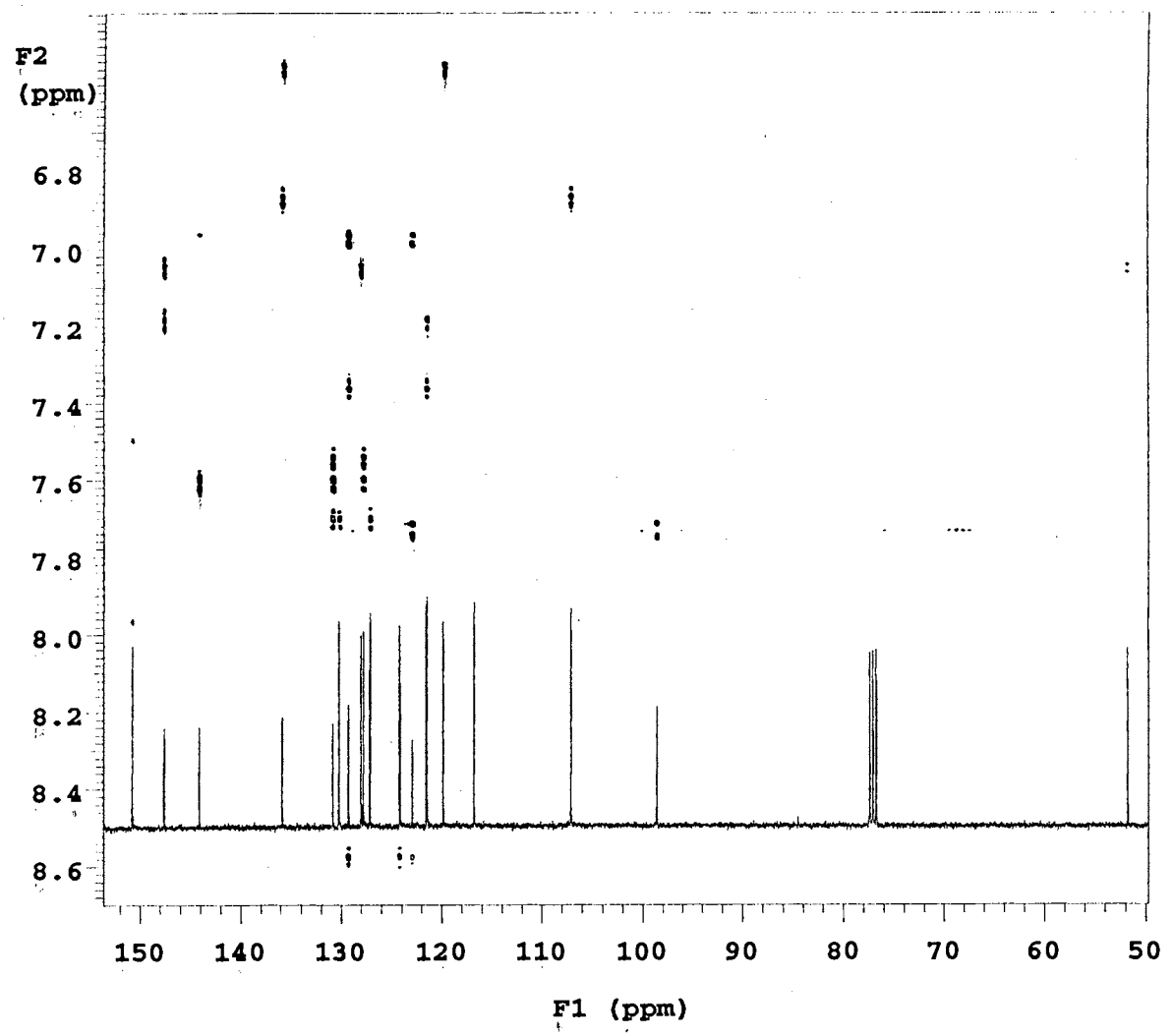


Figure 6-6 The HMBC spectrum of SP1.

ppm) and (6.893 ppm, 107.0 ppm), respectively. Proton 6 will have crosspeaks with carbon 4 and 7a, which are at (7.647 ppm, 121.4 ppm) and (7.647 ppm, 147.4 ppm), respectively. Proton 7 will have crosspeaks with carbon 5 and 4a. They are at (6.569 ppm, 119.7 ppm) and (6.569 ppm, 135.7 ppm), respectively. The assignment of proton and carbon atoms in the spiro ring is described in Figure 6-7.

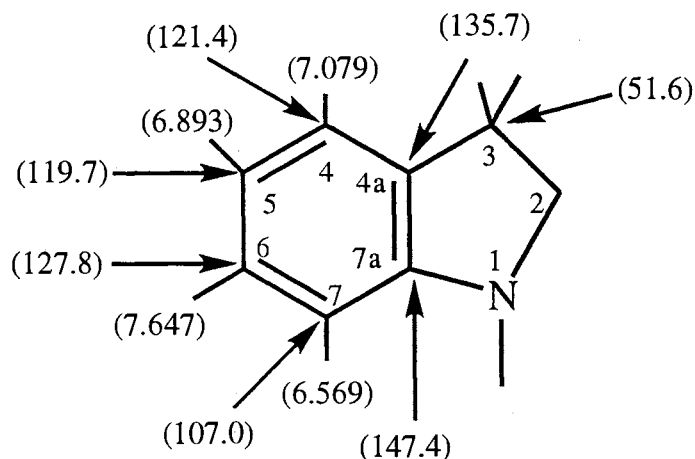


Figure 6-7. The assignment of proton and carbon atoms in the spiro ring from HMBC.

The assignment of carbon atoms in the oxazine ring can be made in the same way and the result is shown in Figure 6-8. Proton 5' will have crosspeaks with carbon 1a' and 6a'. They appear at (7.003 ppm, 122.8 ppm) and (7.003 ppm, 129.1 ppm), respectively. Proton 6' will have crosspeaks with carbon 4a', 10a' and 7'. They are at (7.647 ppm, 143.9 ppm), (7.647 ppm, 130.7 ppm) and (7.647 ppm, 127.6 ppm), respectively. Proton 2' will have crosspeaks with carbon 3' and 1a'. They are at (7.747 ppm, 98.4 ppm) and (7.747 ppm, 122.8 ppm), respectively. Proton 7' will have crosspeaks with carbon 6', 10a' and 9'. They are at (7.736 ppm, 130.1 ppm), (7.736 ppm, 130.7 ppm) and (7.736 ppm, 126.9 ppm), respectively. Proton 8' will have crosspeaks with carbon 6a' and 10'. They are at (7.385 ppm, 129.1 ppm) and (7.385 ppm, 121.31 ppm), respectively. Proton 9' will have crosspeaks with carbon 10a' and 7'. They are at (7.570 ppm, 130.7 ppm) and (7.570 ppm, 127.6 ppm), respectively. Proton 10' will have crosspeaks with carbon 1a', 6a' and

CHAPTER 7

STUDY OF ALUMINOSILICATE GELS DOPED WITH PHOTOCHROMIC SPIROOXAZINE

7.1. Introduction

Sol–gel chemistry provides new and interesting approaches in the field of material science, especially in the area of photonically-active media. Synthesis is typically performed at or near room temperature so that organic molecules, such as photochromic spirooxazine can be incorporated inside the inorganic matrix leading to new hybrid materials. ^{7.1,7.2} Solid state media are achieved through a two step reaction which involves the hydrolysis of an alkoxide precursor, such as tetramethoxysilane, followed by polycondensation. Typically, dopants are incorporated into gel hosts via dissolution of soluble species into the initial precursor sol. Solutions may be coated onto various substrates, thin films or cast into bulk monoliths. Thus, sol–gel based media appear to be promising candidates for the development of new optical device sources.

The sol–gel preparative method provides a route by which a variety of novel solid state materials may be prepared. ^{7.1-7.4} The tremendous inherent processing flexibility and potential for good optical transparency over extended regions of the visible and near IR spectrum make sol–gel materials of potential use in the development photonically-active media. Additionally, the solution synthetic aspect of sol–gel processing facilitates the incorporation of active species within the nanostructured sol–gel network. This method is easily adapted to the deposition of thin films on substrates such as optical fibers and planar waveguides by simple coating methods.

The host gel medium which serves as the basis of this work is prepared using di-*sec*-butoxyaluminumoxytriethoxysilane (DBATES), a silicon-aluminum double-alkoxide

8'. They are at (8.563 ppm, 122.8 ppm), (8.563 ppm, 129.1 ppm) and (8.563 ppm, 124.0 ppm), respectively.

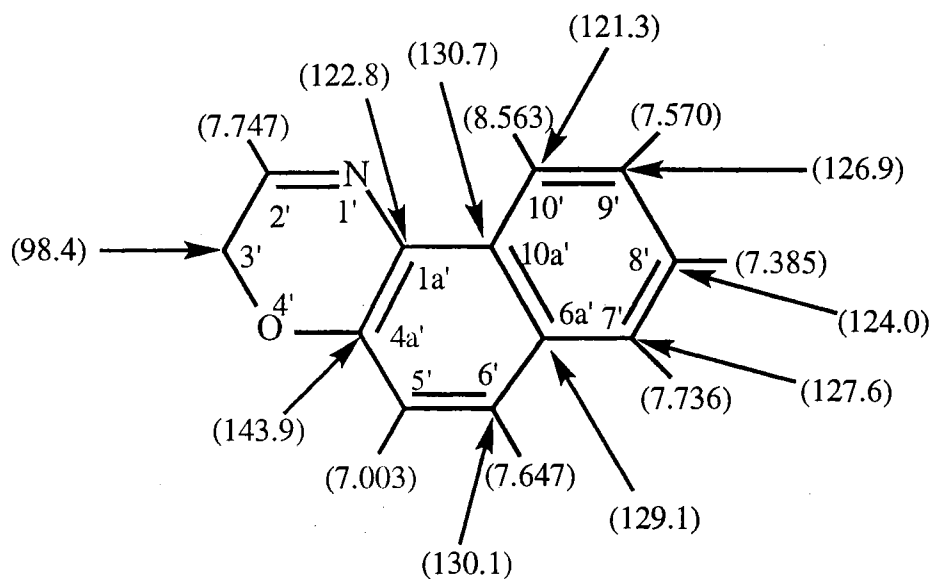


Figure 6-8. The assignment of proton and carbon atoms in the oxazine ring from HMBC.

Based on the above discussion on 2D-NMR spectroscopy, the chemical shifts of all proton and carbon atoms in SP1 have been assigned. The results are summarized as Table 6-1 and 6-2.

Table 6-1

Chemical Shifts (δ /ppm) of Protons and H-H Coupling Constants

No.	δ (ppm)	H-H coupling constants (Hz)
4	7.079, d,d(Q)	$J_{4,5} = 7.6$ Hz, $J_{4,6} = 1.2$ Hz
5	6.898, d,d,d(Hexa)	$J_{5,4} = J_{5,6} = 7.6$ Hz, $J_{5,7} = 1.2$ Hz
6	7.213, d,d,d(Hex)	$J_{6,5} = J_{6,7} = 7.6$ Hz, $J_{6,4} = 1.2$ Hz
7	6.569, d,d(Q)	$J_{7,6} = 7.6$ Hz, $J_{7,5} = 1.2$ Hz
2'	7.747, s	
5'	7.003, d	$J_{5',6'} = 8.6$ Hz
6'	7.647, d	$J_{6',5'} = 8.6$ Hz
7'	7.736, d,d(Q)	$J_{7',8'} = 8.4$ Hz, $J_{7',9'} = 1.2$ Hz,
8'	7.385, d,d,d(Hep)	$J_{8',7'} = 8.4$ Hz, $J_{8',9'} = 7.2$ Hz, $J_{8',10'} = 1.2$ Hz
9'	7.570, d,d,d(Hep)	$J_{9',10'} = 8.4$ Hz, $J_{9',8'} = 7.2$ Hz, $J_{9',8'} = 1.2$ Hz
10'	8.563, d,d(Q)	$J_{10',9'} = 8.4$ Hz, $J_{10',8'} = 1.2$ Hz
8	1.352, s	
9	1.345, s	
10	2.725, s	

Table 6-2
Chemical Shifts (δ /ppm) of Carbon Atoms

Number of carbon atom	Chemical shifts (δ /ppm)
2 (3')	98.4
3	51.6
4a	135.7
4	121.4
5	119.7
6	127.8
7	107.0
7a	147.4
2'	150.7
4a'	143.9
5'	116.6
6'	130.1
6a'	129.1
7'	127.6
8'	124.0
9'	126.9
10'	121.3
10a'	130.7
1a'	122.8
8	20.6

Table 6-2 (Continued)

9	25.2
10	29.4

6.III.C. Conformational Structure of SP1

According to structure I in Figure 6-1, the shielding effect through the bond transfer is the same for C₈ and C₉, but the chemical shift positions of two methyl groups (¹³C and ¹H) are found to be different as shown in Table 6-1 and 6-2.

In Chapter 2, the X-ray crystal analysis of similar spirooxazines indicated that benzo and naphtho rings of SP1 are planar, but the oxazine ring and pyrrole ring are nonplanar. Torsion angles of N(1')-C(2')-C(3')-O(4') and C(3')-O(4')-C(4a')-C(1a') were found to be 17.1(6)° and 14.5(5)°, respectively. Thus, a half boat conformation of the oxazine ring could be described as shown in Structure (II) in Figure 6-9.

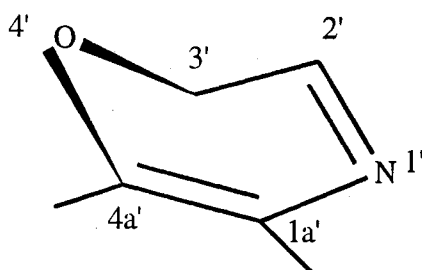


Figure 6-9. Conformational structure of oxazine ring (Structure II)

According to structure (II) in Figure 6-9, C(4a'), C(1a'), N(1'), C(2') and C(3') are almost coplanar, but the O(4') oxygen is forward out of the planar.

Concerning the dihydropyrrole ring, torsion angles of C(2)-C(3)-C(4a)-C(7a), C(2)-C(3)-C(4a)-N(1), and C(4a)-C(7a)-N(1)-C(2) were found to be 14.4(4)°, -0.5(6)°

and $-15.6(4)^\circ$ by X-ray analysis, respectively. The three torsion angles indicated that the dihydropyrrrole ring forms a chair-like conformation. Figure 6-10 shows the conformational structure of SP1 based on these interpretations.

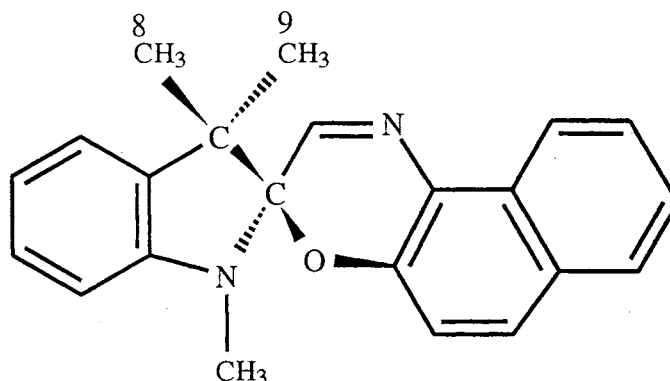


Figure 6-10. Conformational structure of SP1 (Structure III)

According to Figure 6-10, carbon 9 and its bonded hydrogen atoms in SP1 molecule are located in the deshielded area of π -electron conjugated systems. The chemical shift position of ^{13}C is expected to be larger than that of ^{13}C in the other methyl group C(8). The differences between C(8) and C(9) lie in their relationship to the remote naphthalene part of the heterocycle. The nonplanar indole 5-membered ring may also affect where C(8) and C(9) sit in the ring currents of the benzene and naphthalene rings. C(8) at 20.6 ppm must be more crowded by neighboring ^1H 's than C(9) at 25.2 ppm. In addition, methyl groups connected to a saturated tertiary carbon in liquid solution exhibit typical chemical shifts of 28.7 ppm.^{6.1} However, both C(8) and C(9) have chemical shifts much less than this value. The discrepancy may be due to the steric crowding effects between C(8) and C(9) methyl groups with C(2') hydrogen, which results in upfield chemical shift. The results presented indicated the conformational structure derived from X-ray analysis agrees with the NMR data.

6.III.D. *Structure Determination of the Protonated Product of SP1*

Figure 6-11 shows the 1D proton spectrum of SP1 in CD₃OD solvent. The single peak at 2.725 ppm was assigned as proton 10 (Table 6-1). This methyl group is directly bonded to the nitrogen in the spiro ring.

Figure 6-12 shows the 1D proton NMR spectrum of SP1 in CD₃OD solvent after addition of DCl in CD₃OD. The peak at 2.725 ppm almost disappeared, and a new peak at 4.235 ppm is found in Figure 6-12. The proton chemical shift of this methyl appeared at low field, indicating that a conjugated ring system may have formed as a result of protonation. All of the aromatic chemical shifts also appear to change, further evidence for ring opening. The photoproduct of SP1, PMC1 species, is postulated to react with HCl to generate a more stable form, PMC1•HCl, under such conditions. The chemical structure of protonated product of the open form (PMC1•HCl) was proposed in Figure 3-4 in Chapter 3.

Protons are not assigned in Figure 6-12, but clearly there are large changes to both the benzene and naphthalene rings. This result may be useful for the identification of an acidichromic product, and provide more information on the mechanism of the associated acid-base chemistry.

6.IV. *Summary and Conclusions*

High resolution ¹H and ¹³C NMR signals were completely assigned for photochromic compound spiro(1,3,3-trimethylindolo-2,3'-naphth[1,2-*b*]-1,4-oxazine). The signal assignments were performed using 2D DQFCOSY, HMQC and HMBC methods. NMR data is consistent with the result from X-ray structure analysis on conformational structure of spirooxazine. The protonated product of SP1 and/or PMC1 was investigated by proton NMR spectrum. The results presented here indicate NMR spectroscopy method could be potentially used to identify the functional groups and

provide much information on the conformational structure of organic photochromic compounds.

6.V. References

- 6-1 E. Breitmaier, "Structure Elucidation by NMR in Organic Chemistry", J. Wiley & Sons, New York, 1993.
- 6-2 H. Gunther, "NMR Spectroscopy", J. Wiley & Sons, New York, 1992.
- 6-3 E. O. Stejskal, "High Resolution NMR in the Solid State: Fundamental of CP/MAS", Oxford University Press, New York, 1994.
- 6-4 E. Breitmaier and W. Voelter, "Carbon-13 NMR Spectroscopy", VCH Verlagsgesellschaft mbH, D-6940 Weinheim, 1987.
- 6-5 M. Magust, M. LeBaccon, Y. Poirier and R. Guglielmetti, *Can. J. Chem.* **60** (1982) 2544.
- 6-6 A. Samat, G. Martin and R. Guglielmetti, *C. R. Acad. Sci.* **279C** (1972) 573.

sp-1, small filter in 1H channel, CD3OD
as solvent

exp5 presat

SAMPLE		SATURATION	
date	Oct 30 96	sspul	n
solvent	CD3OD	satpwr	0
file	/data2/i400_1-	satfrq	-72.0
-5-97/Knobbe/oct30-		satdly	1.500
qf_sp-1_CD3OD_1H		satmode	ynn
ACQUISITION		composit	n
sfrq	399.939	DEC. & VT	
tn	H1	dn	H1
at	2.008	dof	-72.0
np	16064	dm	nnn
sw	4000.0	dmm	c
fb	2000	dmf	200
bs	16	temp	27.0
ss	2	PROCESSING	
tpwr	52	wtfile	
pw	6.1	proc	ft
d1	0	fn	32768
tof	-72.0	math	f
nt	16		
ct	16	werr	
alock	n	wexp	
gain	36	wbs	
FLAGS		wnt	
il	n	DISPLAY	
in	n	sp	84.0
dp	y	wp	3833.2
hs	nn	vs	447
		sc	20
		wc	160
		hzmm	23.96
		is	500.00
		rfl	61.8
		rfp	0
		th	20
		ins	1.000
		ai	cdc ph

118

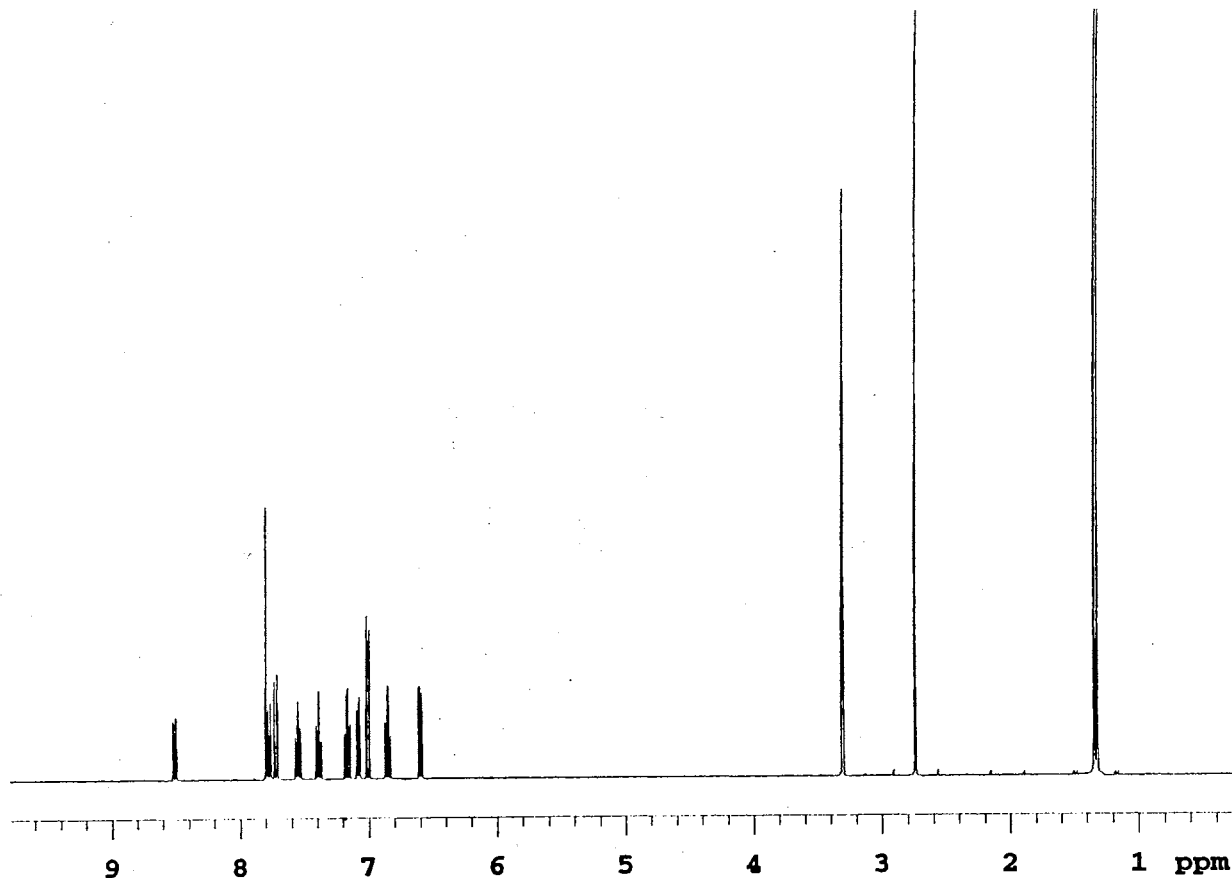


Figure 6-11 Proton spectrum of SP1 in CD₃OD solvent

sp-1, small filter in 1H channel, CD3OD
 as solvent, added DCl, then wait for 5 h
 rs.

exp6 presat

SAMPLE		SATURATION	
date	Oct 30 96	sspul	n
solvent	CD3OD	satpwr	0
file	/data2/i400_1-	satfrq	64.8
	-5-97/Knobbe/oct30-	satdly	1.500
qf_sp-1_acid-after-		satmode	yy
	-5hra_1H	composit	n

ACQUISITION		DEC. & VT	
sfrq	399.939	dn	H1
tn	H1	dof	64.8
at	2.007	dm	nnn
np	19264	dmm	c
sw	4799.9	dmf	200
fb	3000	temp	27.0

		PROCESSING	
bs	16	wtfile	
ss	2	proc	ft
tpwr	52	fn	32768
pw	6.1	math	f
d1	0		
tof	64.8		
nt	32	werr	
ct	32	wexp	
alock	n	wbs	
gain	36	wnt	

FLAGS		DISPLAY	
il	n	sp	39.3
in	n	wp	3562.4
dp	y	vs	487
hs	nn	sc	20
		wc	160
		hzmm	22.26
		is	500.00
		rfl	323.2
		rfp	0
		th	20
		ins	1.000
		ai	cdc ph

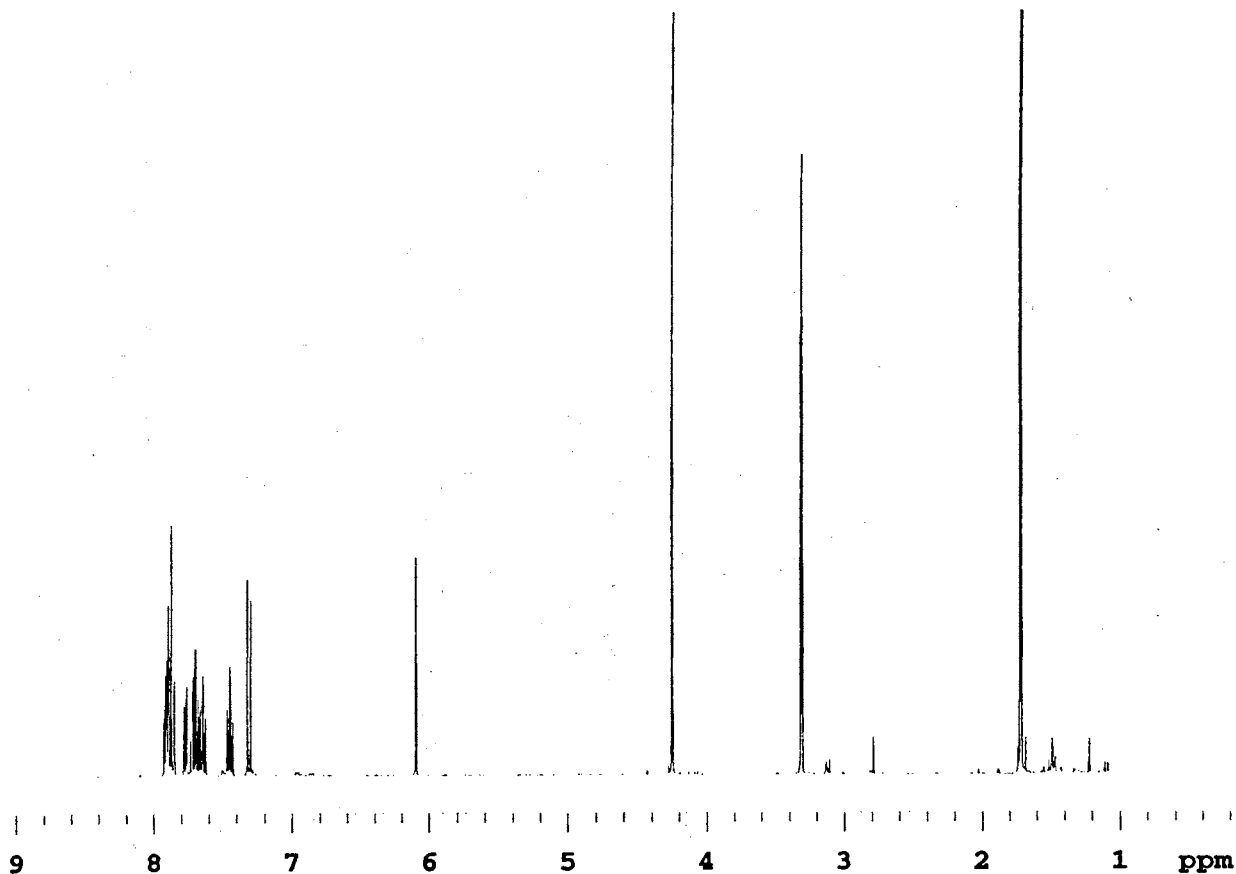


Figure 6-12 Proton NMR spectrum of SP1 after addition of DCl in CD₃OD

CHAPTER 7

STUDY OF ALUMINOSILICATE GELS DOPED WITH PHOTOCHROMIC SPIROOXAZINE

7.1. Introduction

Sol–gel chemistry provides new and interesting approaches in the field of material science, especially in the area of photonically-active media. Synthesis is typically performed at or near room temperature so that organic molecules, such as photochromic spirooxazine can be incorporated inside the inorganic matrix leading to new hybrid materials. ^{7.1.7.2} Solid state media are achieved through a two step reaction which involves the hydrolysis of an alkoxide precursor, such as tetramethoxysilane, followed by polycondensation. Typically, dopants are incorporated into gel hosts via dissolution of soluble species into the initial precursor sol. Solutions may be coated onto various substrates, thin films or cast into bulk monoliths. Thus, sol–gel based media appear to be promising candidates for the development of new optical device sources.

The sol–gel preparative method provides a route by which a variety of novel solid state materials may be prepared. ^{7.1-7.4} The tremendous inherent processing flexibility and potential for good optical transparency over extended regions of the visible and near IR spectrum make sol–gel materials of potential use in the development photonically-active media. Additionally, the solution synthetic aspect of sol–gel processing facilitates the incorporation of active species within the nanostructured sol–gel network. This method is easily adapted to the deposition of thin films on substrates such as optical fibers and planar waveguides by simple coating methods.

The host gel medium which serves as the basis of this work is prepared using di-*sec*-butoxyaluminumoxytriethoxysilane (DBATES), a silicon-aluminum double-alkoxide

Practical device considerations for sol-gel synthesis dictate the encapsulation of monomeric photofunctional compounds into a stable, chemically inert solid state host matrix. Development of photonically-active media requires a good understanding of the structure of doped sol-gel networks and of the conditions that the oxide matrix imposes on the dopant at a molecular level. Such interactions have important effects on the optical properties of entrapped photonically-active species.^{7.4-7.6} Spiro(1,3,3-trimethylindolo-2,3'-naphth[1,2-*b*]-1,4-oxazine), SP1, hereinafter, has been used to investigate as a probe within the gel network at the molecular level.

This chapter is focused on the characterization of spirooxazine-doped aluminosilicate gel specimens. The studies of the nature of spectroscopic changes to SP1 doped in transparent gels prepared by the sol-gel process have been carried out. Changes to the spectral character of spirooxazine dopant yielded insights into the evolution of the DBATES-derived gel due to the strong influence exerted by the local chemical environment on the luminescent photochromic guest.

7.II. *Experimental Methods*

7.II.A. *Materials and Sample Preparation*

Spiro(1,3,3-trimethylindolo-2,3'-naphth[1,2-*b*]-1,4-oxazine) was synthesized from 2-methylene-1,3,3-trimethylindoline and 1-nitroso-2-naphthol by Prof. Meigong Fan as detailed elsewhere.^{7.7} The DBATES precursor was obtained from United Chemical Technology and used without further purification. Anhydrous reagent grade isopropanol was purchased from the Fisher Scientific Company. The water was deionized and distilled.

Bulk gel specimens were prepared using a modified sol-gel process which was previously reported by Pouxviel *et al.*^{7.1-7.3} Briefly, the DBATES precursor was diluted using isopropanol to get a 1:1 volume ratio binary solution (solution 1). A

separate solution containing a 1:1 volume ratio of water to isopropanol was prepared. SP1 was dissolved in the latter, forming solution 2. Solution 2 was subsequently added, in a dropwise fashion with constant stirring, to solution 1, producing the initial sol. The final SP1 concentration was 0.1 mM. The resultant sol was hydrolyzed in a covered container at room temperature overnight, poured into 1×1×4.5 cm³ polystyrene cuvettes, covered, and allowed to gel. Gellation of specimens prepared in this manner occurred within three days. Gels were aged in the covered cuvettes for two weeks. After aging, the covers were perforated to allow solvent evaporation. Gel specimens were allowed to dry under ambient conditions for three weeks until air-stable xerogels were obtained. Optical characteristics of the precursor solutions, aged gels, and air-stable xerogels were periodically determined. The dopant molecular number densities (N_D) of entrapped SP1 in the air-stable xerogel specimens were calculated, based upon the final dimensions of the bulk monoliths, to be $8.2 \times 10^{16} \text{ cm}^{-3}$.

7.II.B. Apparatus and Spectral Measurements

The ultraviolet excitation source was a model 160-W UV Lamp (Fisher Scientific Company) with peak emission at 365 nm and a manufacturer-specified irradiation intensity of 11,600 $\mu\text{W}/\text{cm}^2$. Absorbance spectra were determined using a Cary 5E spectrophotometer (2.0 nm spectral band pass). Continuous wave front face excitation and emission spectra were measured using a Spex Industries Model F112A spectrofluorimeter; excitation and emission band passes were 1.85 and 0.86 nm, respectively. All luminescence spectra were collected in the dark at room temperature and corrected for instrumental response.

7.III. Results and Discussion

7.III.A. SP1 Spectra in the DBATES

Curve 1 of Figure 7-2 shows the fluorescence emission spectra of SP1 doped aluminosilicate sol excited at 370 nm. The intense emission band centered at 430 nm was observed to remain essentially unchanged over excitation wavelengths ranging from 320 to 370 nm. A much smaller peak, which is not apparent on the primary scale shown, can be found at 643 nm in Curve 2 (intensity increased 10-fold with respect to Curve 1). This weak 643 nm emission band was also observed when an excitation wavelength of 540 nm was used as shown as Curve 1 in Figure 7-3.

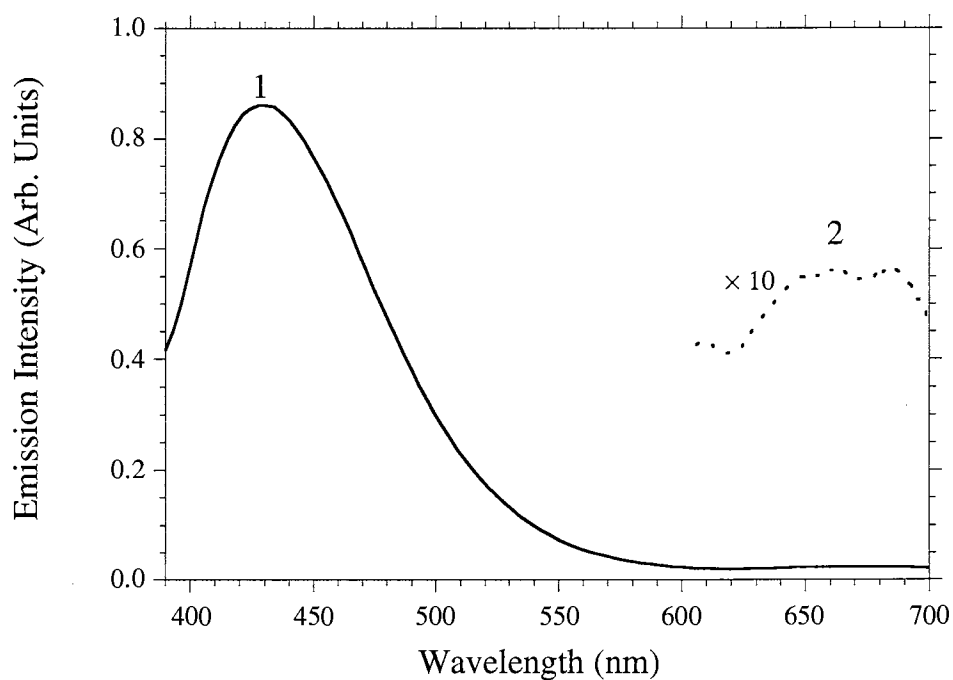


Figure 7-2. Fluorescence emission spectra of SP1 doped DBATES sol, $\lambda_{\text{ex}} = 350$ nm.

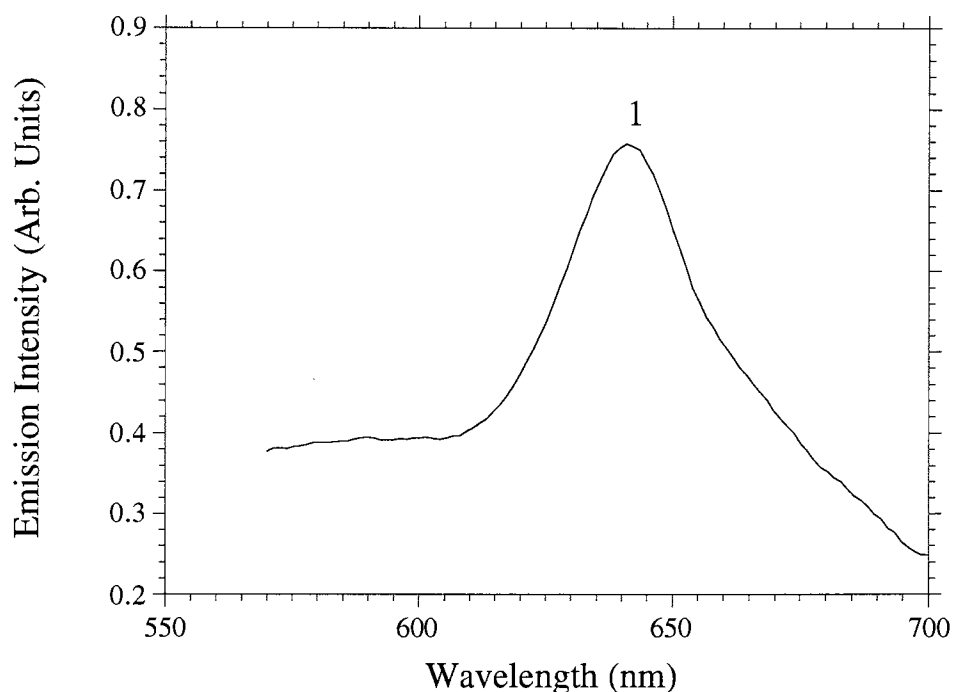
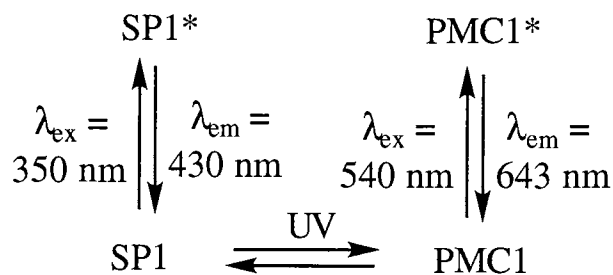


Figure 7-3. Fluorescence emission spectra of SP1 doped DBATES sol, $\lambda_{\text{ex}} = 540$ nm.

These results may be interpreted as follows: An equilibrium state exists between SP1 and PMC1 in the DBATES sol, as indicated in Figure 7-4. The intense emission band centered at 430 nm (Curve 1 of Figure 7-2) is assigned to radiative relaxation from the lowest excited singlet state of SP1. The weak 643 nm (Curve 2 of Figure 7-2) emission band is attributed to radiative relaxation from the lowest excited singlet state of PMC1, which is present at low concentration in the sol. The PMC1 \rightarrow PMC1* transition has a smaller energy gap, and for this transition is more efficiently probed using the 540 nm excitation wavelength (Curve 1 of Figure 7-3). The intense 643 nm emission band (PMC1 \rightarrow PMC1*) is easily observed, to the exclusion of a high energy SP1 \rightarrow SP1* transition.



(where * denotes an excited singlet state)

Figure 7-4. An equilibrium between SP1, PMC1 and their excited states.

The emission band of PMC1 is not observable in pure isopropanol solution, where strong solute–solvent interactions dominate. It is expected that such interactions provide a very rapid collisional nonradiative deactivation pathway for electronically excited states. In the sol stage, however, the viscosity has greatly increased, due to oligomerization in the sol, with respect to alcoholic solution. Thus, the PMC1 product may be spectroscopically observed in the sol even though it is not readily studied in alcoholic solution.

Photochromic effects were studied in the sol as given in Figure 7-5. The optical absorption spectrum of SP1 dissolved in an aluminosilicate sol is shown in Curve 1 of Figure 7-5. This spectrum consists of two absorption shoulders peaking at 320 nm and 350 nm, in the absence of UV irradiation, and corresponds to the SP1 form of the molecule. After 2 minutes of UV irradiation, a new absorption band centered at 610 nm appeared (Curve 2 of Figure 7-5). The onset of a 610 nm absorption band is associated with the formation of the ring-opened merocyanine or PMC1 conformation, a result which is consistent with findings reported by Schneider *et al.* using laser photolysis methods.^{7.8}

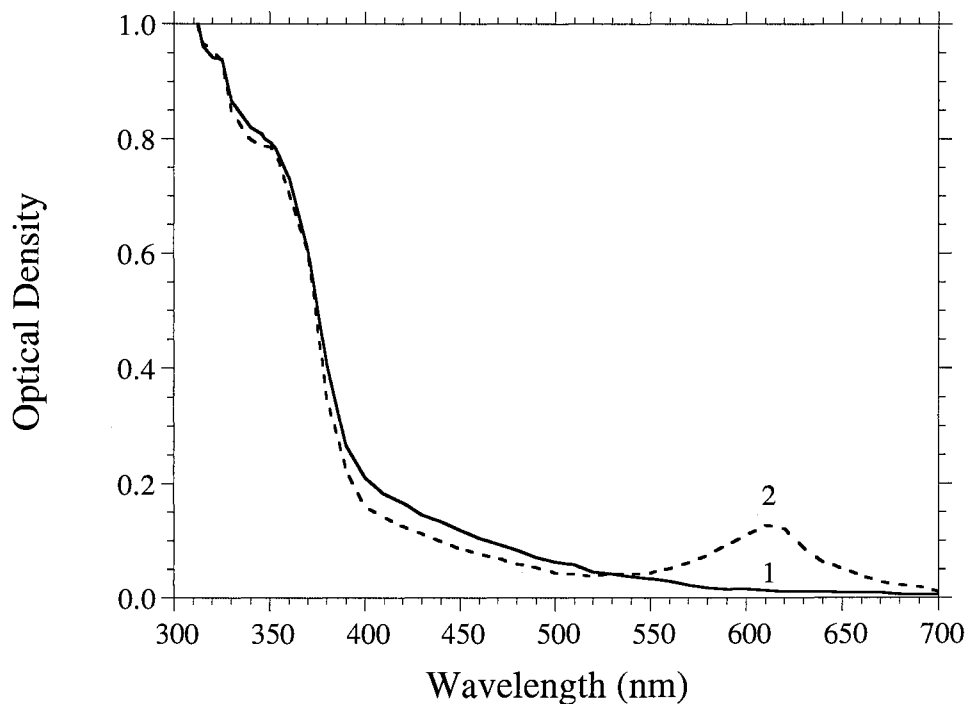


Figure 7-5. Absorption spectra of SP1 doped DBATES sol
 (1). before UV irradiation; (2). after 2-min. UV irradiation.

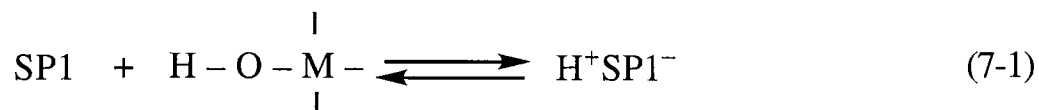
The PMC1 form exhibited a lifetime of approximately 20 seconds in the aluminosilicate sol, a relaxation rate which is much slower than that observed in common solutions, which typically has a lifetime of approximately 0.5 seconds in acetonitrile.^{7.9} This result is consistent with the higher local viscosity in the DBATES sol, showing the molecular rearrangement responsible for the regeneration of SP1 from PMC1. Other mechanisms, such as SP1 molecule binding with the oligomeric fragments in the sol, may also be used to explain this phenomenon.

The most dramatic macroscopically-observed physical changes occur during gellation, when the initial sol is transformed into a rigid solid. At gellation the solvent phase consists of excess isopropanol and water with the additional ethanol and butanol

produced by the hydrolysis of the DBATES alkoxy groups. In an unaged gel, solvated dopants such as SP1 are not constrained by the ramified and open gel structure. Thus, the luminescence spectra of SP1 and PMC1 species in the unaged gel are essentially the same as those observed for these species in a liquid solution.

7.III.B. SP1 Spectra in the Aged Gel

During aging, the gel is kept in a closed container and no evaporation of the organic molecules occurred. Thus, a substantial amount of solvent remains in the 2-phase matrix of an aged gel. The fluorescence spectra of an aged SP1-doped specimen are shown in Figure 7-6. The fluorescence band centered at 440 nm (Curve 1 of Figure 7-6; $\lambda_{\text{ex}} = 370$ nm) is essentially the same as that observed in the sol (Curve 1 of Figure 7-2). An intense new fluorescence band, centered at 540 nm, was observed when the excitation wavelength was increased to 435 nm (Curve 2 of Figure 7-6). This band is quite similar to one found in isopropanol solutions acidified by the addition of HCl as shown as Figure 5-2 in Chapter 5.^{7,10} This band was previously assigned to the protonated product of SP1, $\text{SP1} \cdot \text{HCl}$, in acidic alcoholic solution. The absence of HCl from the preparation, however, necessitates consideration of other possibilities. It is proposed the formation of a new species in the aged gel, which is postulated to be the protonated product of SP1 by acidic metal hydroxide sites in the aluminosilicate network according to equation 7-1:



where M represents Si or Al, and the product is the protonated product.

When the excitation wavelength was increased to 540 nm, in addition to the

weak emission band centered at 643 nm (previously attributed to singlet state emission from (PMC1)*, see Curve 2 of Figure 7-2), a new band centered at 580 nm was also observed (Curve 3 of Figure 7-6).

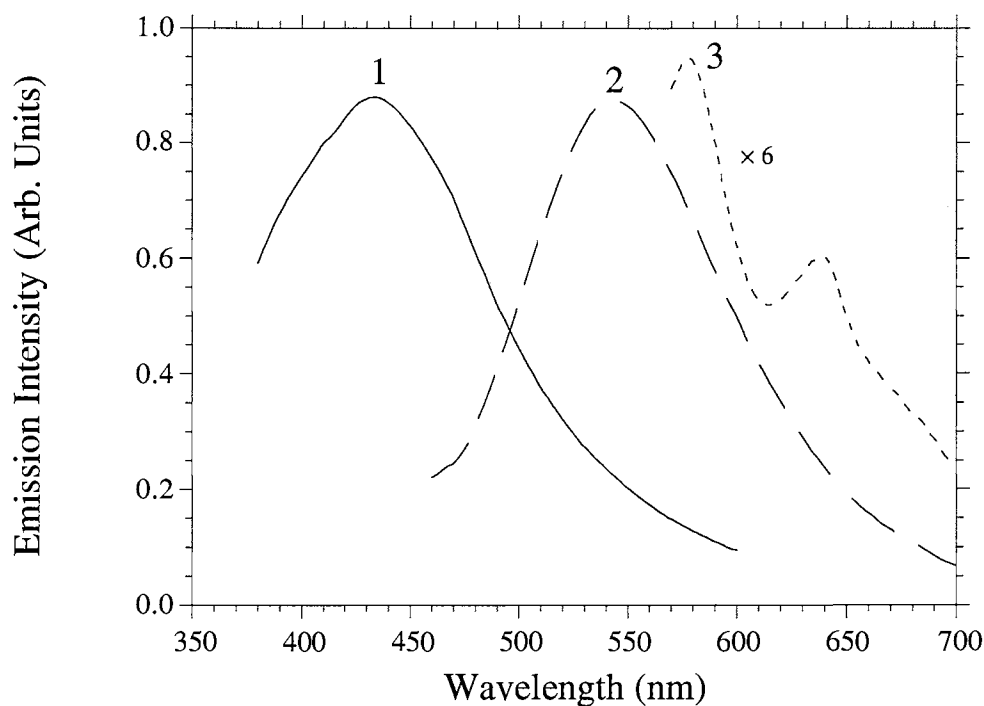
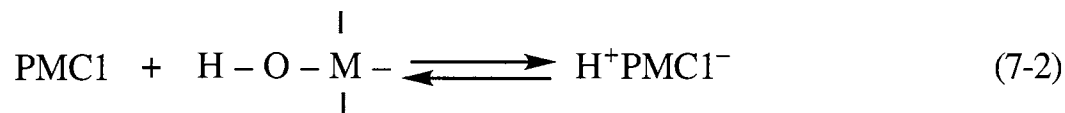


Figure 7-6. Fluorescence emission spectra of SP1 doped aluminosilicate aged gel at different excitation wavelength.

(1). $\lambda_{\text{ex}} = 370 \text{ nm}$; (2). $\lambda_{\text{ex}} = 430 \text{ nm}$; (3). $\lambda_{\text{ex}} = 540 \text{ nm}$.

It is suggested that the new band results from the excited state of a protonated product of PMC1. Similar to SP1, the photochromic compound PMC1 (Figure 7-1) may also interact with acidic metal hydroxide sites to yield the acidichromic product of PMC1, as shown in equation 7-2:



Aged aluminosilicate gels consist of network polymers formed by Si–O–Si, Si–O–Al and Al–O–Al linkages. These systems contain large quantities of charged polar species such as Si–OH and Al–OH groups. SP1 and PMC1 may interact electrostatically with these inorganic species, resulting in the formation of the protonated product such as, SP1•HO-M and PMC1•HO-M type. The ready formation of open-form merocyanine conformers indicates that the aged gel is still comparatively low in density, permitting the necessary molecular rearrangement of SP1 to proceed.

Photochromic behavior of SP1 is retained in the solvent-rich aged gels, as shown in Figure 7-7. Curve 1 of Figure 7-7 shows the absorption spectrum prior to UV irradiation. Two shoulders on the main UV absorption band, peaking at 320 nm and 350 nm, were observed. These shoulders correspond to the presence of the SP1 conformation as previously seen in Curve 1 of Figure 7-5. The intense absorption band centered at 450 nm, which is not seen in Figure 7-5, is assigned to the acidichromic product of SP1 (simplified as SP1•HO-M species). After 2 minutes of 365 nm irradiation, an intense peak centered at 560 nm was observed (Curve 2 of Figure 7-7).

It is believed that the new band, centered at 560 nm, results from the formation of a protonated product of photomerocyanine derived from SP1•HO-M (*e.g.*, PMC1•HO-M). Thus, photochromic effects which are observed in SP1 aluminosilicate sols are also observed for aged gels containing the acidichromic product. Photochromic effects in the aged gels were found to be completely reversible. This result is very similar to the acidichromic effects previously reported for SP1 in alcoholic solutions.^{7.10}

The colored protonated product of merocyanine (PMC1•HO-M) generated by

irradiation with ultraviolet light slowly decays, by a thermally activated mechanism, to $SP1 \bullet HO-M$. The thermal decay event obeys first order kinetics with a rate constant of 0.359 min^{-1} at room temperature (correlation coefficient is 0.992). Because of the interactions between the photochromic compound and condensing polymeric host material, the decay process in the aged gel is orders of magnitude slower than that in alcoholic solutions.

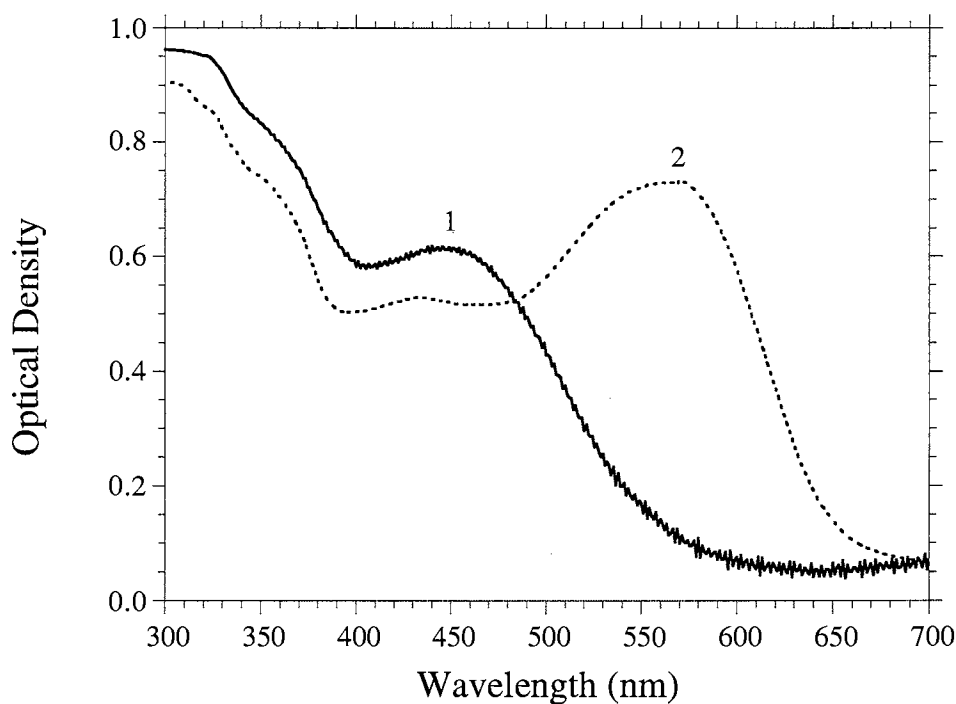


Figure 7-7. Absorption spectra of SP1 doped aluminosilicate aged gel. (1). before UV irradiation; (2). after 2-min. UV irradiation.

7.III.C. *SP1 Spectra in Air-stable Xerogel Specimens*

The third stage of the process is the drying of the gel. When the free solvent species evaporate, the aluminosilicate gel structure collapses and the gel shrinks dramatically. The final volume is approximately one fifth that of the aged wet gel. The

oxide network becomes substantially more compact, and the flexibility decreases with the departure of the solvent. This state is typically referred to as the xerogel phase.

The four species SP1, PMC1, acidichromic product of SP1 (SP1•HO-M) and acidichromic product of PMC1 SP1•HO-M are found in the xerogel stage as shown in Figure 7-8. As discussed earlier, the intense emission band at 460 nm is from the lowest excited singlet state of SP1. This band exhibited a bathochromic shift of 30 nm compared with the result in the aluminosilicate sol, which is due to the changes in matrix rigidity at this stage. This phenomenon was previously reported by Dunn *et al.* for bipyridyltriscarbonylchlororhenium(I), $\text{ReCl}(\text{CO})_3\text{bipy}$ and was described as rigidochromism.^{7,11} The 643 nm peak is from the photochromic product PMC1. The acidichromic product SP1•HO-M is responsible for the fluorescence band centered at 540 nm, whereas PMC1•HO-M is for the peak centered at 580 nm. All four species are also observable at the final stage of the xerogel. However, photochromic behavior is not observed for DBATES-type xerogels because of the acidichromic effects, matrix rigidity changes and solvent loss. The results are of importance for the understanding of interactions between dopant and matrix and provide insight regarding the preparation of photochromic media. The issue of developing a novel, air-stable, solid state photochromic material using sol-gel processing is examined in the next chapter.

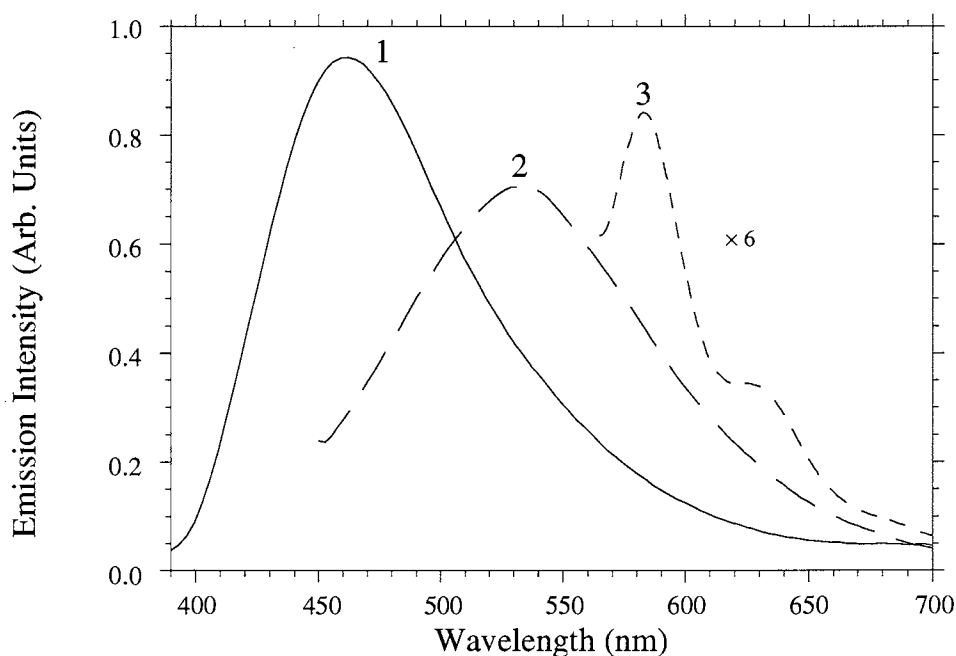


Figure 7-8. Fluorescence emission spectra of SP1-xerogel at different excitation wavelength. (1). $\lambda_{\text{ex}} = 370 \text{ nm}$; (2). $\lambda_{\text{ex}} = 435 \text{ nm}$; (3). $\lambda_{\text{ex}} = 540 \text{ nm}$.

7.IV. Summary and Conclusions

The photochromic compound, SP1, is found to be sensitive to changes in the local environment associated with the various stages of the sol-gel process. The sol, aged gel and xerogel transitions can be monitored by the evolution of absorption, luminescence and photochromic behavior of SP1 doped into the aluminosilicate host gel. Photochromism is retained through the aged gel stage, but is lost in the initial air-stable xerogel. The appearance of new fluorescence peaks, such as those shown in Figure 7-6, is consistent with the formation of protonated product of the probe chromophore by HO-M surface groups in the gel. The observed rigidochromism is in

good agreement with the result previously reported by Dunn.^{7.11} This result also agrees with the previous report of SP1 in alcoholic solution with the formation of protonated product spirooxazine•HCl as detailed in chapter 3, section 3.

7.V. References

- 7-1 J. C. Pouxviel, J. P. Boilot, J. P. Lecomte and A. Dager, *J. Phys. Paris* **48** (1987) 921.
- 7-2 D. Preston, J. C. Pouxviel, T. Novinson, W. Kaska, B. Dunn and J. I. Zink, *J. Phys. Chem.* **94** (1990) 4167.
- 7-3 L. M. Yates, III, X. -J. Wang and E. T. Knobbe, *J. Sol–Gel. Sci. Technol.* **2** (1994) 745.
- 7-4 D. Preston, J. C. Pouxviel, T. Novinson, W. Kaska, B. Dunn and J. I., Zink, *J. Phys. Chem.* **94** (1990) 4167.
- 7-5 D. Levy, S. Einhorn and D. Avnir, *J. Non-Cryst. Solids* **113** (1989) 137.
- 7-6 D. Levy and D. Avnir, *J. Phys. Chem.* **92** (1988) 4734.
- 7-7 X. Y. Zhang, S. Jin, Y. F. Ming, Y. C. Liang, L. H. Yu, M. G. Fan, J. Luo, Z. H. Zuo and S. D. Yao, *J. Photochem. Photobiol. A: Chem.* **80** (1994) 221.
- 7-8 S. Schneider, A. Mindl, G. Elfinger and M. Melzig, *Ber. Bunsenges. Phys. Chem.* **91** (1987) 1922.
- 7-9 C. Bohne, M. G. Fan, Z. J. Li, Y. C. Liang, J. Luszyk and J. C. Scaiano, *J. Photochem. Photobiol. A: Chem.* **66** (1992) 79.
- 7-10 X. D. Sun, M. G. Fan, X. J. Meng and E. T. Knobbe, *J. Photochem. Photobiol. A: Chem.* (in press).
- 7-11 J. Mckiernan, J. C. Pouxviel, B. Dunn and J. I. Zink, *J. Phys. Chem.* **93** (1989) 2129.

CHAPTER 8

PREPARATION OF AIR-STABLE PHOTOCHROMIC XEROGEL USING SPIROOXAZINE DOPANTS

8.1. Introduction

The low temperature synthesis of inorganic oxide glasses by the sol-gel method allows the incorporation of organic molecules into the gel matrices. 8.1,8.2 Unlike most of the other sol-gel matrices, organically modified silicates (ORMOSILs) possess organic functionality, such as acrylate, epoxide, 1,2-ethanediol, *etc.* The precursor for the epoxy ORMOSIL preparation is 3-glycidoxypropyltrimethoxysilane (GPTMS, an epoxy modified silicate). The chemical structure of GPTMS is shown in Figure 8-1. The GPTMS has three hydrolyzable alkoxide groups which will form Si-O-Si linkages upon complete condensation. After the alkoxide hydrolysis and condensation reactions, a hybrid organic/inorganic polymer can be formed by crosslinking of the organic phase. Thus, ORMOSILs are widely used in sol-gel synthesis for the purpose of making photonically-active media. 8.3,8.4

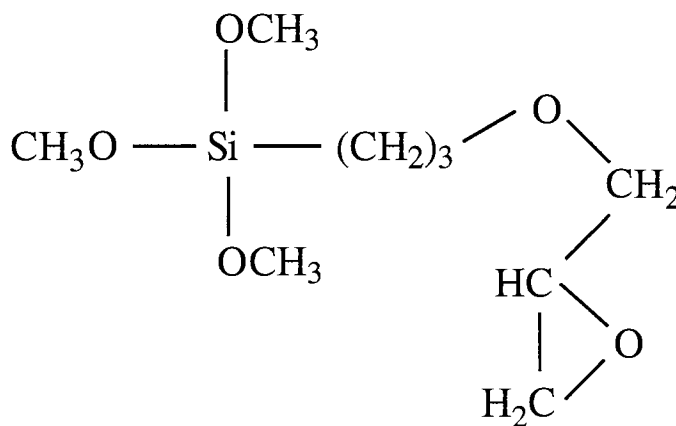


Figure 8-1. Chemical structure of 3-glycidoxypropyltrimethoxysilane (GPTMS)

they must be dissolved in an appropriate solvent. Device applications dictated the use of all solid state media. The goal with the work described in this chapter is the development of a solid state spirooxazine-doped medium that retain its photochromic character in an air-stable form.

The studies on preparation of sol-gel derived photochromic materials have been of interest to many researchers. Avnir *et al.* 8.1,8.6-8.8 were the first to study the photochromic dye aberchrome-670 and spiropyran in sol-gel. They observed unusual optical properties in these materials using tetramethoxysilane or polydimethylsiloxane precursors. They concluded that the photochromic behavior was strongly tied to the polarity of the cage within which chromophores were prepared. reverse photochromism They found that the photomerocyanine form of spiropyran compound was stabilized by strong hydrogen bonds to silanols of the cage. Thus, the stable state for spiropyran in these gel hosts was the PMC rather than the spiro form. They termed this behavior as reverse photochromism. Previous work on the encapsulation of photochromic compounds included two major motivations: First, photochromic glasses used in the real world are based on a very limited selection of inorganic dopants. The ability to entrap photochromic materials in sol-gel glasses provides the possibility to use a much wider variety of photochromic molecules to tailor desired properties such as the nature of photochromism. The successful preparation of solid state photochromic materials using organic dopants is very important for practical device applications, and is the focus of much activity for companies such as Transition Optics. 8.1,8.8,8.9 A second aspect of this research pertains to the natural sensitivity advantage for molecules that undergo photochromic rearrangements. This promotes the study of environmental parameters, subtle influences exerted by permitting one to follow the structural and chemical changes which occur during the sol-gel process. For example, polymerization, aging, and drying are associated with physicochemical changes that may be probed spectroscopically. 8.2,8.10,8.11 The studies of photochromic properties of spirooxazine in sol-gel media

began in 1994. ^{8.12,8.13} Spirooxazine doped materials have been previously prepared using ethyltriethoxysilane or di-*sec*-butoxyaluminumoxytriethoxysilane as sol-gel precursors. ^{8.14-8.17} However, little is known concerning the interaction between guest and sol-gel matrix in spirooxazine doped photochromic glasses. The photochromic properties and luminescence of spirooxazine doped sol-gel derived ORMOSIL materials have not been reported.

This chapter includes the study of the of spirooxazine doped air-stable ORMOSIL gels prepared by the sol-gel process. The ORMOSIL gel system of interest is an epoxy-diol modified silicate containing ethylene glycol and GPTMS ORMOSIL. The preparation and investigation of photochromism and luminescence effects of spirooxazine in air-stable sol-gel media is the major focus in this work.

8.II. Experimental Methods

8.III.A. Materials

SP1 was synthesized from 2-methylene-1,3,3-trimethylindoline and 1-nitroso-2-naphthol by Prof. Meigong Fan. ^{8.18} Tetramethoxysilane (TMOS) was obtained from Fluka Company and used without further purification. GPTMS (96%) was purchased from Aldrich. Anhydrous reagent grade ethylene glycol (EG) was obtained from Fisher Scientific Company. The water was deionized and distilled. The ultraviolet excitation source was a model 160-W UV Lamp (Fisher Scientific Company) with peak emission at 365 nm and a manufacturer-specified irradiation intensity of 11,600 $\mu\text{W}/\text{cm}^2$.

8.III.B. Sample Preparation

Bulk epoxide ORMOSIL gel specimens were prepared using TMOS, GPTMS, EG, and 0.040 *M* aqueous hydrochloric acid as precursors. Molar ratios of 1.0 TMOS:

1.0 GPTMS: 1.0 EG: 4.5 H₂O: 3.2×10⁻³ HCl were employed. A typical synthesis involved reacting 15.7 ml of TMOS and 6.7 ml of 0.040 M HCl in a Bransonic model 3 ultrasonic cleaner until it forms a sol within 5 minutes at room temperature. Then 23.6 ml of GPTMS, 1.9 ml of additional 0.040 M HCl, and 5.9 ml of EG were added to the mixture. The resulting sol was allowed to react in the sonicator for an additional 15 minutes.

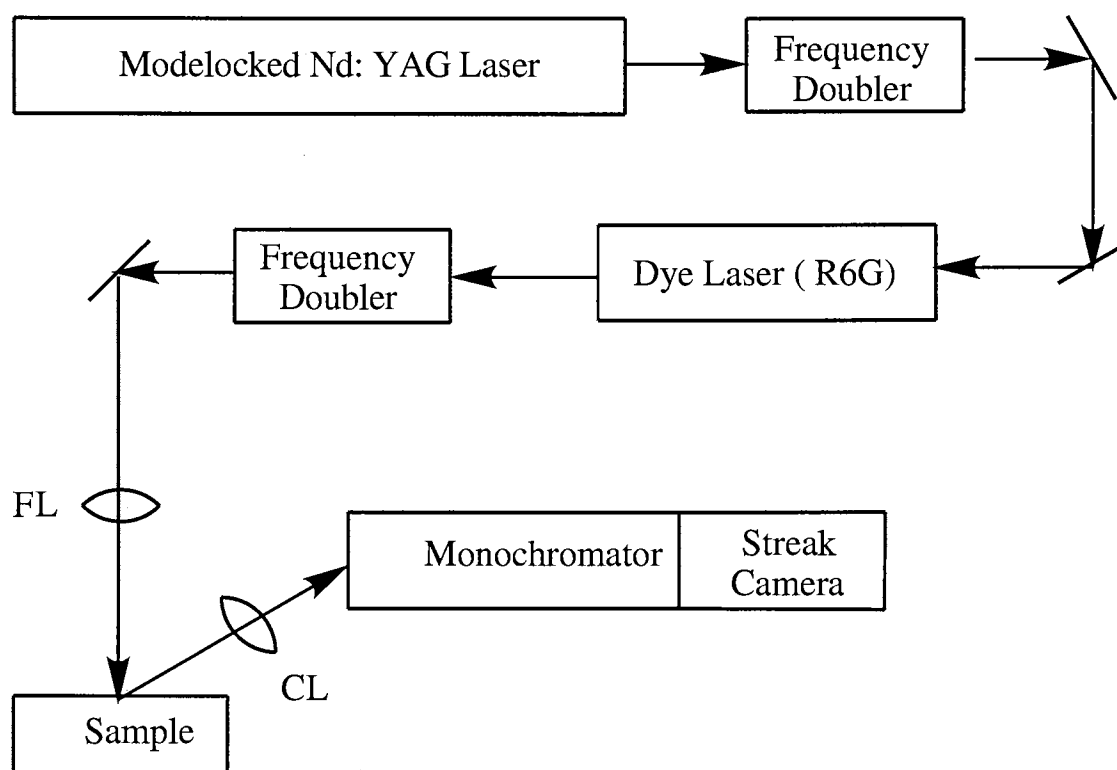
Doping was achieved by the addition of SP1 in ethanol to the precursor solution, providing a final dopant concentration of 1×10⁻⁴ M. Since the SP1 compound is very sensitive to high proton activity in alcoholic solution,^{8,19} a 0.2 M ammonium hydroxide solution in ethanol was added to the hydrolyzed sol in a dropwise fashion, with stirring to adjust the pH back to about 7 (using pH paper) before the addition of SP1. The resulting solution was poured into transparent polystyrene cuvettes and kept in covered containers at room temperature until the onset of gellation. After gellation, the covers were perforated to allow solvent evaporation. Aging and drying were allowed to proceed under ambient conditions for 3 to 4 weeks. Optical characteristics of the air-stable xerogels were subsequently determined. The final SP1 dopant number densities (N_D) in the air-stable epoxide ORMOSIL gels were calculated to be 3.0×10¹⁷ cm⁻³.

8.III.C. *Spectral Measurements*

Absorbance spectra were determined using a Cary 5E spectrophotometer (2.0 nm spectral band pass). Continuous wave front face excitation and emission spectra were measured using a Spex Industries Model F112A spectrofluorimeter; excitation and emission band passes were 1.85 and 0.86 nm, respectively. All luminescence spectra were collected in the dark at room temperature and corrected for instrumental response.

Time-resolved luminescence measurements of the SP1-doped gels utilized a frequency-doubled dye laser (5 ps pulse width; 82 MHz repetition rate). 300 nm output

from the dye laser was obtained upon frequency doubling of the 600 nm oscillation produced upon pumping *via* modelocked Nd:YAG laser (Spectral Physics 3800; frequency doubled 532 nm output). Temporal luminescence characteristics were obtained using a 0.5 M dispersing monochromator in conjunction with a synchronscan streak camera (Hamamatsu C5690, temporal resolution < 2 ps). The overall time resolution of detection system, including timing jitter, was less than 20 ps. The experimental apparatus is schematically shown in Figure 8-3.



FL = Focusing Lens; CL = Luminescence Collection Lens

Figure 8-3. Schematic diagram of experimental setup for time-resolved measurements of photochromic SPI-doped gels.

8.III. Results and Discussion

8.III.A. Photochromic Effects in SP1-doped ORMOSIL Xerogels

Figure 8-4 shows the optical absorption spectra of SP1-doped epoxide ORMOSIL xerogels before (Curve 1) and after (Curve 2) a 1 minute UV irradiation. The gel samples were observed to be colorless before exposure to the UV light source. Their absorption spectrum (Curve 1 of Figure 8-4) showed an intense band centered around 350 nm. There was no peak in the visible region. Upon exposure to UV irradiation, the samples turned blue, resulting from the onset of an absorption band at 612 nm with a shoulder around 575 nm (Curve 2 of Figure 8-4). After irradiation ceased, the samples returned to their original colorless form and the bands in the visible region disappeared. The appearance of the 612 nm band was attributed to the formation of the photomerocyanine (PMC) product, as described in Chapter 3, section III (Figure 3-3). These results indicated that the SP1-doped ORMOSIL matrices result in the formation of air-stable photonically-active solid state bulk media. The retention of photochromic activities in the ORMOSIL gels, in contrast to the findings for the aluminosilicate gels, is attributed to the presence of organic groups, which provide the local environment for the molecular rearrangement.

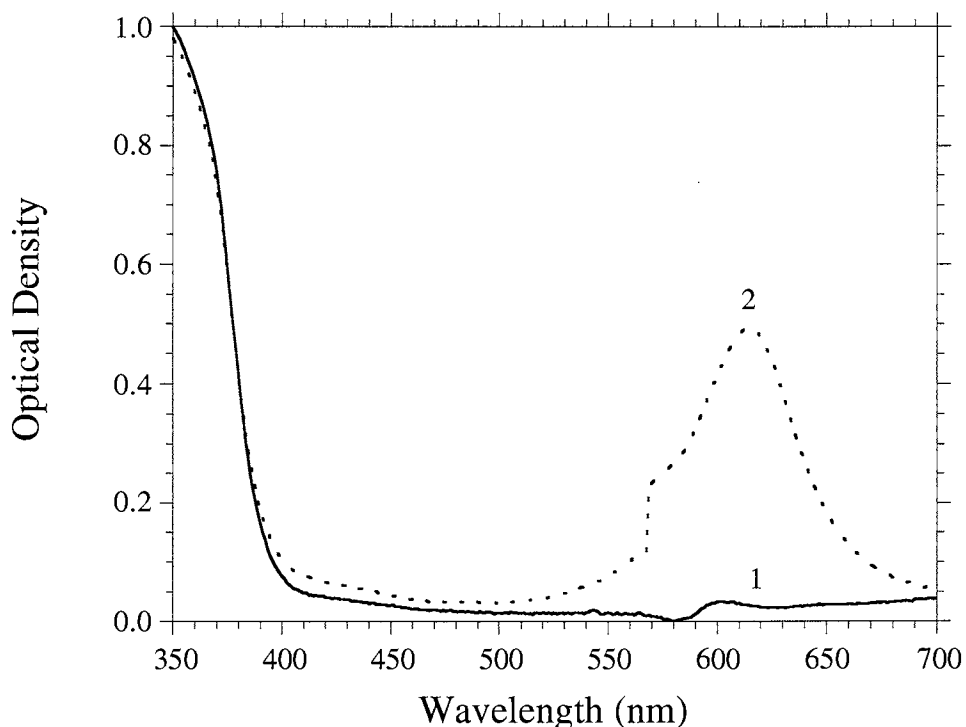


Figure 8-4. Absorption spectra of SP1-doped epoxide ORMOSIL gels (1). before UV irradiation; (2) after 1 min. UV irradiation.

8.III.B. Decay Rate Measurements

The colored form (PMC) generated by illumination with ultraviolet light decays over a period of 50 seconds at room temperature to the colorless form in the ORMOSIL xerogel specimens. A typical thermal decay rate measurement is shown in Figure 8-5. The plot shows the decrease in the optical density for epoxide ORMOSIL after removing the UV irradiation. A plot of the natural logarithm of relative absorbance (A/A_0) versus decay time (inset of Figure 8-5) is linear, indicating that the decay is a first order reaction.

The lifetime for SP1 doped gels is calculated from the slope of the natural logarithm of the absorbance versus time plot. It is calculated to be 7.4 seconds for air-stable epoxide ORMOSIL gels. The lifetime of photomerocyanine (PMC) in epoxide

ORMOSIL gels is much longer than that in the common solvents, which is reported to be approximately 0.5 seconds in common solvents.^{8.20} Interactions between the photochromic compound and gel host material cause the thermalization process in the solid state sol-gel media to be much slower than that in common solutions. Molecular rearrangements clearly occur much more slowly in the dense, solid host.

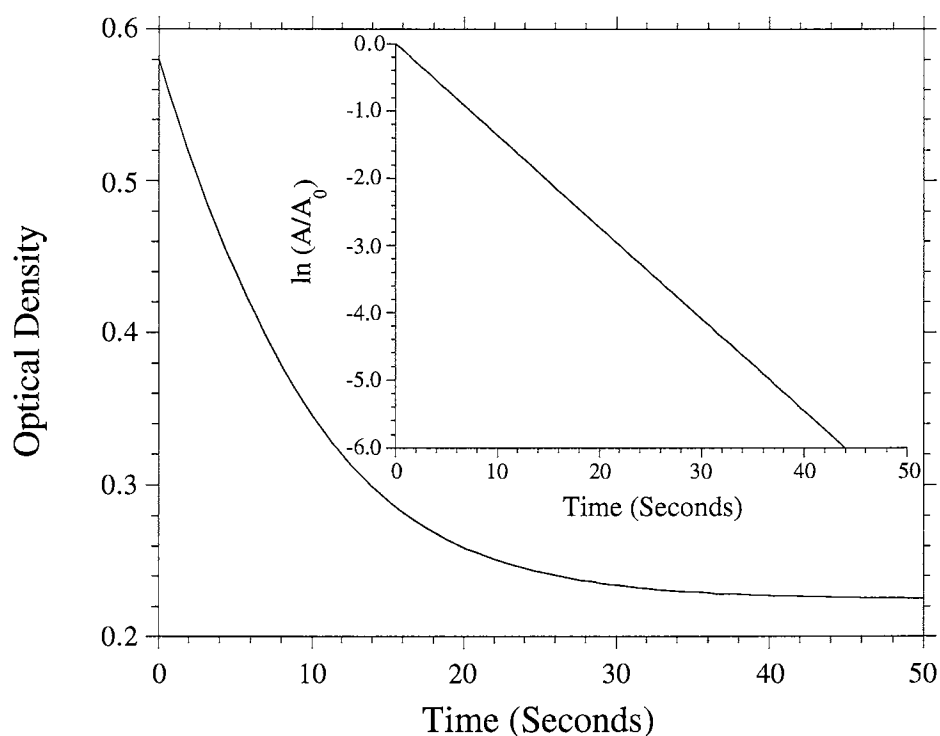


Figure 8-5. Time evolution for SP1 doped air-stable epoxide ORMOSIL xerogel absorbance at 612 nm following UV irradiation.

Inset: $\ln(A/A_0)$, versus decay time ($\lambda = 612$ nm);

(...) = actual data, (—) = single exponential fit.

8.III.C. *Fluorescence Studies of SP1-doped ORMOSIL Xerogels*

Figure 8-6 shows the fluorescence emission spectra of SP1 doped epoxide ORMOSIL xerogels excited at 350 nm (Curve 1) and 480 nm (Curve 2). The intense emission band centered at 430 nm was observed to remain essentially unchanged over excitation wavelengths ranging from 320 to 370 nm. This band is assigned to radiative relaxation from the lowest excited singlet state of SP1. A new much weaker fluorescence band, centered at 550 nm, was observed when the excitation wavelength was increased to 480 nm (Curve 2 of Figure 8-6). This band did not exist at the beginning of the sol, but was detected as the gellation processed. It was found that the 550 nm band is quite similar to one found in isopropanol solutions acidified by the addition of HCl as shown in Figure 5-2 in Chapter 5. This band was previously assigned to the protonated product of SP1, $\text{SP1}\cdot\text{HCl}$, in acidic alcoholic solution. This suggests the formation of a new species in the aged gel, $\text{SP1}\cdot\text{HO-Si}$, which is postulated to result from protonation of SP1 by acidic Si-OH sites in the gel network. This finding is consistent with that reported for the all-inorganic aluminosilicate gel specimens.

These results indicate that the acidichromic process is observed to occur in the sol to gel transition process for both the aluminosilicate gel (Chapter 7, section 7.III.B.) and ORMOSIL hosts.^{8,11} Unlike SP1 in aluminosilicate gel, the acidichromism process did not dominate during the development of air-stable organically silicate gel preparations. A small portion of SP1 was retained in the form of a protonated product prior to irradiation, while the majority of SP1 remained in its spiro form. This is part of the reason that the photochromism is still observed in the xerogel stage for ORMOSIL, while the photochromism is lost for aluminosilicate gel.

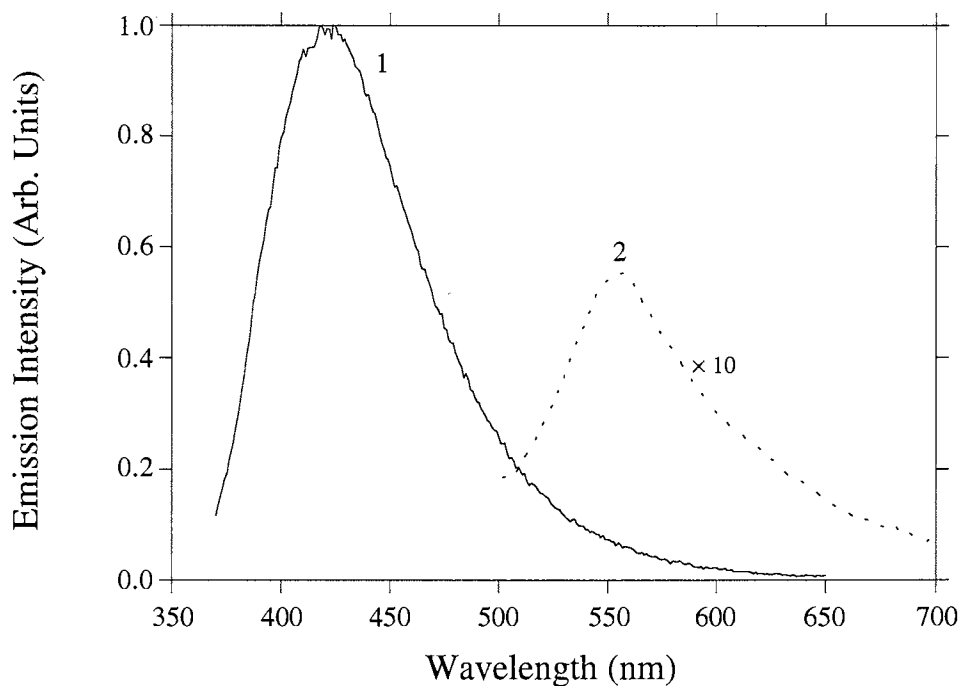


Figure 8-6. Fluorescence emission spectra of SP1 doped epoxide ORMOSIL gels.

(1: $\lambda_{\text{ex}} = 350 \text{ nm}$; 2: $\lambda_{\text{ex}} = 480 \text{ nm}$)

8.III.D. *Time-resolved Fluorescence Decay of SP1 Doped Gels*

Fluorescence decay curve for epoxide ORMOSIL xerogel is shown in Figure 8-7 ($\lambda_{\text{ex}} = 300 \text{ nm}$; $\lambda_{\text{em}} = 430 \text{ nm}$). Radiative decay curves of the SP1 guest were fit to a double-exponential relaxation behavior according to equation (8-1). Correlation coefficient of 0.993 were found for epoxide ORMOSIL gels.

$$k = f i_1 \exp(-x/\tau_1) + f i_2 \exp(-x/\tau_2) \quad (8-1)$$

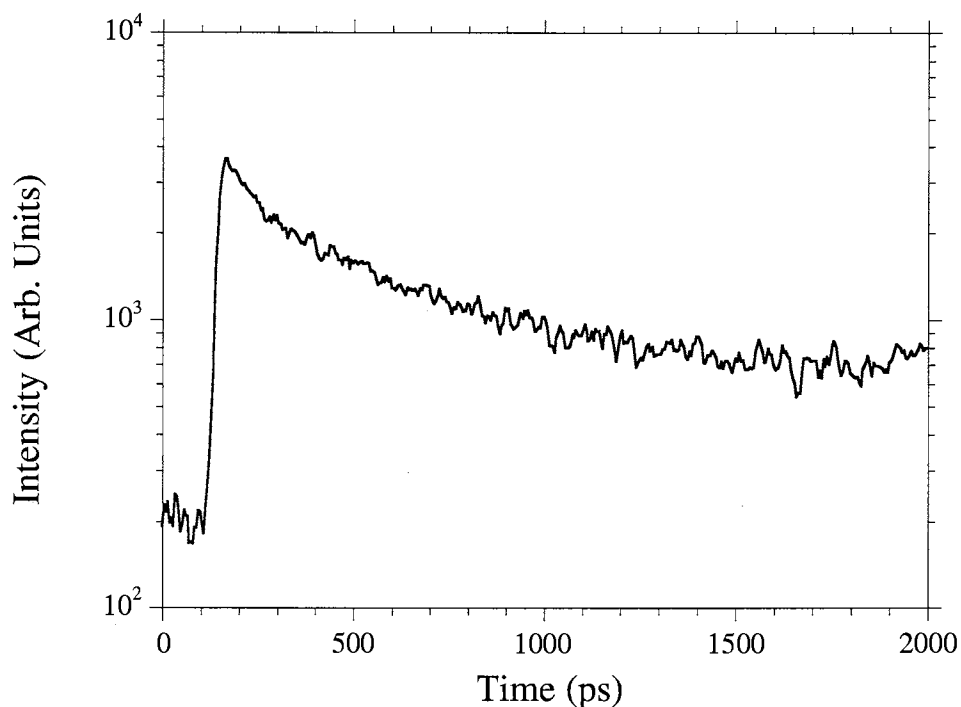


Figure 8-7. Radiative decay curve of SP1 doped epoxide ORMOSIL gel

The radiative lifetime of the long (τ_1) and short (τ_2) components were found to be 2.64 nsec and 194 psec for epoxide ORMOSIL gels. The fractional intensity of the components were $fi_1 = 0.22$ and $fi_2 = 0.78$; fluorescence decay was fitted using a double-exponential model. The longer lifetime (2.64 nsec) has been tentatively assigned to a radiative relaxation from the lowest excited singlet state of SP1 to the ground state. The fractional intensity of this radiation is only 22% of the total emission intensity. This indicates that most of the first excited singlet state S_1 energy is transferred to a secondary intermediate. According to the literature,^{8,21} there is no excited triplet state involved in the photochromic process of SP1. The second decay component, having a very short lifetime of 194 psec, is tentatively assigned to a radiation process out of the excited state

intermediate, designated X_1^* . It is noted in the literature^{8.20} that cleavage of the spiro C-O bond, which initiates photochromic rearrangement of SP1, occurs on a picosecond scale. Because the ultrafast photochromic reaction, the lifetime of X_1^* is very short. In other words, the observed fluorescence lifetime τ_2 will depend on the competition between the radiative, photo-initiated chemical reactions, and other competing non-radiative processes according to equation (8-2):

$$\tau = 1/(k_f + k_r + k_n) \quad (8-2)$$

In this equation, k_f is the radiation relaxation rate, k_r is the initial chemical reaction rate of photochromism of SP1 and k_n refers to all of the non-radiative relaxation rate except mentioned chemical reaction. τ_2 represents the lifetime of the first excited singlet state of the intermediate, X_1^* .

The results of the radiative lifetimes indicate that only part of the fluorescence is from the lowest singlet state of SP1. The fast radiative lifetime is very short compared with the longer S_1 to S_0 transition. The photochromism is observed for this organic modified sol-gel derived media in the air-stable xerogel stage. It is postulated that the sol-gel host slows the photo-initiated molecular rearrangement reaction to the extent that it may be observed using the apparatus shown in Figure 8-3.

8.IV. Summary and Conclusions

Photochromic epoxide ORMOSIL glasses containing spirooxazine have been prepared and investigated. These specimens show regular photochromism instead of reverse photochromism which was observed by Avnir *et al.*^{8.1,8.6-8.8} for spiropyran. The photochromic properties and thermal decay of these sol-gel derived glasses are studied. The thermal decay of spirooxazine doped xerogels is found to be much slower

than that in common solutions because of the presence of hybrid organic/inorganic polymers. The fluorescence spectra of SP1 doped specimens have been conducted indicating that acidichromism which observed in aluminosilicate is not a main process for ORMOSIL preparation. Picosecond lifetime studies show a double exponential decay. The photophysical process of SP1 derived media has been discussed.

8.V. References

- 8-1 D. Levy and D. Avnir, *J. Phys. Chem.* **92** (1988) 4734.
- 8-2 D. Preston, J. C. Pouxviel, T. Novinson, W. Kaska, B. Dunn and J. I. Zink, *J. Phys. Chem.* **94** (1990) 4167.
- 8-3 C. J. Brinker and G. Scherer, *J. Non-Cryst. Solids* **70** (1985) 301.
- 8-4 C. J. Brinker and G. Scherer, *J. Non-Cryst. Solids* **100** (1988) 31.
- 8-5 L. L. Hench and J. K. West, *Chem. Rev.* **90** (1990) 33.
- 8-6 D. Levy, D. Avnir and R. Reisfeld, *J. Phys. Chem.* **88** (1984) 5956.
- 8-7 V. R. Kaufman, D. Levy and D. Avnir, *J. Non-Cryst. Solids* **82** (1986) 103.
- 8-8 D. Levy, S. Einhorn and D. Avnir, *J. Non-Cryst. Solids* **113** (1989) 137.
- 8-9 T. Yoshida and A. Morinaka, *J. Photochem. Photobiol. A: Chem.* **78** (1994) 179.
- 8-10 J. Mckiernan, J. C. Pouxviel, B. Dunn and J. I. Zink, *J. Phys. Chem.* **93** (1989) 2129.
- 8-11 X. D. Sun, M. G. Fan and E. T. Knobbe, *Mol. Cryst. Liq. Cryst.* (in press).
- 8-12 L. Hou, M. Menning and H. Schmidt in *Sol-Gel Optics III*, ed. J. D. Mackenzie, *Proc. SPIE* **2288**, 328 (1994).
- 8-13 H. Nakazumi, R. Nagashiro, S. Matsumoto and K. Isagawa in *Sol-Gel Optics III*, ed. J. D. Mackenzie, *Proc. SPIE* **2288**, 402 (1994).
- 8-14 L. Hou and H. Schmidt, *J. Mater. Sci.* **31** (1996) 3427.

- 8-15 L. Hou, B. Hoffmann, M. Nennig and H. Schmidt, *J. Sol-Gel Sci. Tech.* **2** (1994) 635.
- 8-16 J. Biteau, F. Chaput and J-P. Boilot, *J. Phys. Chem.* **100** (1996) 9024.
- 8-17 L. Hou and H. Schmidt, *Mater. Lett.* **27** (1996) 215.
- 8-18 X. Y. Zhang, S. Jin, Y. F. Ming, Y. C. Liang, L. H. Yu, M. G. Fan, J. Luo, Z. H. Zuo and S. D. Yao, *J. Photochem. Photobiol. A: Chem.* **80** (1994) 221.
- 8-19 X. D. Sun, M. G. Fan, X. J. Meng and E. T. Knobbe, *J. Photochem. Photobiol. A: Chem.* (in press).
- 8-20 C. Bohne, M. G. Fan, Z. J. Li, Y. C. Liang, J. Lusztyk and J. C. Scaiano, *J. Photochem. Photobiol. A: Chem.* **66** (1992) 79.
- 8-21 S. Schneider, F. Baumann, U. Kluter and M. Melzig, *Ber. Bunsenges. Phys. Chem.* **91** (1987) 1225.

2

VITA

Xiaodong Sun

Candidate for the Degree of

Doctor of Philosophy

Thesis: PHOTOCROMIC CHARACTERISTICS OF SPIROOXAZINE-CONTAINING MEDIA

Major Field: Chemistry

Biographical:

Personal Data: Born in Beijing, China, on May 10, 1964, the son of Xiancheng Sun and Lansheng Zhang.

Education: Received a Bachelor of Science degree and Master of Science degree in chemistry from Peking University, Beijing, China in July 1986 and in August 1989, respectively. Completed requirements for the Degree of Doctor of Philosophy with a major in chemistry at Oklahoma State University in May 1997.

Experience: Employed by Oklahoma State University, Department of Chemistry, as a graduate teaching and research assistant; Oklahoma State University, Department of Chemistry, 1991 to present.